EVALUATION OF THE EFFECT OF THE pH OF CONCRETE PORE SOLUTION ON THE CORROSION PERFORMANCE OF REINFORCING BARS

By
Yaseen Mazin Ameen Al-Rifaie

Submitted to the graduate degree program in Civil Engineering
and the Graduate Faculty of the University of Kansas in partial fulfillment
of the requirements for the degree of Master of Science

_____Matt O'Reilly____
Chairperson

_____David Darwin____

____Lequesne Remy____
Committee Members

Date Defended: January / 4 / 2018

The thesis committee for Yaseen Al-Rifaie
Certifies that this is the approved version of the following thesis:

EVALUATION OF THE EFFECT OF THE pH OF CONCRETE PORE SOLUTION ON THE CORROSION PERFORMANCE OF REINFORCING BARS

____Matt O'Reilly____
Chairperson

____David Darwin____

___Lequesne Remy____
Committee Members

Date Defended: January / 4 / 2018

ABSTRACT

In this study, the effect of the pH of concrete pore solution on the corrosion resistance of reinforcement is evaluated using the rapid macrocell test (outlined in Annex A2 of ASTM A955-14). Tests are conducted on five different types of reinforcing bars; Type 2304 duplex stainless steel bar, Type 304 stainless steel clad bar, MMFX Type CS (MMFX(9%)) reinforcing bar, galvanized reinforcing bar, and dual-coated reinforcing bar (zinc-coated bars covered with a layer of epoxy coating). Specimens are exposed to two different pore solutions (standard and modified) with pH values of 13.9 and 13.5, respectively, simulating the conditions found in concrete environments. The corrosion activity of the specimens is monitored using macrocell corrosion rate, corrosion potential, and microcell corrosion rate (as measured by linear polarization resistance measurements (LPR)).

The results show that the pH of the pore solution (or of the concrete) has a major influence on the corrosion resistance of reinforcing bars. MMFX(9%) and dual-coated reinforcing bars exhibit better corrosion resistance in the standard pore solution compared to the modified pore solution. Conversely, the corrosion resistance of galvanized reinforcement decreases as pH increases, likely due to the formation of large isolated hydroxyzincate crystals. Stainless steel reinforcement generally exhibits similar corrosion resistance in the standard and modified pore solutions.

Keywords: corrosion, concrete, pH, pore solution, reinforcing bar, stainless steel, dual-coated reinforcing bars

ACKNOWLEDGMENTS

I would first like to thank the Higher Committee for Education Development in Iraq (HCED) for awarding me their scholarship.

I would also like to thank my advisor Dr. Matt O'Reilly for his continuous help whenever I ran into a trouble or had a question about my research or writing since the first day I worked with him, Dr. David Darwin for his advice and support, and Dr. Remy Lequesne for his continuous motivation and support.

My appreciation is continued to my friends and colleagues who have helped me throughout my years of study.

Last but not least, I would like to extend my profound thanks to my parents (Mazin Al-Rifaie and Asmaa Al-Rifaie) and to my brothers (Mustafa, Tahseen, and Younis) for providing me with constant support and encouragement throughout the time I spent on this work.

CONTENTS

LIST OF FIGURES

LIST OF TABLES

CHAPTER 1: INTRODUCTION

1.1 GENERAL

Reinforced concrete is a composite material characterized by high durability and good performance during the service life of the structure. These characteristics have made reinforced concrete one of the most widely used construction materials. However, the corrosion of reinforcing steel in concrete is a major durability problem, causing degradation and reducing the service life of reinforced concrete structures (Broomfield 1997, Zhang et al. 2009, Ranjith et al. 2016). Corrosion-related damage is also a major expense; a result of a comprehensive study on the financial impacts of metallic corrosion in the United States estimated the direct cost related to the corrosion in the United States at $276 billion per year, approximately 3.1% of the U.S gross domestic product for that period (Koch et al. 2002).

Reinforced concrete bridge components are one of the structures most likely to be damaged by corrosion, particularly bridge decks, due to the use of chemicals (deicers) in snow and ice control operations. These chemicals are the major source of chloride ions that cause severe corrosion in bridge decks reinforcement (as discussed in Section 1.4.2). As of 2016, the Federal Highway Administration (FHWA) reported that of the 614,387 bridges in the United States, approximately 11% of these bridges, 56,007, were classified as structurally deficient, many due to corrosion (FHWA 2016).

The annual direct cost related corrosion for bridges is estimated to be $8.3 billion in the United States, with indirect costs due to traffic delays and productivity loss estimated at more than 10 times that value (Koch et al. 2002). Thus, a large amount of research has been conducted to develop effective methods to prevent corrosion of reinforcing steel.

Increasing concrete cover, using higher quality concrete, and using alternatives to conventional reinforcing steel, such as epoxy-coated bars, stainless steel bars, clad bars, MMFX

(9%) bars, zinc (galvanized) bars, and dual-coated reinforcing bars, are some of the methods used now to increase the resistance of reinforcing steel to corrosion and hence increase the service life of bridge decks. Section 1.5 provides more information about the corrosion protection systems incorporated in this study.

1.2 CORROSION OF REINFORCING STEEL IN CONCRETE

Corrosion is an electrochemical oxidation of a metal by a destructive chemical reaction with its environment. Corrosion as a chemical reaction requires four factors: an anode, a cathode, an electronic circuit, and an electrolyte or ionic connection.

The anode, where ferrous ions and electrons are released by the oxidation process of iron, is the site where corrosion begins and where the corrosion products are accumulated. With presence of oxygen, the oxidation reaction of iron at the anode causes ferrous ions to go into solution, and produces two electrons [Eq. (1.1)]:

$$Fe \rightarrow Fe^{2+} + 2e^{-} \tag{1.1}$$

The cathode, where the electrons released at the anode are consumed by a reaction of moisture with oxygen to form hydroxyl ions, can be located on the same bar of the reinforcing steel as the anode or a different bar if an electrical connection is provided. The oxygen reduction process at the cathode, when moisture and released electrons from the anode are present, produces hydroxyl ions [Eq. (1.2)]:

$$2H_2O + O_2 + 4e^{-} \rightarrow 4OH^{-} \tag{1.2}$$

An electrical circuit, the third requirement of corrosion to occur, provides a path for electrons to flow from anode to cathode. This electrical connection can be provided by reinforcing bars embedded in concrete or tie wires.

The fourth requirement for corrosion of reinforcing steel, the electrolyte or ionic connection, can be provided by the pore solution in concrete, where the pore solution acts as a path for the hydroxyl ions formed at the cathode to migrate to the anode. The hydroxyl ions react with the ferrous ions existing at the anode to produce ferrous hydroxide [Eq. (1.3)]:

$$Fe^{2+} + 2OH^{-} \rightarrow Fe(OH)_2 \quad (1.3)$$

Reinforcing steel in concrete is normally protected from corrosion due to the high pH environment provided by concrete pore solution. This high alkalinity causes a passive layer of γ-ferric oxyhydroxide to be formed, which acts as a protective film covering the reinforcing bar surface and protecting against corrosion Eq. (1.4):

$$4Fe(OH)2 + O2 \rightarrow 4\ \gamma\text{-}FeOOH + 2H_2O \quad (1.4)$$

This passive layer, however, can be damaged in presence of chloride ions, which can be diffuse inside of concrete from interior or exterior sources, and the carbonation process, which reduces the pH level of concrete, hence decreasing the passivity of reinforcing steel (as discussed in Section 1.3).

Ferrous hydroxide, when moisture and oxygen are present, is oxidized to yield ferric hydroxide. Ferric hydroxide forms ferric oxide (rust) through the following reactions, [Eq. (1.5) and Eq. (1.6)]:

$$4Fe(OH)_2 + 2H_2O + O_2 \rightarrow 4Fe(OH)_3 \quad (1.5)$$

$$2Fe(OH)_3 \rightarrow Fe2O_3 + 3H_2O \quad (1.6)$$

Rust can occupy as much as five times the original size of the reinforcing steel. This produces internal tensile stresses in the surrounding material at the interface of reinforcing bar causing cracking and spalling of concrete. These cracks increase the permeability of concrete

allowing more chloride, oxygen, and moisture to penetrate into the concrete and reach the reinforcement.

1.3 THE EFFECT OF CONCRETE pH LEVEL ON CORROSION OF REINFORCING BARS

In the present work, the influence of changes alkalinity (pH value of concrete) on the corrosion potential of steel in concrete is evaluated.

The concrete environment is characterized by different phases, including an interstitial electrolyte. The main component of this electrolyte is a saturated solution of $Ca(OH)_2$, containing a significant amount of soluble compounds of alkali metal elements such as sodium hydroxide (NaOH) and potassium hydroxide (KOH) (Freire et al. 2010). The alkali metal ions can be released into the surrounding solution due to the formation of new hydration products with water as a result of hydration reactions, thereby; causing an increase in the pH value of the concrete pore solution (Šiler et al. 2016).

As stated in Section 1.2, reinforcing steel embedded in concrete is normally protected from corrosion by a microscopically thin passive layer of γ−ferric oxide coating that forms on the steel surface. The pH of the concrete pore solution must be between 11.5 and 13.8 in order to keep this passive layer intact. (Gong et al. 2002, Figueira et al. 2015). However, when the pH of concrete pore solution drops below this level such as occurs when sufficient amounts of CO_2 enter the concrete, the passive layer breaks down and reinforcement corrosion will take place. Whereas corrosion initiates at pH level below 11.5, the passive film on the steel surface completely disappears at a pH level of 8, and a rapid form of corrosion occurs when the pH drops to less than 7 (Berkeley & Pathmanaban 1990, Ahmad 2003).

The passive layer can also break down in the presence of chlorides. The critical chloride corrosion threshold is the minimum concentration of chloride ions at the surface of the steel required to cause passive film breakdown and initiate corrosion (Page & Treadaway 1982). The pH level of the pore solution of concrete influences the critical threshold value. Prior research (Hartt & Nam 2008) has shown that greater thresholds for corrosion initiation were exhibited by specimens with higher pH. Hartt et al. (2003) tested a series of concrete specimens that subjected to cyclic wet-dry ponding with a solution containing 15 % NaCl for four years and fabricated using three different cements with different levels of alkalinity to evaluate the effect of the pH level of the concrete pore solution on the chloride threshold and time-to-corrosion. The pH for the specimens tested ranged from 13.05 to 13.20 for the low alkalinity mix (LA), 13.19 to 13.36 for the normal alkalinity (NL), and 13.53 to 13.65 for the high alkalinity (HA). The results reflect that the high alkalinity specimens presented the highest chloride threshold. The effective diffusion coefficient (D_{eff}) was about 40% lower for HA concrete specimens compared to the NA and LA ones; thereby, less Cl^- penetration occurred for specimens prepared with the HA cement, leading to an increase in time-to-corrosion of five times over the NA and LA specimens (Hartt et al. 2003).

Mammoliti et al. (1996) tested steel with different surface finishes in two different pore solutions, a saturated solution of $Ca(OH)_2$ with pH 12.5 and a simulated concrete pore solution containing NaOH and KOH and an excess of $Ca(OH)_2$ with pH 13.3. The results showed that even at chloride ion concentrations as high as 10%, the simulated pore solution of pH 13.3 provided sufficient protection against corrosion whereas the pH 12.5 solution did not (Mammoliti et al. 1996).

Hartt et al. (2004) evaluated the corrosion performance of different types of high-performance reinforcement in aqueous solutions of different pH levels. The results of the threshold

Cl^- concentrations showed that the thresholds of AISI 304 and 2304 stainless steel at levels of pH 13.9 and 12.6 were 4 times the thresholds at pH 9. Type AISI 304 stainless steel provided threshold (at levels of pH 13.9 and 12.6) 10 times the threshold provided at pH 7.5, while the 2304 stainless steel provided threshold (at levels of pH 13.9 and 12.6) 6.6 times more than the threshold provided at pH 7.5 (Hartt et al. 2004). These results showed that the threshold Cl^- concentration decreased as the alkalinity of the pore solution decreased.

Flint and Cox (1988) showed that the pH of high alkalinity concrete ranges from 13 to 14 in the early stages of curing. This alkali concentration, however, may fall to about 12.6 when expose to high concentrations of chloride, which can lower the potential of stainless steel to a value which pitting corrosion may occur (Flint & Cox 1988).

Smith et al. (1992) monitored the performance of solid stainless steel bars and a single type of stainless steel clad bar using severe cyclic wetting and drying tests with high pH (pH 13) and low pH (pH 7) environments. The results of 28 days of cyclic testing showed that the corrosion rate of conventional steel in the environment of pH 13 was 8% of the corrosion rate in the pH 7 solution.

Ai et al. (2016) studied the passive behavior of a Cr10Mo1 alloy in alkaline solutions simulating the pore solutions of fresh and carbonated concrete, monitoring the effects of pH on the structure and characteristics of surface film formed on the steel. An aqueous saturated solution of 0.3 M $Ca(OH)_2$ with 0.5 M KOH + 0.2 M NaOH was prepared for alkaline medium with pH 13.5, to simulate the condition found in normal concrete. Lower pH (12.0, 10.5, and 9.0) solutions were also prepared by adding $NaHCO_3$ into the saturated solution of 0.3 M $Ca(OH)_2$, to simulate the carbonation process. The results showed that Cr10Mo1 steel exhibited better passivity as the pH decreased because the passive film formed on its surface involves a bilayer structure with an

exterior layer of Fe oxides and an interior layer containing Cr. The more stable Cr oxides form on the Cr10Mo1 steel surface as the pH level decreased, reflecting higher corrosion resistance. For carbon steel, lowering the pH resulted in lower corrosion resistance due to the gradual degradation of the protective Fe oxides (Ai et al. 2016).

Galvanized steel (Section 1.5.5) has been considered as an effective alternative to conventional steel. The zinc coating layer, which formed by the galvanizing process, is oxidized forming calcium zincate salt (calcium hydroxyzincate), which acts as a barrier layer protecting the underlying steel from corrosion. This protective layer continues to be stabilized in pH level of concrete ranging from 6 to 13 (Maslehuddin et al. 1994, Yeomans 2004). In environments with a pH above 13.3, however, calcium hydroxyzincate forms large isolated crystals that cannot protect the underlying steel from corrosion (Andrade & Macias 1988).

Epoxy-coated reinforcing steel has also exhibited good corrosion protection, as described in Section 1.5.1. Damage in the coating of steel may accrue during the shipment, handling at the job site, and concrete placement; this is considered a disadvantage of this system. Blisters may take place close to the damage sites and form by osmotic pressure due to accumulation of concrete pore water under the coating. Corrosion initiates inside the blisters due to the drop in the pH of the pore solution of concrete from 12 to 5, causing the formation of an acidic environment under the coating (Weyers et al. 1998).

1.4 FACTORS AFFECTING THE pH OF CONCRETE

Corrosion is greatly affected by the pH level of the pore solution of concrete, which in turn can be influenced by several factors, as detailed below.

1.4.1 Carbonation

The pore solution in fresh concrete starts its life at a highly pH level of about 13. However, in relatively dry environments, the pH value of this medium can be reduced at the exposed surfaces down to pH values of about 8.5 due to a process known as carbonation, where carbon dioxide from the atmosphere penetrates into the concrete and react with the hydrated cement compounds (Grubb et al. 2007, Liu et al. 2017).

In the carbonation process, carbonic acid is produced due to dissolution of CO_2 in water which in turn reacts with calcium hydroxide generated in cement hydration process producing calcium carbonate. Calcium carbonate causes a severe reduction in the pH level of the pore solution of concrete (Gong et al. 2003). The mechanism of carbonation is shown in the following reactions, [Eq. (1.7) and Eq. (1.8)]:

$$CO_2 + H_2O \rightarrow H_2CO_3 \quad (1.7)$$

$$H_2CO_3 + Ca(OH)_2 \rightarrow CaCO_3 + 2H_2O \quad (1.8)$$

1.4.2 Chlorides

Compared with the carbonation process, chlorides can cause much more rapid corrosion of reinforcing steel in concrete, as the ingress of chloride ions are usually faster than the carbonation process (Ranjith et al. 2016).

When chlorides diffuse into concrete and accumulate at the surface of the reinforcing steel, breakdown of the passive film formed on the steel surface may take place due to the formation of an iron-chloride complex as a result of the reaction between the chloride ions and available iron ions from the passive layer. The following reactions occur when chloride ions are available at the surface of steel [Eq. (1.9) and Eq. (1.10)]:

$$Fe^{2+} + 4Cl^{-} \rightarrow (FeCl_4)^{2-} \quad (1.9)$$

$$(FeCl_4)^{2-} + 2H2O \rightarrow Fe(OH)_2 + 2H^{+} + 4Cl^{-} \quad (1.10)$$

The ratio of chloride ions to the weight of cement, the critical threshold of chloride required to initiate corrosion, can vary greatly. In design, these values have been limited to be not greater than 0.15% (water-soluble) or 0.40% (acid-soluble) (Thomas 1996). The critical threshold of chloride can also be specified as a ratio of chloride to hydroxyl ions, [Cl-]/[OH-], and should not exceed 0.6 (Hausmann 1967).

Chloride can be found or transported into concrete due to addition of admixtures, contaminated constituents, exposure to seawater, or exposure to deicing salts (Byfors 1987).

1.4.3 Supplementary Cementitious Materials

The influence of using supplementary cementitious materials on alkali contents of cement paste pore solutions was investigated by several researchers (Diamond 1981, Diamond 1983, Page & Vennesland 1983, Byfors 1987, Muralidharan et al. 2008, Diab et al. 2011, King et al. 2012, Ortolan et al. 2016). All the results agreed that using supplementary cementitious materials as a partial replacement of portland cement causes a reduction in the concentration of calcium hydroxide; therefore, the pH level of the pore solution of concrete will be reduced.

A study by Ortolan et al. (2016) evaluated the influence of cement replacement by silica fume on the pH value of concrete mixtures, hydrating for up to 91 days, with replacement ratios of 0, 5 and 10% by volume. The results showed that, after the first three days of testing, the pH was influenced by the difference in the percentage of substitution. The mixture with 10% silica fume obtained the lowest pH value of about 12.6 at the end of the testing period (91 days). Likewise, the mixture with no replacement showed the highest pH value of 13.2 at 91 days (Ortolan et al. 2016).

The study by Byfors (1987) showed that a reduction of the pH value by 0.4 and 0.7 units occurred when silica fume was used as a replacement (10 and 20% by volume, respectively) in portland cement paste with a water-binder ratio of 0.5. Additions of 15-40% fly ash led to reductions in pH by 0.3 and 0.2 units, respectively.

1.4.4 Inhibitors

The use of some corrosion inhibitors causes a reduction in the pH of the pore solution of concrete. Calcium nitrite is an example of one of the inhibitors that lower the pH of the pore solution in concrete (Li et al. 1999)

O'Reilly et al. (2011) showed that the pore solution of specimens with no calcium nitrite obtained a pH level of 13.5 after 25 days of the test period, while the pore solution of specimens with calcium nitrite had a pH level of 13.2 at 25 days.

1.5 CORROSION PROTECTION SYSTEMS

Corrosion is a concern threatening the integrity of reinforcing steel in concrete structures, especially in structures like bridge decks. For that reason, a variety of strategies have been developed to protect reinforcing steel in concrete from corrosion by developing several protection methods.

Increasing concrete cover over conventional reinforcing steel and using a high quality concrete have not been adequate to improve the durability of concrete. Supplementary protection, therefore, is required for structures exposed to corrosive environments such as bridge decks. Thus, alternatives to conventional steel reinforcement such as stainless steel, epoxy-coated bar, and other species of corrosion protection systems have been used to provide sufficient protection from corrosion and increase the service life of structures (Vassie 1996, Kepler et al. 2000).

The service life of a structure can be considered as the period of time expected for a structure to achieve its function without extraordinary maintenance or repair (Ranjith et al. 2016). For reinforcing concrete structures exposed to corrosive environments due to chloride, two phases to service life occur, an initiation phase and a propagation phase (Ahmad 2003), as demonstrated in Figure **1.1**.

The initiation phase, depassivation, is the period of time until the passive layer over the reinforcing steel fails due to a presence of chlorides or carbonation, t_p. The propagation phase, t_{corr}, represents the time between the initiation phase and repair of the concrete (Ahmad 2003).

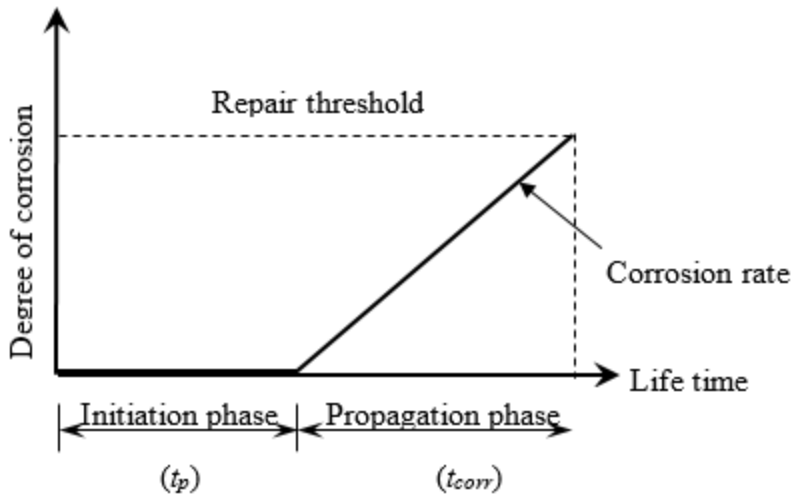

Figure 1.1: Service life model of steel corrosion in concrete (Berkeley & Pathmanaban 1990, Ahmad 2003)

Using alternative reinforcing steel is one of the methods used to increase the initiation time or lower the corrosion rate. In the current study, the alternate steels under consideration are discussed below.

1.5.1 Epoxy-Coated Reinforcement (ECR)

Epoxy-coated reinforcing steel is the most common corrosion protection system used in highway bridge decks in the United States. Epoxy-coated reinforcing steel was developed in the early 1970s (Manning 1996). Study by Clifton et al. (1975) evaluated 47 different coating materials to be used on reinforcing steel embedded in concrete of bridge decks to provide protection from corrosion due to chloride ions from deicing salts applied over the bridge decks. These coating materials were tested for chemical and physical durability, chloride permeability, and protective qualities of coting. The study showed that powder epoxy coatings had better performance than the liquid epoxies. Moreover, only the epoxy-coated reinforcing bars had acceptable performance in bond and creep characteristics when used in concrete (Clifton et al. 1975).

Epoxy coatings provide protection for reinforcing steel embedded in concrete in two ways, first by creating a barrier to keep oxygen and chlorides from reaching the reinforcing steel surface, and second by isolating the reinforcing steel electrically to avoid any electrical connection between bars (Kepler et al. 2000, O'Reilly et al. 2011). Therefore, epoxy coatings significantly reduce the macrocell corrosion by reducing the macrocell electrical currents between anode and cathode (Clear & Virmani 1983). Localized corrosion, however, can still occur. Since the efficiency of epoxy coatings depends on their ability to provide a physical and electrical barrier, special measures must be taken during coating, shipping and storage process of the reinforcing steel to protect it from damage (Clear 1995). In 1986, the first signs of severe corrosion of epoxy-coated reinforcing steel were discovered in the substructure of five marine bridges in the Florida Keys. After only six years, loss of adhesion of the epoxy to the reinforcement surface occurred and was followed by spalling of concrete in the bridge substructure (Smith et al. 1993, Manning 1996).

The corrosion of epoxy-coated rebar can be occurred due to the presence of small imperfections in the epoxy coating. These small imperfections, called holidays, allow for a very small area of the underlying steel to be exposed to the corrosive materials, causing localized corrosion. Damage incurred to the epoxy coating during casting concrete, shipment and placement of the rebar may also be weaknesses where corrosion occurs. Results of a study by Samples (1998) showed an average of 12.2 defects per foot (40 defects per meter) were created during placement of concrete, placement of rebar, and shipment. An average of 75 percent of those holidays (30 holidays per meter or 9 holidays per foot) were created during the concrete casting operation. Samples found that an increase in the coating thickness by 2 mils (50.8 μm) reduced the defects (holidays) created during shipment and fabrication by 85 percent.

Several studies proved that functional service life was significantly increased when bridge decks were reinforced with epoxy-coated reinforcement compared to use of conventional reinforcing bars (Treadaway & Davies 1989, Fanous & Wu 2005, Darwin et al. 2011). However, it was found that the epoxy lost adhesion to the steel surface over time when the concrete remains saturated, such as in bridge piers in salt water (Sagüés et al. 1994, Smith & Virmani 1996, Manning 1996, Darwin et al. 2007, Darwin et al. 2011). The adhesion of the coating to steel decreases after a period of exposure to corrosive materials such as chlorides. This reduction in adhesion increases as chloride content increases (Darwin et al., 2011).

Regardless of these imperfections, epoxy-coated reinforcing steel significantly improves the service life of the structure compared to conventional steel. Draper (2009) compared the performance of epoxy-coated reinforcement to that of conventional steel reinforcement, using the Southern Exposure and cracked beam tests. Results showed that the epoxy-coated reinforcement exhibited a critical chloride threshold several times higher than that of conventional reinforcement. Also, the epoxy-coated reinforcement exhibited low corrosion losses, whether in uncracked or cracked concrete specimens, well below the magnitude of corrosion loss required to cause corrosion-induced surface deterioration. Epoxy-coated reinforcing steel exhibits a significant reduction in corrosion rates compared to bare reinforcement (Darwin et al. 2007, O'Reilly et al. 2011). The Federal Highway Administration (FHWA) published a report, which summarized results of investigations that have been performed by highway agencies in the United States and Canada to evaluate the corrosion resistance of epoxy-coated reinforcing bars (Smith & Virmani 1996). A total of 92 bridge decks, two bridge barrier walls, and one noise barrier wall located in 11 different states, were evaluated at service ages of 3 to 20 years. The results of the investigations showed that the structures were generally in good condition. Erdoğdu et al. (2001) examined

epoxy-coated reinforcing steel bars in concrete slabs subjected to synthetic seawater and a 3% salt solution to simulate marine and bridge deck environments. Epoxy-coated bars with no damage as well as bars with 1% and 2% damage to the coating were embedded in the concrete slabs. After two years of monitoring, the results showed that epoxy-coated bars, even with damaged coatings, provided excellent performance as a corrosion protection system in corrosive environment, even with damage. Overall, the epoxy-coated reinforcing steel bars significantly contribute to the service life improvement of structures that exposed to corrosive environment.

1.5.2 Stainless Steel

Stainless steels are steel alloys that contain at least 10.5 percent chromium (ASTM A955-14). Stainless steel is well known for its corrosion resistance due to the high chromium content, which forms a thin protective layer on the surface of the steel. Activation of this protective layer (passive layer) can be accelerated by washing the steel in an acid solution bath to oxidize the surface of the metal, a process known as pickling. Stainless steels are classified as martensitic, austenitic, ferritic, or duplex depending on their grain structure. Several types of stainless steel have been used as reinforcement, such as 405 (12% chromium, 0.5% nickel), 430 (17% chromium, 0.75% nickel), 304 (18% chromium, 8% nickel), 316 (17% chromium, 12% nickel) and 316 LN (16% chromium, 10% nickel) as well as three types of duplex stainless steel, 2101 (21% chromium, 1% nickel), 2205 (22% chromium, 5% nickel) and 2304 (23% chromium, 4% nickel).

Stainless steel has shown very good performance in concrete. Zoob et al. (1985) tested 304 solid stainless steel as well as conventional reinforcing bars. The reinforcing steel samples were embedded in concrete slabs exposed to high chloride concentrations by using alternating cycles (4 days wet and 3 days dry) of elevated temperature and exposure to a 15 percent sodium chloride

solution for a total of 48 weeks. The macrocell corrosion current between the anode and cathode was measured for both stainless steel and conventional steel bars to monitor corrosion activity. Slabs reinforced with conventional bars exhibited cracks during the test. The results showed that the corrosion threshold of stainless steel was 7 to 10 times that of conventional steel (Zoob et al. 1985).

Treadaway et al. (1989) evaluated Type 405 and 430 ferritic stainless steel reinforcement as well as Type 316 austenitic stainless steel reinforcement; reinforcing bars were also tested. Concrete containing 0.96% and 3.2% chlorides added by weight of cement was used during the tests, results showed that the concrete specimens containing austenitic stainless steel reinforcement exhibited no cracking after 10 years of exposure. Types 405 and 430 ferritic stainless steel reinforcement presented substantial pitting when embedded in concrete with 0.96% chloride by weight of cement. At lower chloride contents, however, ferritic stainless steel performed better in delayed cracking time than conventional bars. The austenitic stainless steels provided very high corrosion resistance, even in the concrete with 3.2% chlorides by weight of cement, while the specimens that reinforced with conventional bars exhibited cracking after less than six months of testing (Treadaway et al. 1989).

Srensen et al. (1990) investigated conventional steel and Type 304 and 316 stainless steel bars. The samples were cast into concrete with admixed chloride Results showed that the threshold for stainless steel reinforcing was 10 times higher than that of conventional steel. They also found that the critical chloride content by weight of cement was 0.5% of admixed chloride for conventional bar, 5 % to 8% for Type 304 stainless steel, and greater than 8% for Type 316 stainless steel. Rasheeduzzafar et al. (1992) also tested stainless steel and conventional reinforcing steel and found that concrete specimens with stainless steel containing 19.2 kg/m^3 (32.4 lb/yd^3) of

admixed chloride ions exhibited no sign of corrosion or cracking of the concrete over a test period of 7 years.

McDonald et al. (1995) reviewed several studies and concluded that all the field and laboratory data for testing stainless steels showed that stainless steel reinforcing bars presented excellent corrosion resistance in very high chloride content environments, whether inside concrete or from outside chloride exposure during storage in the field.

Duplex stainless steels have become widely used as alternatives to austenitic stainless steels due to their higher mechanical strength, good corrosion performance, and lower alloying costs (Chen et al. 2012, Tan et al. 2012). Balma et al. (2005) tested Type 2101 and 2205 duplex steels, using the rapid macrocell test and bars cast in concrete (Southern Exposure and cracked beam tests, referred to as bench-scale tests). Bars were tested in both the pickled and unpickled condition. Results showed that the duplex steels exhibited corrosion losses between 0.3% and 1.8% of the corrosion losses for conventional steel with, 2205 duplex steel exhibiting better performance than Type 2101 steel during tests. The pickled bars presented lower rate of corrosion than that of unpickled bars for the same type of steel (Balma et al. 2005).

Ji (2005) tested pickled and unpicled 2101 and 2205 duplex steel, using rapid macrocell tests, corrosion potential tests, bench-scale tests, and two modified versions of the Southern Exposure test to determine the critical chloride threshold. The results showed that the duplex steel performed significantly better than conventional steel. The results also showed that the corrosion resistance of duplex steels depends on the ratio of chromium (Cr) to nickel (Ni) in the steel and whether the bars are pickled or unpickled. The corrosion performance of the 2205 steel (22% chromium and 5% nickel) was better than that of 2101 steel (21% chromium and 1% nickel) when evaluated in the same condition. Also, pickled bars exhibited corrosion resistance higher than

unpickled bars, and pickled 2101 steel performed better than unpickled 2205 steel (Ji 2005). Duarte et al. (2014) evaluated the electrochemical behavior of austenitic (304 and 316) and duplex (2205 and 2304) stainless steels when embedded in concrete specimens exposed to solutions containing high concentration of chloride periodically, simulating the condition found in sea water environments. The result showed that the austenitic 316 stainless steel was more resistant to corrosion than others. The duplex steel Type 2304 showed the lowest corrosion resistance compared with the others during the test period (Duarte et al. 2014). Another study by Alvarez et al. (2011) tested duplex 2304 steel in eight alkaline solutions (carbonated and non-carbonated, saturated $Ca(OH)_2$ solutions with different chloride contents), and the results of the investigation compared to those of austenitic 304 and duplex 2205 tested under similar conditions. The final results showed that the duplex 2304 presented better corrosion behavior than the 304, but less than that of the 2205 duplex in simulated concrete solutions (Alvarez et al. 2011).

A study by Lafikes et al. (2011) tested different type of steels, including Type 2304 stainless steel using rapid macroceel and bench-scale tests. The rapid macroceel test results showed that Type 2304 stainless steel exhibited an average corrosion rate below 0.25 μm/yr, but the corrosion rate of individual specimens exceeded 0.50 μm/yr. The 2304 stainless steel was re-pickled; the re-pickled 2304 stainless steel exhibited not more 0.25 μm/yr for average corrosion rate and below 0.50 μm/yr for individual specimens' corrosion rate. The bench-scale test results showed that the duplex 2304 steel satisfied the requirement of the ASTM A955 for maximum allowable corrosion rate. Overall, the duplex 2304 steel showed significant increase in corrosion resistance when compared to conventional steel (Lafikes et al. 2011).

O'Reilly et al. (2011) tested various types of reinforcing steel including 2205 stainless steel, using bench-scale tests. The results showed that the 2205 stainless steel reinforcement

exhibited excellent corrosion resistance in concrete containing high chloride concentration compared with its counterparts. Bridge deck reinforced with pickled 2205 stainless steel presented the longest design life of all corrosion protection system tested (O'Reilly et al. 2011).

When long-term corrosion resistance is required and the goal is achieving a longer service life, using stainless steel is often the optimum option to reach the requirements. The increase in overall cost due to using the stainless steel is considered to be reasonably low (McDonald et al. 1995).

1.5.3 Stainless Steel Clad Reinforcement

The use of solid stainless steel has been limited due to its high cost. Stainless steel clad bars have been used as a lower cost alternative to using solid stainless steel reinforcement (Head et al. 2015). The cladding of the stainless steel clad bars, however, can be damaged during shipping, handling or bending, and any cut or exposed ends must be protected before using the stainless steel clad bars as reinforcement.

Rasheeduzzafar et al. (1992) examined the performance of corrosion resistance of conventional, galvanized, Type 304 stainless clad conventional bars, and epoxy-coated steel embedded in concrete specimens containing 32.4 lb/yd3 (19.2 kg/m3) of admixed chlorides for seven years. The stainless steel clad reinforcement had the best performance of the bars evaluated. Upon completion of the tests (7 years), neither signs of cracking of the concrete or corrosion were observed on any of the stainless steel bars. The chloride threshold was estimated to be 24 times the corrosion threshold of conventional reinforcement (Rasheeduzzafar et al. 1992). Clemeña (2004) compared the corrosion performance of a bar cladded with stainless steel 316L with a solid 316LN stainless steel bar as well as with conventional reinforcement. The steel samples were

embedded in concrete blocks subjected to alternating ponding with a saturated salt solution and drying cycles over the test period. After three years of embedment in concrete, results showed that clad bars exhibited protection against corrosion no less important than that exhibited by the solid 316LN stainless steel bars. Darwin et al. (1999) compared the performance of 304 stainless steel clad reinforcing bars with that of conventional reinforcement. The No. 6 [No. 19] bars were tested using rapid corrosion potential and macrocell tests, which were carried out in two phases. In the first phase, bare reinforcing steel was tested; in the second phase, reinforcement encased in mortar was tested. Results showed that intact cladding significantly improved the performance of corrosion as long as the mild steel core of the clad bars were kept isolated from chlorides. For bare bars of clad reinforcement, corrosion rate ranged from 0 to 0.3 μm/yr, about 1/100 of that for conventional reinforcement. For bars encased in mortar, corrosion rate ranged from 0 to 0.2 μm/yr, averaging about 1/20 to 1/50 of the value observed for conventional bars. Another study by Kahrs et al. (2001) evaluated 304 stainless steel clad reinforcing bars (damaged and undamaged) and conventional reinforcing steel following the same test process followed by Darwin et al. (1999). The cut ends of stainless steel clad bars were protected with epoxy or with a sealed. The undamaged bars exhibited approximately the same results showed by Darwin et al. (1999); the bars with holes drilled through the cladding exhibited corrosion rate ranged from 0.0 to 0.75 μm/yr, averaging about 1/70 of that observed for conventional reinforcement. The results also showed that epoxy coating applied to the ends of bars will not provide protection to the mild steel core of the clad bars because the stainless steel clad bars were coated with epoxy exhibited corrosion rate similar to that of conventional reinforcing bars. Therefore, caps filled with epoxy or other techniques should be used to seal the ends of clad bars (Kahrs et al. 2001).

Cross et al. (2001) found that the lack of metallurgical bond between the mild steel core and cladding could lead to voids at the core-cladding interface, which in turn results in premature cracking of the cladding and reduces the resistance of the material against corrosion.

Clemena & Virmani (2002) compared the behavior of clad bars, three solid stainless steel (316LN, 304, and 2205) bars, and conventional steel bars. The steel samples were embedded in concrete blocks exposed to alternating ponding with a saturated salt solution and drying cycles over the test period. The clad bars and the three solid stainless steel bars exhibited virtually the same excellent resistance to corrosion even after 700 days, while signs of corrosion were observed on the traditional steel only after 90 days of exposure. The chloride threshold of the clad bars and stainless steel bars was estimated to be at least 15 times more than the chloride threshold of the conventional steel (Clemena & Virmani 2002).

Gong et al. (2006) compared the corrosion performance of 316 LN stainless steel clad reinforcement and multiple corrosion protection systems (specimens with more than one corrosion resistant system, such as epoxy-coated reinforcement and Multiple coated reinforcement with a zinc layer underlying the epoxy), using conventional steel and conventional epoxy-coated steel as control systems. Macrocell and bench-scale tests were used for monitoring corrosion activity. The results found very good performance for stainless steel clad bars with intact cladding. The stainless steel clad bars exhibited average corrosion loss ranging from 0.1% to 3% of that for conventional steel and 2.5% to 100% of that for conventional epoxy-coated reinforcement (Gong et al. 2006).

1.5.4 MMFX Reinforcing Steel

Microcomposite steel (MMFX) was first introduced in North America by MMFX Steel Corporation of America as an economic option of reinforcing steel that provides combination of a high performance of corrosion resistance along with high strength resulting from its ferritic-martensitic microstructure (Kahl 2007). MMFX steel is less expensive than stainless steel because it has a lower chromium content (4% or 9% chromium).

The first use of MMFX steel was in Iowa, in 2001 in a bridge over South Beaver Creek. The bridge deck of the eastbound lane of the structure was constructed with MMFX bars while the westbound lane was reinforced with conventional epoxy-coated reinforcement. Corrosion activity was monitored for 3 years by using reference electrodes that were installed throughout the bridge. The results of monitoring after 3 months showed initial corrosion current of the epoxy-coated reinforcing steel to be six times higher than that of the MMFX reinforcement (Phares et al. 2006). The epoxy-coated bars may had a higher initial corrosion due to defects in the coating surface of the epoxy-coated steel (Phares et al. 2006). In the laboratory, Phares et al. (2006) also investigated the corrosion performance based on ASTM G109 and rapid macrocell accelerated corrosion tests. The test results showed that, after 40 weeks, initiation of corrosion had not occurred on either the MMFX or the undamaged epoxy-coated reinforcement. Uncoated reinforcing steel, however, exhibited initiation of corrosion within the fifth week, while epoxy-coated reinforcement with induced defects initiated corrosion between 15 and 30 weeks (Phares et al. 2006).

Gong et al. (2003) compared the performance of MMFX reinforcing steel with that of epoxy-coated and uncoated conventional reinforcement. The rapid macrocell test and two bench-scale techniques, Southern Exposure and cracked beam tests, were used. The results showed that MMFX bars exhibited higher corrosion resistance than conventional bars, but lower than that of

epoxy-coated reinforcing steel. Gong et al. (2003) recommended MMFX reinforcement should not be used as alternative to epoxy-coated reinforcing steel unless it is used with a supplementary corrosion protection system.

Darwin et al. (2002) evaluated corrosion resistance, mechanical properties, applicability for structural applications, life expectancy, and cost effectiveness of MMFX bars. Corrosion performance was evaluated using rapid macrocell, Southern Exposure, and cracked beam tests. The MMFX steel exhibited corrosion rate between one-third and two-thirds that of conventional bars; however, it exhibited lower corrosion resistance compared to epoxy-coated reinforcement. The time between construction and the first repair required was estimated to be 30 years for bridge decks containing MMFX microcomposite reinforcing steel, compared to 10 to 25 years for bridge decks containing conventional steel and 30 to 40 years for bridge decks containing epoxy-coated reinforcement. These results also showed that MMFX reinforcing steel is not cost effective compared to epoxy-coated reinforcement (Darwin et al. 2002)

A study by Clemeña (2003) evaluated seven types of reinforcing steel; 304 stainless steel, 316LN stainless steel, 316L stainless steel-clad carbon steel bars, MMFX bars, 2101LDX duplex stainless steel, dual-coated bars (conventional bars coated with a 2-mil layer of zinc followed by a layer of epoxy), and conventional reinforcing bars. These samples were embedded in concrete blocks and exposed to weekly wet dry cycles of a saturated salt solution. The results showed that the MMFX bars exhibited better corrosion resistance than that of 2101 LDX, but less corrosion resistance than that of the other bars tested. (Clemeña 2003).

Balma et al. (2005) compared MMFX bars with conventional reinforcement, using rapid macrocell, Southern Exposure, and cracked beam tests. Results showed that MMFX bars had corrosion losses ranging from 26% to 60% of the corrosion losses of conventional steel. Results

also showed that the chloride corrosion threshold of the MMFX steel was higher than that of the conventional bars. On average, conventional steel initiated corrosion at week 11, but MMFX bars initiated corrosion at week 25 (Balma et al. 2005). A study by Ji et al. (2005) showed that the corrosion resistance of MMFX reinforcing steel was higher than the corrosion resistance of conventional bars, with corrosion losses of MMFX steel ranging between 16% and 66% of the value of conventional reinforcing bars. Results also showed the chloride threshold of the MMFX bars to be four times that of conventional reinforcing steel (Ji et al. 2005).

Kahl (2007) evaluated the corrosion performance of MMFX reinforcement, using No. 6 bar specimens were directly exposed to 3.5 percent salt solution, and #4 bar samples were embedded in ten concrete blocks, and exposed to 3.5 percent by weight salt solution (NaCl) in water by using alternating cycles (wet/dry cycling), to simulate a severe corrosion environment. The results showed that MMFX bars exhibited greater corrosion resistance than epoxy-coated steel. Based on the life cycle cost analysis of the study, the use of MMFX bars will provide an estimated additional 12 years of service life over epoxy-coated steel.

1.5.5 Zinc Coated (Galvanized) Reinforcement

Zinc coating is another technique has been used to protect reinforcing steel from corrosion since the 1930s. Zinc coating, like an epoxy-coating, provides protection to the underlying steel by acting as a barrier to moisture, oxygen, and chloride ions. Moreover, zinc provides cathodic protection to the underlying steel even when there is damage in the coating by acting as a sacrificial anode, which corrodes preferentially to exposed steel (Jones 1996).

Due to the highly alkaline environment of the pore solution in concrete (pH between 12.2 and 13.3) zinc is oxidized forming a calcium zincate salt (calcium hydroxyzincate), and the

cathodic reaction leads to form hydrogen gas on the galvanized surface [Eq. (1.11) and Eq. (1.12)] (Figueira et al. 2015):

$$2H^+ + 2e^- \rightarrow H_2 \uparrow \quad (1.11)$$

$$Zn + 2H_2O \rightarrow Zn(OH)_2 + H_2 \uparrow \quad (1.12)$$

The formation of calcium hydroxyzincate creates a barrier layer protecting the underlying steel from corrosion. This layer is stable in pH levels between 6 and 13 (Maslehuddin et al. 1994, Yeomans 2004). In environment with pH above 13.3, calcium hydroxyzincate forms large isolated crystals that cannot protect the underlying steel from corrosion (Andrade & Macias 1988). Hydrogen gas produced in the cathodic reaction also has a negative effect on the passive layer by increasing the permeability of the surrounding concrete. Therefore, ASTM A767/A767M-16 requires galvanized reinforcing steel to be treated by chromate to inhibit the evolution of hydrogen and protect the zinc coating layer in highly alkaline environments (Andrade & Macias, 1988). With the presence of chlorides in concrete, the passive layer of calcium hydroxyzincate will be broken down in a manner similar to that of iron. This passive layer can also be destroyed due to the carbonation process of concrete which in turn produces amorphous products of $ZnCO_3$ and $Zn_5(CO_3)_2(OH)_6$, which have limited properties of passivating (Roventi et al. 2014).

Hot-dip galvanization is the most common method used for applying zinc on the surface of steel. The hot-dip process immerses the steel in a bath of molten zinc at a controlled temperature between 840 and 850 ˚F, forming a metallurgical bond between the underlying steel and zinc coating (Hamad and Mike 2005). The adhesion of the zinc coating to steel surface is at least ten times greater than that of any other coatings, such as powder coatings, paints, and electroplated coatings. This characteristic has been made the zinc coating to resist abrasion and damage due to

shipment, storage process, and concrete placement. It also allows galvanized reinforcing steel bars to be fabricated and bended without damage the zinc coating (Yeomans 2004).

Many studies have examined the effectiveness of zinc coating in protecting reinforcing steel from corrosion, with mixed results. Research by Treadaway and Davies (1989) found that galvanized bars embedded in concrete slabs subjected to accelerate testing for five years demonstrated more cracking than slabs cast with conventional reinforcement. A study by (Saraswathy & Song 2005) examined the corrosion protection performance of four types of galvanized bars in accordance with ASTM G109-07 and found that only one type of galvanized bars presented better corrosion resistance than conventional bars. Conversely, Haran et al. (2000) showed that, although the zinc layer of galvanized rebar corroded heavily in the presence of chlorides, corrosion protection was provided to the underlying reinforcing steel. Hime and Machin (1993) found that the zinc coating of galvanized reinforcing steel embedded in concrete exposed to high concentration of chlorides forms crystallites of zinc hydroxychloride II ($Zn_5[OH]_8Cl_2.H_2O$) as a product of the corrosion process. These crystallites increase in volume to 3 1/2 times the volume of the original zinc and expand even more than iron corrosion products due to presence of voids between the crystallites. Based on these results, if ($Zn_5[OH]_8Cl_2.H_2O$) is formed, galvanized bars can cause cracking in concrete when used as reinforcement (Hime & Machin 1993).

Darwin et al. (2009) found that the critical chloride threshold of concrete specimens with zinc bars, 2.57 lb/yd^3 (1.52 kg/m^3), was 1.6 times greater than the critical chloride threshold exhibited by concrete specimens with conventional reinforcement (1.63 lb/yd^3 (0.97 kg/m^3)). O'Reilly et al. (2011) calculated the corrosion loss of galvanized and conventional reinforcement required to crack concrete with 0.5, 1, and 2 in. concrete cover. For galvanized steel, the required corrosion loss was estimated to be four times more than that of conventional steel in specimens

with 0.5 in. concrete cover, and two times more than that of conventional steel for specimens with 1 in. and 2 in. concrete cover. Farshadfar (2017) compared the corrosion performance of conventional bare and epoxy-coated reinforcement with alternative forms of reinforcement including galvanized steel, MMFX steel, and epoxy-coated MMFX reinforcement, using bench-scale specimens (Southern Exposure, cracked beam, and beam specimens) and rapid macrocell tests. The results showed that the galvanized steel bars required corrosion loss over twice and time to crack concrete almost four times longer compared to specimens with conventional reinforcement.

1.5.5.1 Dual-Coated Reinforcement

Dual-coated steel reinforcing bars are used as another method of corrosion resistance. Dual-coated bars are zinc-coated bars covered with a layer of epoxy coating to provide a barrier and sacrificial protection against corrosion (Frosch et al., 2014). Dual-coated reinforcement is governed by ASTM A1055. O'Reilly et al. (2011) compared the performance of dual-coated reinforcement to that of conventional epoxy-coated reinforcement, using rapid macrocell, bench-scale, and field tests. Results showed that dual-coated reinforcement exhibited greater corrosion losses than conventional epoxy-coated reinforcement in bench-scale and rapid macrocell specimens, but comparable performance in field test specimens. This was expected because the zinc layer provides cathodic protection to the underlying steel by acting as a sacrificial anode. Dual-coated reinforcement exhibited less disbondment compared to conventional epoxy-coated reinforcement (O'Reilly et al. 2011). Another study by Gong et al. (2006) also compared the performance of dual-coated reinforcement to that of conventional epoxy-coated reinforcement, using rapid macrocell and bench-scale tests. Same dual-coated bars were damaged by penetrating

only the epoxy, while the others of them were damaged by penetrating both the epoxy and zinc coating layers. Results showed that dual-coated reinforcement with only the epoxy penetrated exhibited 23 to 231% of that for conventional epoxy-coated steel. Dual-coated reinforcement with both layers penetrated exhibited average corrosion loss 13 to 455% of that for conventional epoxy-coated steel (Gong et al. 2006).

1.6 OBJECTIVES AND SCOPE

The purpose of this study is to determine the corrosion resistance of reinforcing steel in concrete, focusing on the effect of pH level of the pore solution. The following systems are included in this study:

1. Dual-coated steel reinforcement – epoxy-coated reinforcement with a 2-mil (0.05-mm) thick coating consisting of 98% zinc and 2% aluminum underneath the epoxy coating.
2. 2304 duplex stainless steel reinforcement containing 23% chromium and 4% nickel.
3. Stainless steel-clad carbon reinforcing bar using 304 stainless steel as the cladding.
4. MMFX Microcomposite reinforcing bar containing 9% chromium.
5. Galvanized reinforcement, average thickness 6 mil (0.150 mm), without a chromate treatment.

The performance of the corrosion protection systems is evaluated using rapid macrocell test, as described in Chapter 2. Corrosion activity is monitored (as described in Chapter 2) using measurements taken during rapid macrocell testing including macrocell voltage drop, corrosion potential, and linear polarization resistance.

CHAPTER 2: EXPERIMENTAL WORK

2.1 GENERAL

This chapter describes the equipment, materials, and procedures used to prepare and fabricate specimens for corrosion testing, as well as the electrochemical tests performed to monitor and record corrosion behavior. The rapid macrocell test is used to evaluate corrosion protection systems in a pore solution simulating the conditions found in concrete, focusing on the effect of pH level of the pore solution. Two different simulated concrete pore solutions (with pH values of 13.9 and 13.5) are used during the test to evaluate the influence of the pH of concrete pore solution on the corrosion resistance of reinforcing bars.

2.2 CORROSION PROTECTION SYSTEMS (Reinforcement)

The reinforcing bars tested in this study are listed below:

2304 – 2304 duplex stainless steel reinforcement containing 23% chromium and 4% nickel.

304 SSC – Stainless steel-clad carbon reinforcing bar using 304 stainless steel as the cladding material.

MMFX –Microcomposite reinforcing bar containing 9% chromium (ASTM A1035 Type CS).

Zn – Galvanized reinforcement, average thickness 6 mil (0.150 mm), without a chromate treatment.

DC – Dual-coated steel reinforcing bars; epoxy-coated reinforcement with a 2-mil (0.05-mm) thick layer consisting of 98% zinc and 2% aluminum underneath the epoxy coating.

2.3 RAPID MACROCELL TEST

2.3.1 Description

The rapid macrocell test is used for monitoring the corrosion performance of the corrosion protection systems (reinforcement) in a simulated concrete pore solution by measuring the macrocell corrosion rates and corrosion potentials of the reinforcing bar. The rapid macrocell test was first developed at the University of Kansas and is described in Annex A2 of ASTM A955. This test allows the reinforcing bars to be directly exposed to chloride ions to accelerate the corrosion process. The rapid macrocell test system is shown in Figure 2.1. The rapid macrocell system is composed of two containers. One container contains a single 5-in. (127-mm) long No. 5 (No. 16) reinforcing bar, which represents the anode, in a simulated concrete pore and salt solution at a depth of 3 in. (76 mm). The other container consists of two 5-in. (127-mm) long No. 5 (No. 16) reinforcing bars, which represent the cathode in a simulated pore solution at a depth of 3 in. (76 mm). In this system, the anode and cathode are both connected by electrical and ionic connection. Air, scrubbed to eliminate any CO_2, is bubbled into the pore solution surrounding the cathode to provide an adequate supply of oxygen. In the present study, two different pore solutions are used with pH values of 13.5 and 13.9. The test duration is 15 weeks; each pore solution is changed every 5 weeks to maintain the pH.

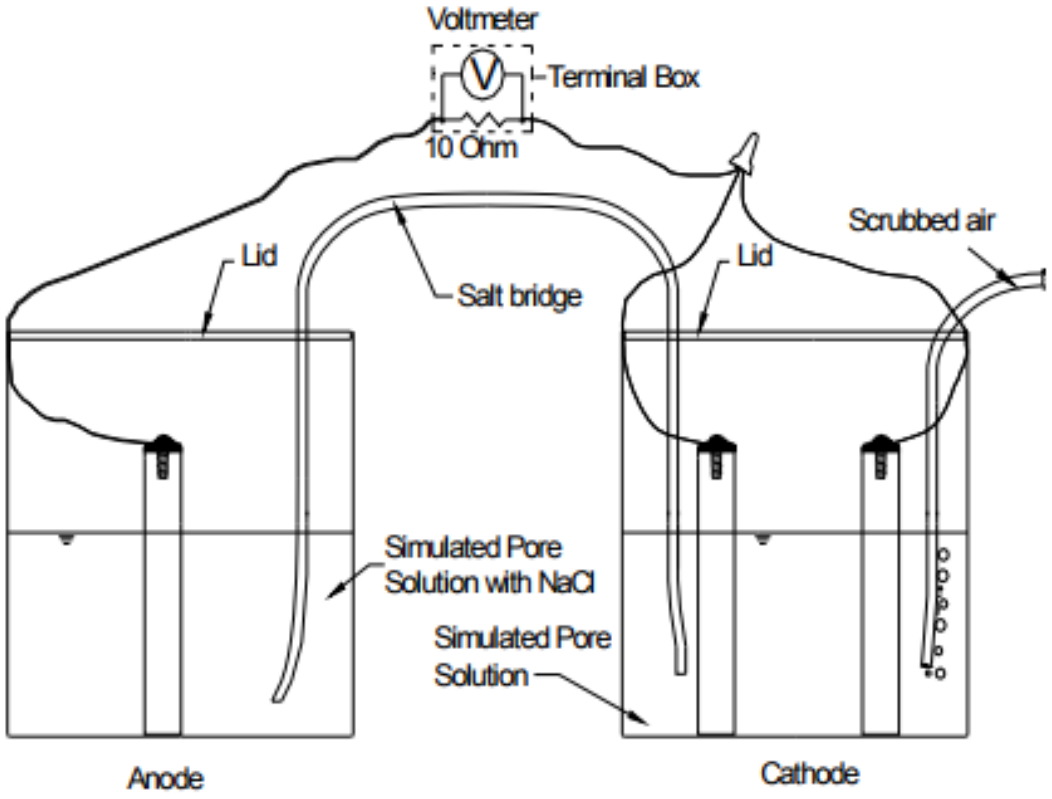

Figure 2.1: Rapid macrocell test system

2.3.2 Materials and Equipment

Materials and equipment needed for the rapid macrocell test are listed below:

Wire – Electrical connections from the cathode and anode bars to the terminal box are made with 16 gauge multi-strand copper wire.

Terminal Box – The terminal box provides an electrical connection between the single bar of the anode and the two bars of the cathode and simplifies corrosion measurements. Each macrocell specimen has its own station on the terminal box, consisting of a red binding post and a black binding post connected across a 10-ohm resistor and a single throw switch. The single reinforcing bar of the anode is connected to the red binding post and the two reinforcing bars of the cathode are connected to the black binding post. The voltage drop

across the 10-ohm resistor can be easily measured and used to determine macrocell corrosion rate, as described in Section 2.3.5.1. The switch is used for disconnecting the circuit to allow measurements of corrosion potential and linear polarization resistance.

Voltmeter – The voltmeter is used to obtain the macrocell voltage drop across the resistor in the test specimens and corrosion potential measurements. The voltmeter used for this study was a Keithley model 2182A nanovoltmeter.

Reference Electrode – the reference electrode is used together with the voltmeter to obtain corrosion potential measurements. A saturated calomel electrode (SCE) was used for rapid macrocell readings in the current study.

Caps – Vinyl caps with an internal diameter of 0.627 in. (16 mm) and a height of 0.5 in. (13 mm) are used to protect the cut ends of dual-coated, galvanized and stainless steel-clad reinforcing bar samples from the salt solution.

Stainless Steel Screws/Washers – They are used to connect wire to the upper end of reinforcing bar specimens during testing.

Epoxy – The epoxy is used to protect the electrical connections at the upper end of the reinforcing bar and is also used to fix the vinyl caps at the lower end of the reinforcement.

Containers – 3.8-L (1-gal) high density polyethylene food storage containers are used to hold specimens in pore solution. Lids are fitted above the containers to minimize evaporation, and perforated to allow the salt bridge (ionic connection) pass through to be in contact with pore solution and facilitate the process of taking readings by the reference electrode.

Pore solution (standard) – Simulates the pore solution in concrete with a pH level of 13.9. One liter of standard pore solution consists of 18.81 g of potassium hydroxide (KOH) and 17.87 g of sodium hydroxide (NaOH) dissolved in 974.8 g of distilled water.

Pore Solution (standard) with Salt – Simulates pore solution with chloride contamination. In this study, a 6.04 molal ion (15%) NaCl solution is used, created by adding 172.1 g of NaCl to one liter of standard pore solution.

Pore solution (modified) – Simulates the pore solution in concrete with a pH level of 13.5. One liter of modified pore solution consists of 8.99 g of potassium hydroxide (KOH) and 7.45 g of sodium hydroxide (NaOH) dissolved in 982.9 g of distilled water.

Pore Solution (modified) with Salt – Simulates pore solution with chloride contamination. In this study, a 6.04 molal ion (15%) NaCl solution is used, created by adding 172.1 g of NaCl to one liter of modified pore solution.

Salt Bridge – The salt bridge is used to provide an ionic connection and allow ionic movement between the anode and cathode. The salt bridges consist of 4.5 g agar and 30 g potassium chloride dissolved in 100 g of distilled water and heated in a metal bowl over a hot plate until the solution begins to congeal. Then, 2-ft (0.61-m) long sections of vinyl tubing with an internal diameter of 0.25 in. (6.4 mm) and an external diameter of 0.375 in. (9.5 mm) are filled with the coagulated mixture. The ends of the tubing are tied into a teardrop form by using a rubber band. The bridges are then kept in boiling water for one hour to remove the bubbles formed inside the vinyl tubing within the coagulated mixture, with the cut ends facing up. The rubber bands are removed after cooling and the ends of the tubing a cut near the coagulated mixture such that continuous gel is exposed and able to be in contact with the pore solution. Bridges with internal voids are rejected.

Air Scrubber – The air scrubber is used to remove CO_2 from the air bubbled to the container holding the pore solution of the cathode in order to avoid carbonation of the solution and maintain the pH. To prepare the air scrubber, a 5-gal (19-L) airtight container is fitted with

a barbed fitting and vinyl tubing. Inside the container, a 6-ft (1.8-m) long section of perforated vinyl tubing is connected to the inner end of the barbed fitting and sealed from the other end. The outer end of this barbed tubing is connected to a compressed air supply; the perforated tubing is used to supply and bubble the air through a 1 N NaOH solution. The perforated vinyl tubing is kept coiled and weighted inside the container to keep the perforations submerged in the solution. Another barbed fitting, located above the level of the NaOH solution at the top of the container, is used as the air outlet to deliver air scrubbed of CO_2 to the macrocell specimens via vinyl tubing. Barbed plastic T-fittings with small C-clamps are used in order to distribute the air to multiple specimens and regulate flow of air to individual specimens. The 1 N NaOH solution in the 5-gal (19-L) container is changed as required.

2.3.3 Macrocell Container Setup

The containers for the rapid macrocell tests are installed as follows:

1. Two containers (buckets) are required for each macrocell specimen. One container is used to hold the anode bar in the pore solution with salt and the other one is used to hold the pore solution and the bars of the cathode. Lids are drilled such that the reinforcing bar samples, salt bridge, air scrubber line, and reference electrode are easily inserted into the solution. In order to avoid inadvertent chloride contamination on future tests, containers holding the pore solution with and without salt are labeled “Salt” and “Pore”, respectively.
2. The standard and modified pore solution with and without salt are prepared described in Section 2.3.2. These solutions are poured into the appropriate container to a depth of 3 in. (76 mm).

3. A salt bridge is inserted through the holes of the lids so that one of its ends is immersed in the anode pore solution and the other end is immersed in the cathode pore solution to provide an ionic connection between the anode and the cathode.
4. An air line from the scrubber is inserted into the bucket holding the cathode pore solution. The flow rate is regulated via small C-clamps to provide a moderate flow of air to the cathode.

2.3.4 Bar Fabrication

The fabrication of reinforcing bars for rapid macrocell specimens proceeds as follows:

1. Reinforcing bar samples are cut to a length of 5 in. (127 mm).
2. One end of each reinforcing bar sample is drilled and tapped to a depth of 0.75 in. (19 mm) using a 10-24 threading.
3. Dual-coated reinforcing bar samples are intentionally damaged with a total of four holes on each test bar, with two holes on each side placed 1 in. (25 mm) and 2 in. (51 mm) away from the untapped end of the reinforcing bar, using a 0.125 in. (3 mm) diameter four-flute drill bit. The intentional damages are made by penetrating the epoxy surface to a depth of 15 mils (0.4 mm) using a milling machine to expose the underlying steel to the pore solution of the anode and cathode. This damage simulates the damage incurred at a work site from shipment, placement and pouring concrete. The dual-coated reinforcing bar sample is intentionally damaged as shown in Figure 2.2.

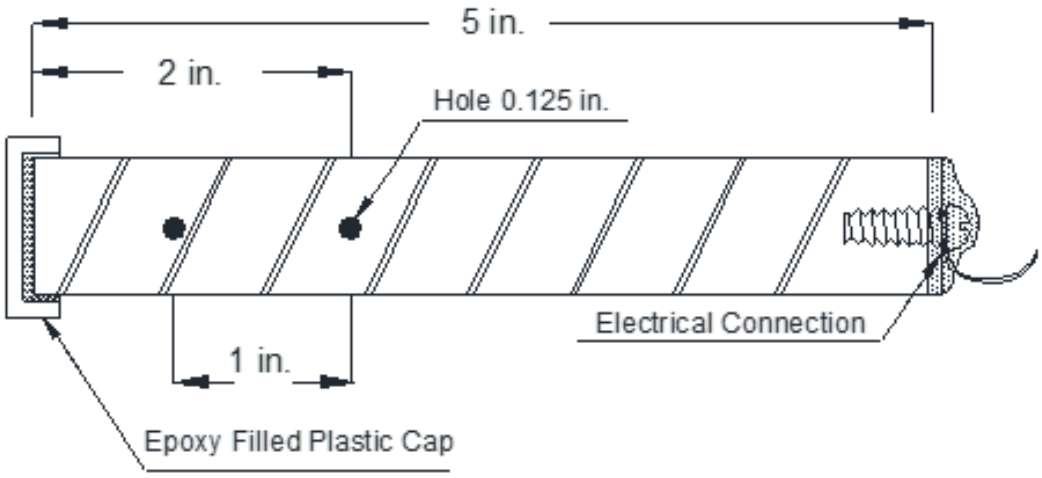

Figure 2.2: Intentionally damaged dual-coated reinforcing bar sample in rapid macrocell test (Farshadfar 2017)

4. Dual-coated reinforcing bar samples are cleaned using warm water with soap and then dried while the uncoated reinforcing bar samples are cleaned with acetone to remove any oils or impurities from the surface of the steel samples.
5. A 16-gauge insulated multi-strand copper wire is used for the electrical connection. One end of the wire is connected to the tapped end of each reinforcing bar sample using a 0.5 in. (13 mm) 10-24 stainless steel screw and a No. 10 stainless steel washer and the other end is connected to the appropriate binding post jack in the terminal box.
6. The electrical connection at the tapped ends of all reinforcing bar samples and all untapped cut ends of dual-coted, galvanized and stainless steel-clad reinforcements are coated with two layers of epoxy to protect them from corrosion. For coated or clad bars, the cut end is also sealed with epoxy and a vinyl cap.
7. A single test reinforcing bar is placed inside the container holding the pore solution with salt to represent the anode while two test reinforcing bars are placed inside the container holding the pore solution without salt to represent the cathode. The test bars are vertically

placed inside the containers and electrically connected to the appropriate binding post jack across a 10-ohm resistor via terminal box.

2.3.5 Rapid Macrocell Test Procedure

The rapid macrocell tests run for 15 weeks. The pore solutions for the anode and the cathode specimens are changed every five weeks to prevent carbonation caused by atmospheric CO_2. Measurements of macrocell corrosion rate and corrosion potential are taken daily for the first week and on a weekly basis thereafter. Linear polarization resistance readings are taken every three weeks just prior to the corrosion potential readings. These measurements are described in detail in 2.3.5.1.

2.3.5.1 Corrosion Monitoring and Measurements

The measurements taken during rapid macrocell testing are a macrocell voltage drop, corrosion potential, and linear polarization resistance. The voltage drop across the 10-ohm resistor is taken to measure macrocell corrosion rate. By measuring the voltage drop across the resistor connecting the anode and cathode, the current density between the anode and cathode can be calculated using Ohm's Law:

$$i_{\text{corr}} = 10^6 \times \frac{V}{RA} \tag{2.1}$$

where

i_{corr} = current density, µA/cm^2

V = measured voltage drop across resistor, volts

R = resistance, ohms

A = surface area of anode, cm^2

For the rapid macrocell test, R = 10 ohm and A = 6.197 $in.^2$.

The relationship between current density and corrosion rate is established using Faraday's Law:

$$r = k\frac{ia}{nF\rho} \tag{2.2}$$

where

r = corrosion rate, µm/year

k = conversion factor, $315360\frac{\mathrm{A}\cdot\mu\mathrm{m}\cdot\mathrm{s}}{\mu\mathrm{A}\cdot\mathrm{cm}\cdot\mathrm{yr}}$

i = current density, $\mu A/cm^2$

a = atomic weight of the corroding metal, g/mol

n = number of electrons lost per atom of metal oxidized

F = Faraday's constant, 96,485 Coulombs/equivalent

ρ = density of metal, g/cm^3

For iron, a = 55.85 g/mol, n = 2, and ρ = 7.87 g/cm^3. Eq. (2.2) simplifies to

$$R = 11.6i \tag{2.3}$$

For zinc, a = 65.38 g/mol, n = 2, and ρ = 7.13 g/cm^3. Eq. (2.2) simplifies to

$$R = 15.0i \tag{2.4}$$

Macrocell corrosion rate can only be measured and used in laboratory specimens where the anode and the cathode can be practically separated. This method, however, does not capture microcell corrosion, where the anode and the cathode are located on the same bar. To capture microcell corrosion, linear polarization resistance is used. Linear polarization resistance readings are taken every three weeks just prior to the corrosion potential readings.

Linear polarization resistance (LPR) is an electrochemical analysis used for determining the total corrosion rate (macrocell and microcell) of a bar by applying external voltage (polarization) to the bar and measuring the response of the bar to that applied voltage (polarization). When no external voltage is applied, the current density and potential of a metal during corrosion reaction will be i_{corr} and E_{corr}, respectively. Applying external voltage will shift the potential of the metal by an amount $\Delta\varepsilon$, which in turn shift the current by an amount Δi. The slope of the potential-current function is called the polarization resistance (R_p), as defined in Equation 2.5 (Jones 1996).

$$R_p = \left[\frac{\Delta\varepsilon}{\Delta i}\right]_{\varepsilon\to 0} \tag{2.5}$$

where

R_p = polarization resistance

$\Delta\varepsilon$ = imposed potential change

Δi = current density change caused by $\Delta\varepsilon$

The linear polarization resistance is inversely proportional to the corrosion current density

$$i_{corr} = \frac{B}{R_p} \tag{2.6}$$

Where, B is the Stern-Geary constant:

$$B = \frac{\beta_a\beta_c}{2.3(\beta_a + \beta_c)} \tag{2.7}$$

Eq. (2.6) then becomes:

$$i_{corr} = \frac{\beta_a\beta_c}{2.3R_p(\beta_a + \beta_c)} \tag{2.8}$$

Where

β_a, β_c = anodic and cathodic Tafel constants, V/decade

R_p = polarization resistance

The Stern-Geary constant will be equal to 0.026 V when anodic and cathodic Tafel constants (β_a, β_c) applied in Eq. (2.8) are set to 0.12 V/decade, as recommended for reinforcing steel in concrete by several studies (Lambert et al. 1991, McDonald et al. 1998). Eq. (2.8) then simplifies to:

$$i_{corr} = \frac{0.026}{R_p} \tag{2.9}$$

This form [Eq. (2.9)] is used to determine the current densities for all linear polarization resistance tests obtained in the current study. The total corrosion rate is then determined using Eq. 3.2 or 2.4.

After macrocell voltage drop readings are taken, the anode and cathode bar specimens are electrically disconnected via the switch at the terminal box for a minimum of two hours to allow the corrosion potentials of the anode and cathode specimens to stabilize. The corrosion potential measurements are then taken with respect to a saturated calomel electrode. The anode and cathode bars are then reconnected to allow corrosion to continue.

2.3.6 End of Life Autopsy

The following steps are taken after testing is completed:

1. The test bars are removed from the solutions and photographed to document any corrosion.
2. A disbondment test is performed to evaluate the integrity of the epoxy of the dual-coated reinforcement. This test is accomplished by using a sharp utility knife to make two cuts through the epoxy at a 45° angle with the axis of the bar at the sites of intentional damage,

forming the shape of an ‘X’. The knife tip is then used to attempt to remove the coating. Then, the area of disbondment and the distance, in four directions, from the center of the hole to the perimeter of the disbondment area are measured. If the area of the disbondment exceeds 1.05 in.^{2} (677 mm^2), the specimen is considered to have experienced total disbondment.

3. The capped specimens are checked for corrosion under the cap. If the area of the end cut of the specimen under the cap exhibits signs of corrosion, the results from that specimen are excluded from analysis.

CHAPTER 3: RESULTS AND DISCUSSION

3.1 GENERAL

In this chapter, the results of the corrosion performance of five types of reinforcing steel (2304 duplex stainless steel bar, 304 stainless steel clad bar, MMFX Microcomposite bar, galvanized bar, and dual-coated steel reinforcing bar) are presented and discussed.

The corrosion performance is evaluated using macrocell corrosion rate, corrosion potential, microcell corrosion rate (as measured by linear polarization resistance measurements (LPR)) corrosion loss (based on corrosion rates obtained from LPR test results), and a disbondment test, as discussed in Chapter 2.

3.2 TEST RESULTS

3.2.1 2304 Duplex Stainless Steel Bar

The average corrosion rates for 2304 duplex stainless steel reinforcement tested in standard and modified pore solutions (with pH levels of 13.9 and 13.5, respectively) are shown in Figure 3.1. Corrosion rates for individual specimens are shown in Appendix A. Although the specimens tested in the modified pore solution exhibit slightly higher corrosion rates than specimens tested in the standard pore solution during the period of the test. The specimens tested in the modified pore solution exhibit a peak corrosion rate of 0.65 µm/yr at week 5, whereas the peak corrosion rate exhibited by the specimens tested in the standard pore solution is 0.096 µm/yr at week 3.

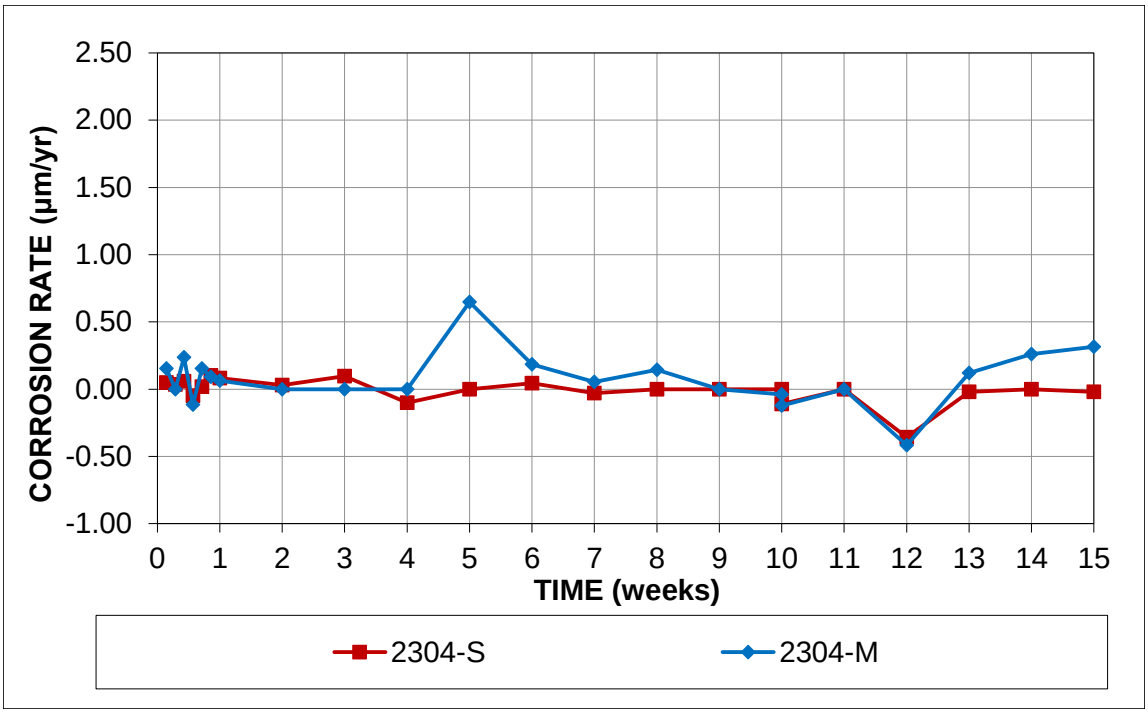

Figure 3.1: Rapid macrocell test. Average corrosion rates (µm/yr) of 2304 duplex stainless steel bar in standard (S) and modified (M) pore solutions

Figure 3.2 shows the average anode potentials, taken with respect to a saturated calomel electrode (SCE), for the 2304 duplex stainless steel specimens tested in standard and modified pore solutions. The anode and cathode potentials for individual specimens are shown in Appendix A. During the first week of testing, the corrosion potentials of the specimens tested in standard and modified pore solutions are comparable. After the first week, the specimens tested in the modified pore solution exhibit a less negative anode potential than the specimens tested in the standard pore solution during the period of the test. The average anode potentials for the specimens tested in the modified pore solution ranges between –0.108 V and –0.186 V, whereas the average anode potentials for the specimens tested in the standard pore solution ranges between –0.134 V and –0.183 V after the first week of testing.

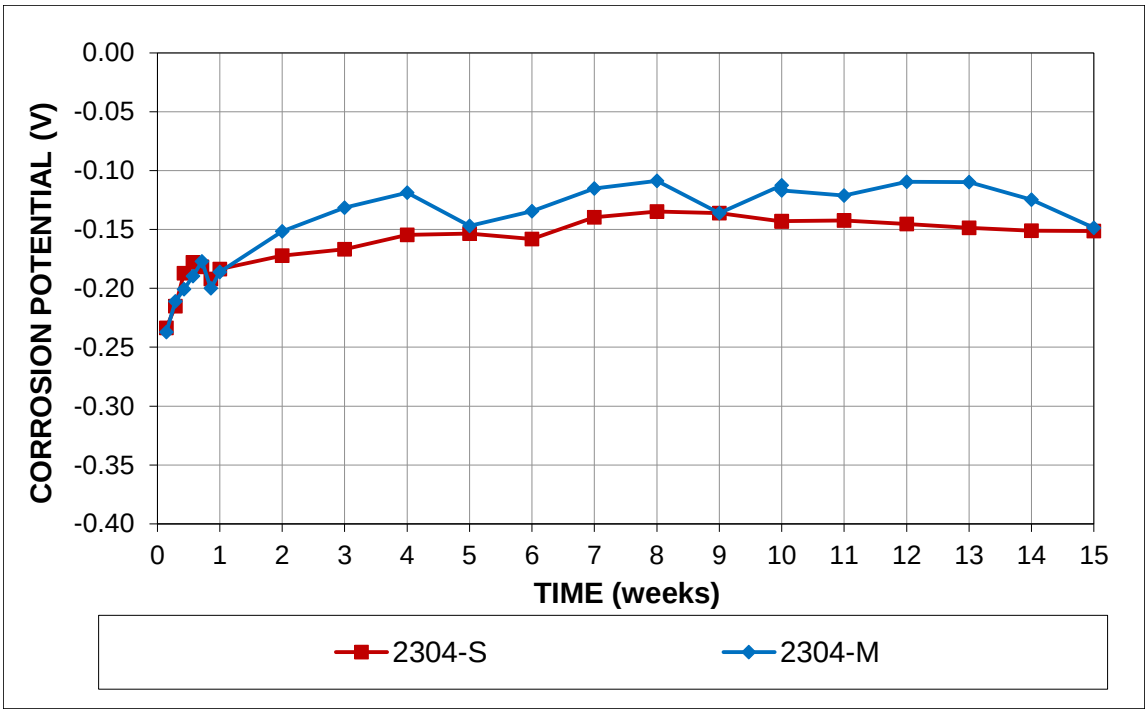

Figure 3.2: Rapid macrocell test. Average corrosion anode potentials (SCE) of 2304 duplex stainless steel bar in standard (S) and modified (M) pore solutions

The average corrosion rates obtained from LPR for the 2304 duplex stainless steel specimens are shown in Figure 3.3. The specimens tested in the modified pore solution exhibit a maximum average corrosion rate of 0.558 µm/yr at week 15. The specimens tested in the standard pore solution exhibit a maximum average corrosion rate of 0.155 µm/yr at the same week. A Student's T-test was performed to determine the statistical significance of the differences in corrosion rate in standard and modified pore solutions. For this study, a value of $p \leq 0.05$ is considered as the threshold for statistical significance. For 2304 duplex stainless steel bars, the difference in LPR corrosion rate between specimens tested in standard and modified pore solutions is not statistically significant ($p = 0.273$).

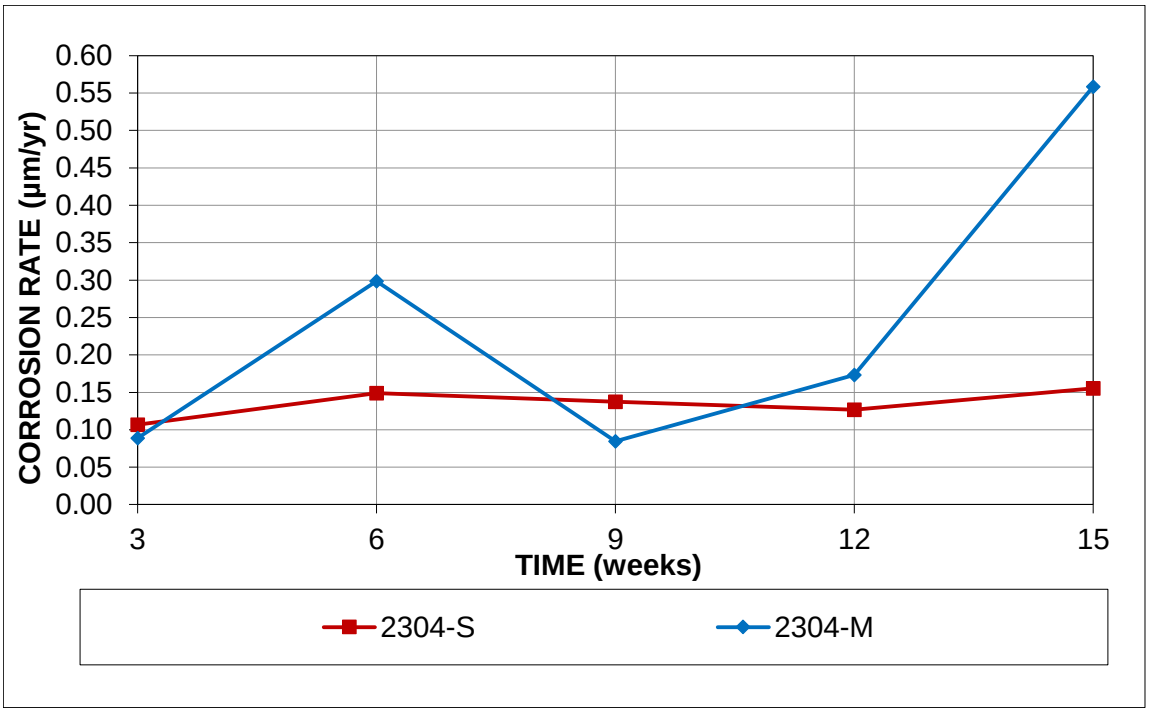

Figure 3.3: Rapid macrocell test. Average corrosion rates (µm/yr) of 2304 duplex stainless steel bar in standard (S) and modified (M) pore solutions from LPR test results

Figure 3.4 shows the average corrosion losses based on average corrosion rates obtained from LPR test results for the 2304 duplex stainless steel specimens. The specimens tested in the modified pore solution generally exhibit higher corrosion losses than specimens tested in the standard pore solution. The average corrosion loss of the specimens tested in the modified pore solution after 15 weeks is 0.070 µm, whereas the specimens tested in the standard pore solution exhibit lower average corrosion loss (0.040 µm). The difference in corrosion losses is not statistically significant (p = 0.229).

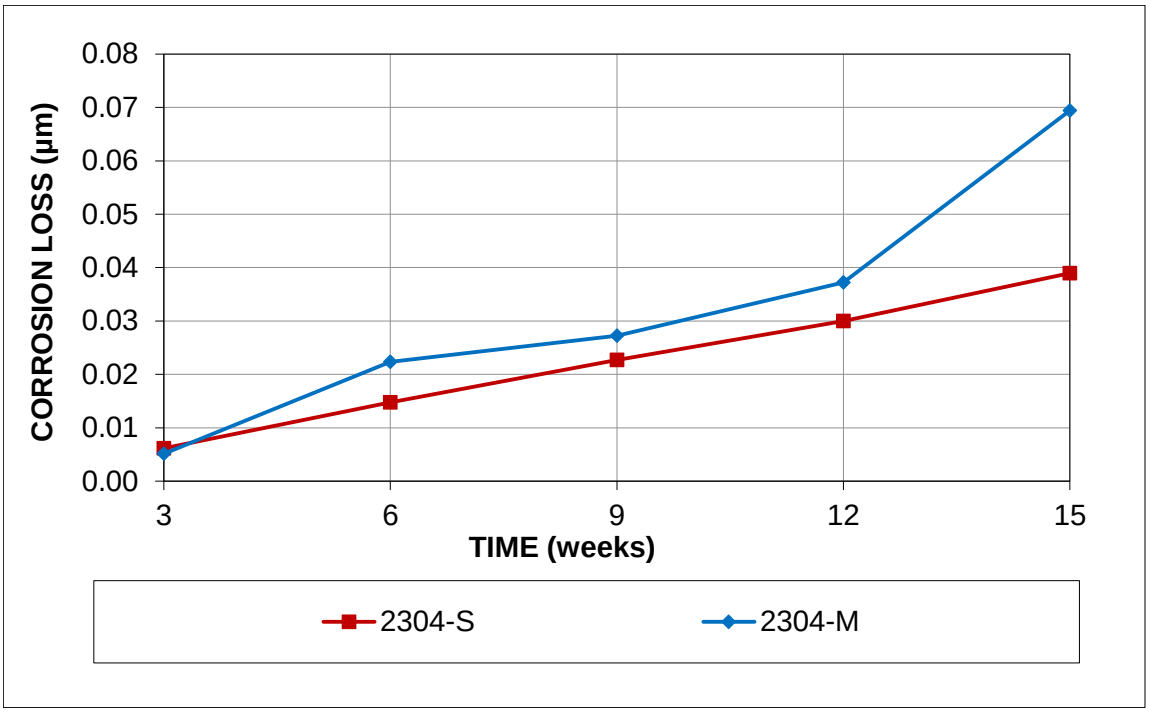

Figure 3.4: Rapid macrocell test. Average corrosion losses (µm) of 2304 duplex stainless steel bar in standard (S) and modified (M) pore solutions based on average corrosion rates obtained from LPR test results

After reaching the end of testing (15 weeks), all specimens were visually inspected and photographed. For 2304 stainless steel reinforcement, corrosion products were observed on some anode bars for specimens tested in standard pore solution (as shown in Figure 3.5 (a)). Corrosion products, however, were clearly visible on all bars for specimens tested in modified pore solution, as shown in Figure 3.6 (a). Representative cathode bars for specimens tested in standard and modified pore solution are shown in Figure 3.5 (b) and 3.6 (b) respectively. No cathode bars showed signs of corrosion.

(a)

(b)

Figure 3.5: Rapid macrocell test, anode bar (a) and cathode bars (b) of specimen 2304-4 in standard pore solution (S) after 15 weeks

(a)

(b)

Figure 3.6: Rapid macrocell test, anode bar (a) and cathode bars (b) of specimen 2304-4 in modified pore solution (M) after 15 weeks

3.2.2 304 Stainless Steel Clad Bar

The average corrosion rates for 304 stainless steel clad reinforcement tested in standard and modified pore solutions are shown in Figure 3.7. Corrosion rates for individual specimens are shown in Appendix A. The specimens tested in the modified pore solution exhibit lower corrosion rates than specimens tested in the standard pore solution during the first 9 weeks of testing. After week 9, the specimens tested in the modified pore solution generally present higher corrosion rates with a peak corrosion rate of 0.43 µm/yr at week 15, whereas the peak corrosion rate exhibited by the specimens tested in the standard pore solution is 0.11 µm/yr at the same week.

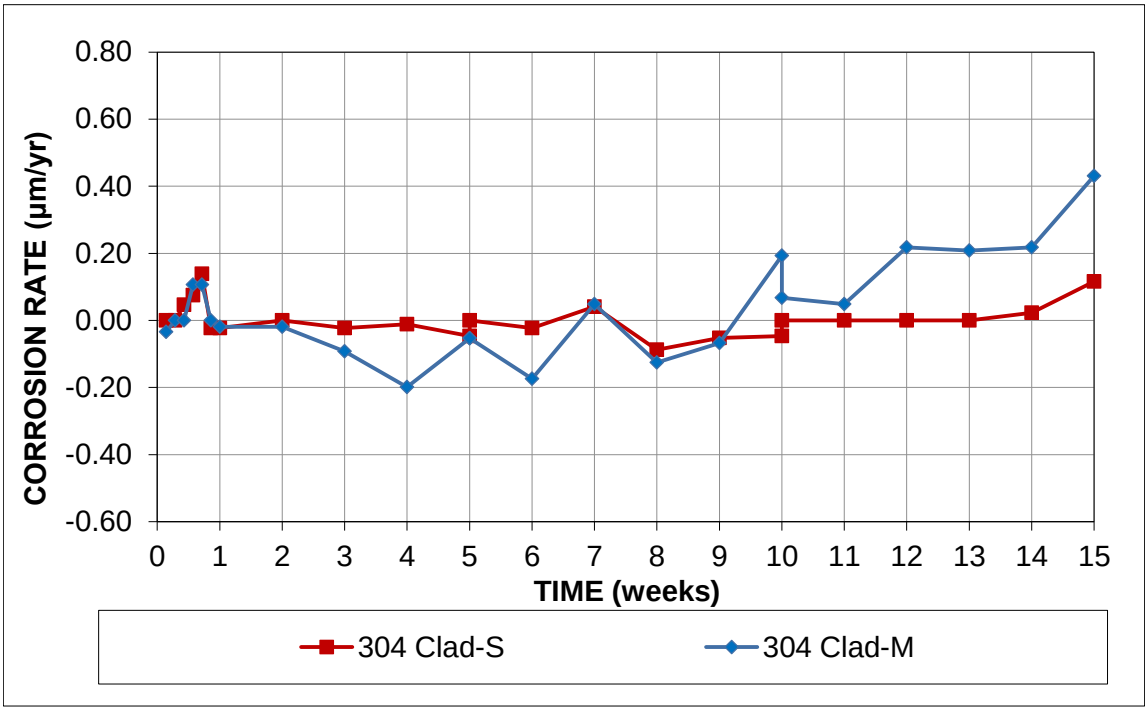

Figure 3.7: Rapid macrocell test. Average corrosion rates (µm/yr) of 304 stainless steel clad bar in standard (S) and modified (M) pore solutions

Figure 3.8 shows the average anode potentials, taken with respect to a saturated calomel electrode (SCE), for the 304 stainless steel clad bar specimens tested in standard and modified pore solutions. The anode and cathode potentials for individual specimens are shown in

Appendix A. The specimens tested in the modified pore solution exhibit a less negative anode potential than the specimens tested in the standard pore solution. The average anode potentials for the specimens tested in the modified pore solution ranges between –0.149 V and –0.097 V, whereas the average anode potentials for the specimens tested in the standard pore solution ranges between –0.131 V and –0.169 V.

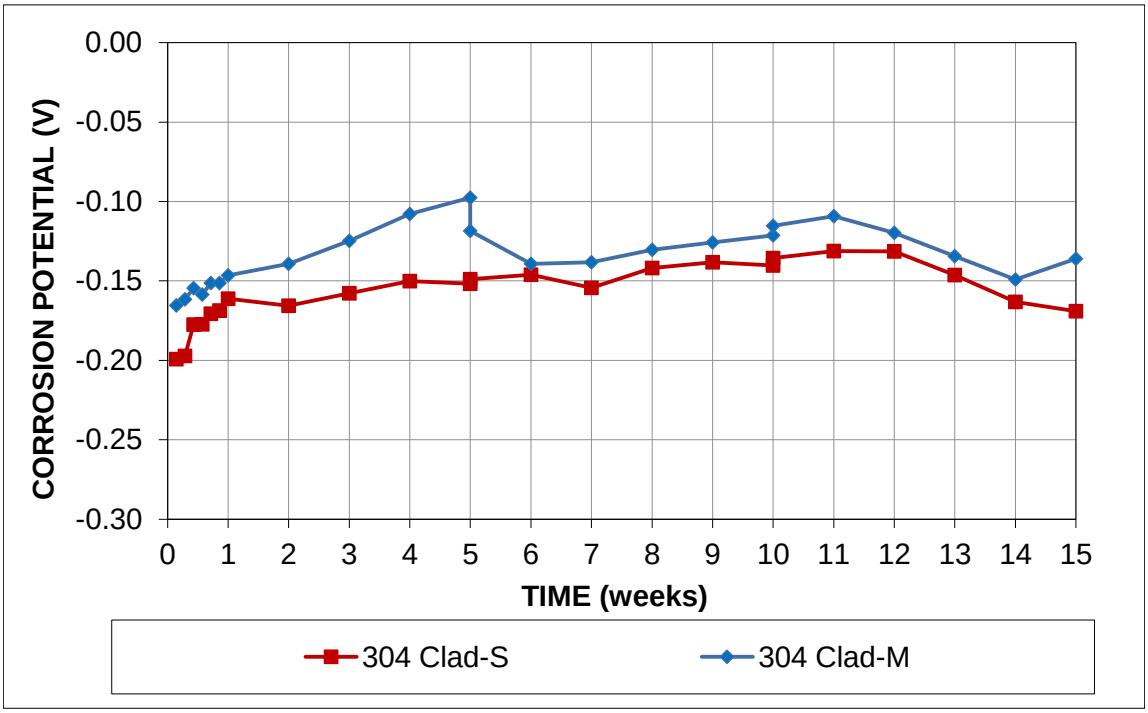

Figure 3.8: Rapid macrocell test. Average corrosion anode potentials (SCE) of 304 stainless steel clad bar in standard (S) and modified (M) pore solutions

The average corrosion rates obtained from LPR for the 304 stainless steel clad bar specimens are shown in Figure 3.9. The specimens tested in the standard pore solution generally exhibit higher corrosion rates than that of the specimens tested in the modified pore solution. However, the difference in LPR corrosion rate between specimens tested in standard and modified pore solutions is not statistically significant (p = 0.537). The specimens tested in standard pore

solution exhibit a peak of corrosion rate of 0.209 µm/yr at week 15, while the specimens tested in modified pore solution exhibit a peak corrosion rate of 0.153 µm/yr at week 9.

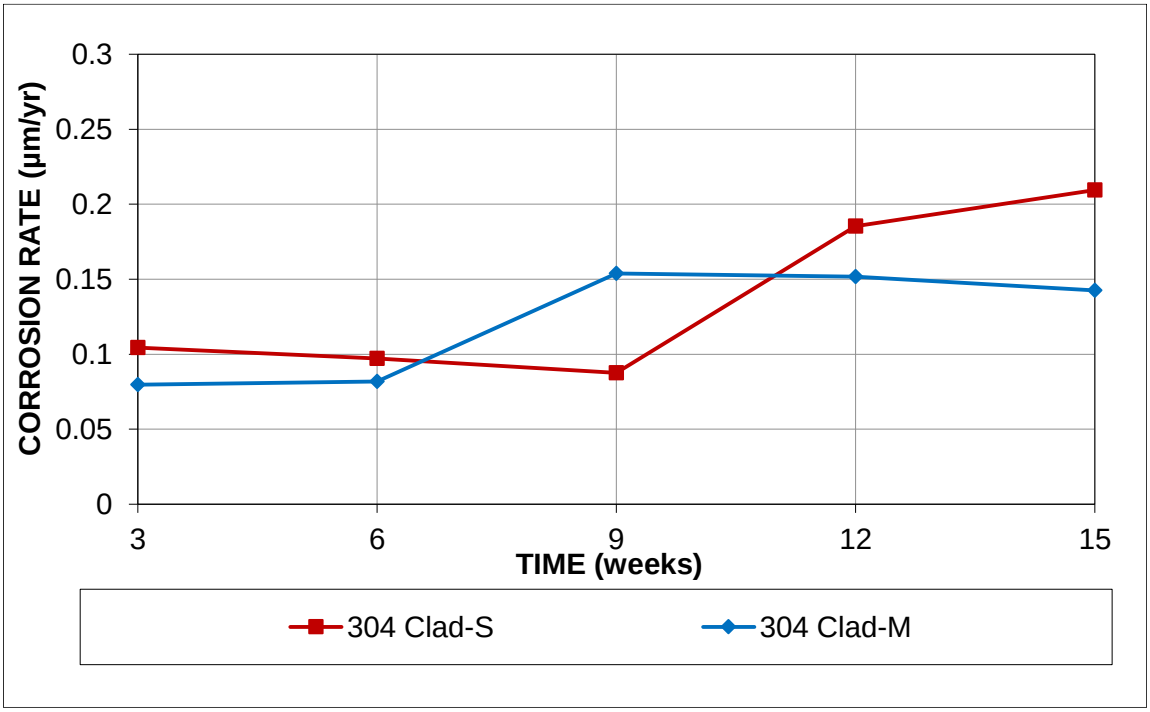

Figure 3.9: Rapid macrocell test. Average corrosion rates (µm/yr) of 304 stainless steel clad bar in standard (S) and modified (M) pore solutions from LPR test results

Figure 3.10 shows the average corrosion losses based on average corrosion rates obtained from LPR test results for the 304 stainless steel clad bar specimens. The average corrosion losses for the specimens tested in standard and modified pore solutions are comparable (p = 0.776).

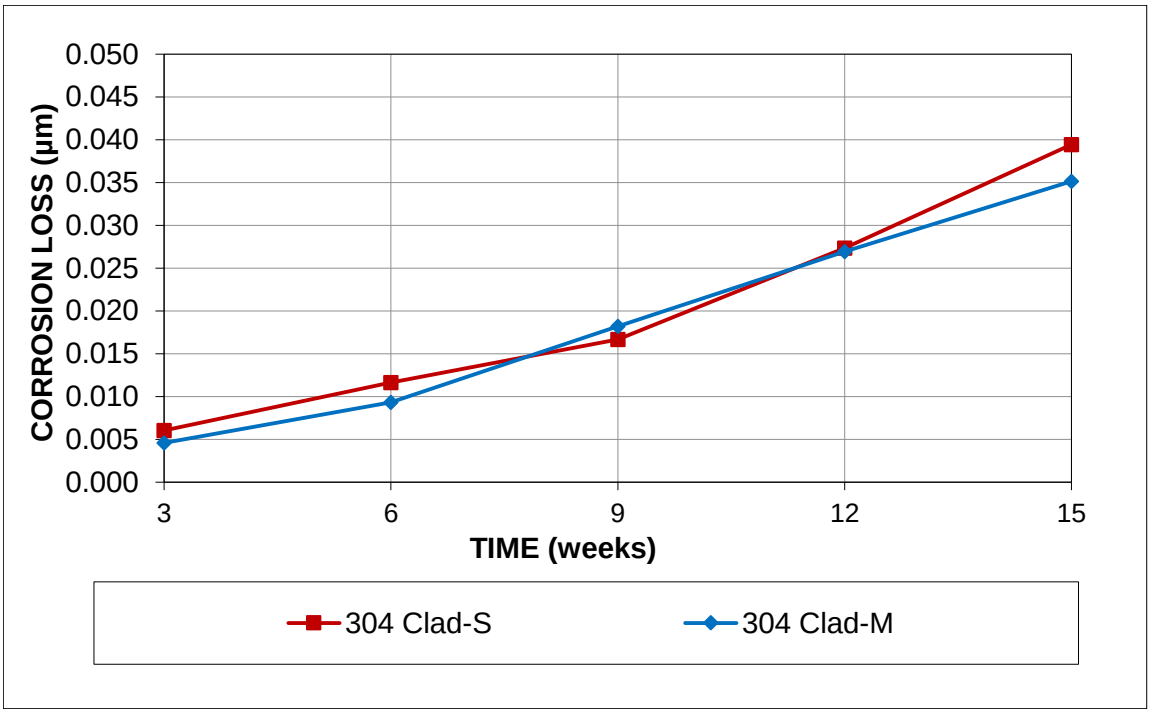

Figure 3.10: Rapid macrocell test. Average corrosion losses (µm) of 304 stainless steel clad bar in standard (S) and modified (M) pore solutions based on average corrosion rates obtained from LPR test results

For 304 stainless steel clad reinforcement, corrosion was observed on some anode bars tested in both standard and modified pore solution, as shown in Figures 3.11 (a) and 3.12 (a) respectively. After the end of life autopsy, the results from one specimen tested in standard pore solution was excluded from analysis due to corrosion under the cap at the cut end, as shown in Figure 3.13. Corrosion products are also observed at the top ends of some cathode bars tested in modified pore solution as shown in Figure 3.14. Corrosion in this case may also be due to crevice corrosion. Representative cathode bars for specimens tested in standard and modified pore solution are shown in Figures 3.11 (b) and 3.12 (b) respectively.

(a)

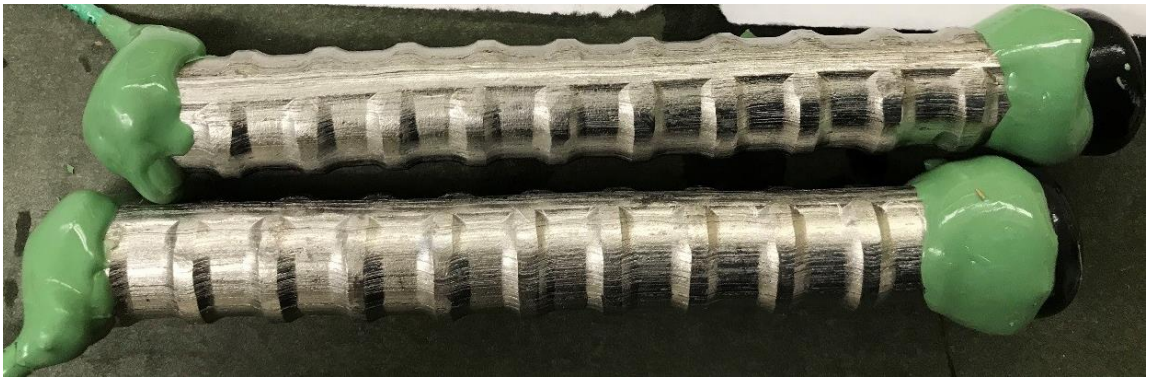

(b)

Figure 3.11: Rapid macrocell test, anode bar (a) and cathode bars (b) of specimen 304 Clad-1 in standard pore solution (S) after 15 weeks

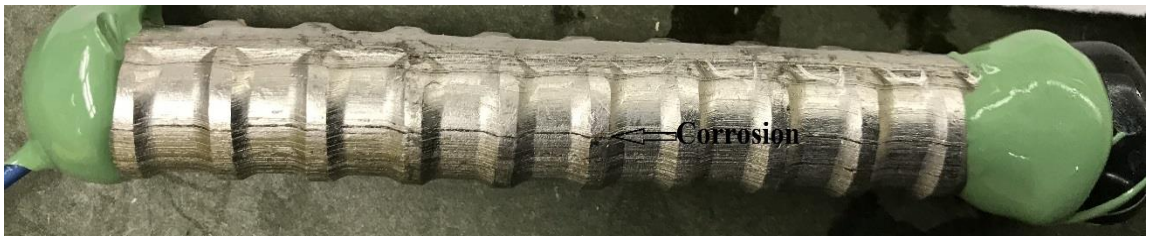

(a)

(b)

Figure 3.12: Rapid macrocell test, anode bar (a) and cathode bars (b) of specimen 304 Clad-2 in modified pore solution (M) after 15 weeks

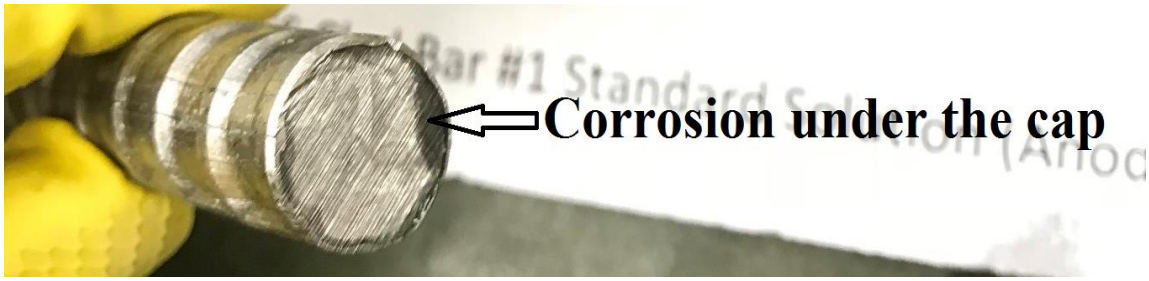

Figure 3.13: Rapid macrocell test, anode bar of specimen 304 Clad (excluded due to corrosion under the cap) in standard pore solution (S) after 15 weeks

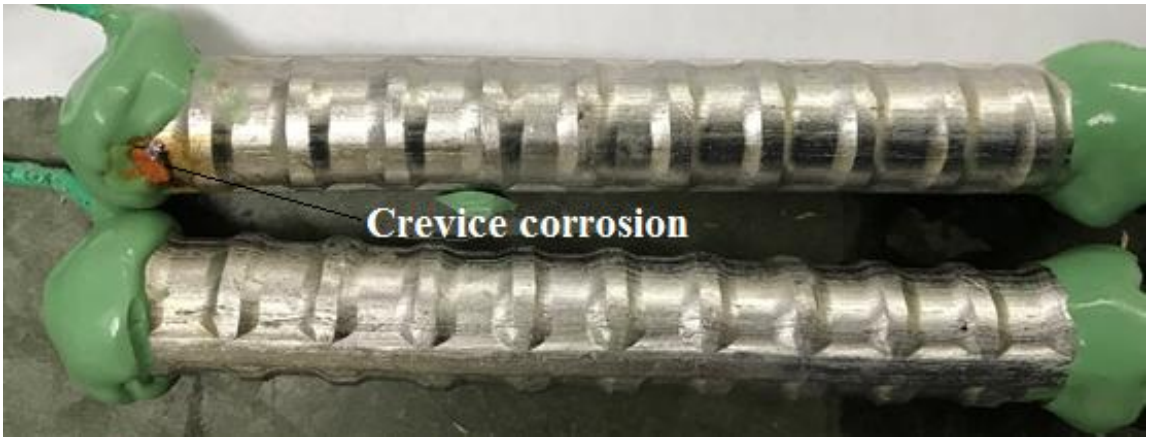

Figure 3.14: Rapid macrocell test, cathode bars of specimen 304 Clad-3 (with crevice corrosion at the top end) in modified pore solution (M) after 15 weeks

3.2.3 MMFX Microcomposite Reinforcing Bar

The average corrosion rates for MMFX bar specimens tested in standard and modified pore solutions are shown in Figure 3.15. Corrosion rates for individual specimens are shown in Appendix A. During the first 10 weeks of testing, the specimens tested in the modified pore solution generally exhibit higher corrosion rates than the specimens tested in the standard pore solution. After 10 weeks, the corrosion rates of the specimens tested in the modified and standard pore solutions are comparable. The specimens tested in the modified pore solution exhibit a peak corrosion rate of 36.99 µm/yr at week 5, whereas the peak corrosion rate exhibited by the specimens tested in the standard pore solution is 20.80 µm/yr at week 6.

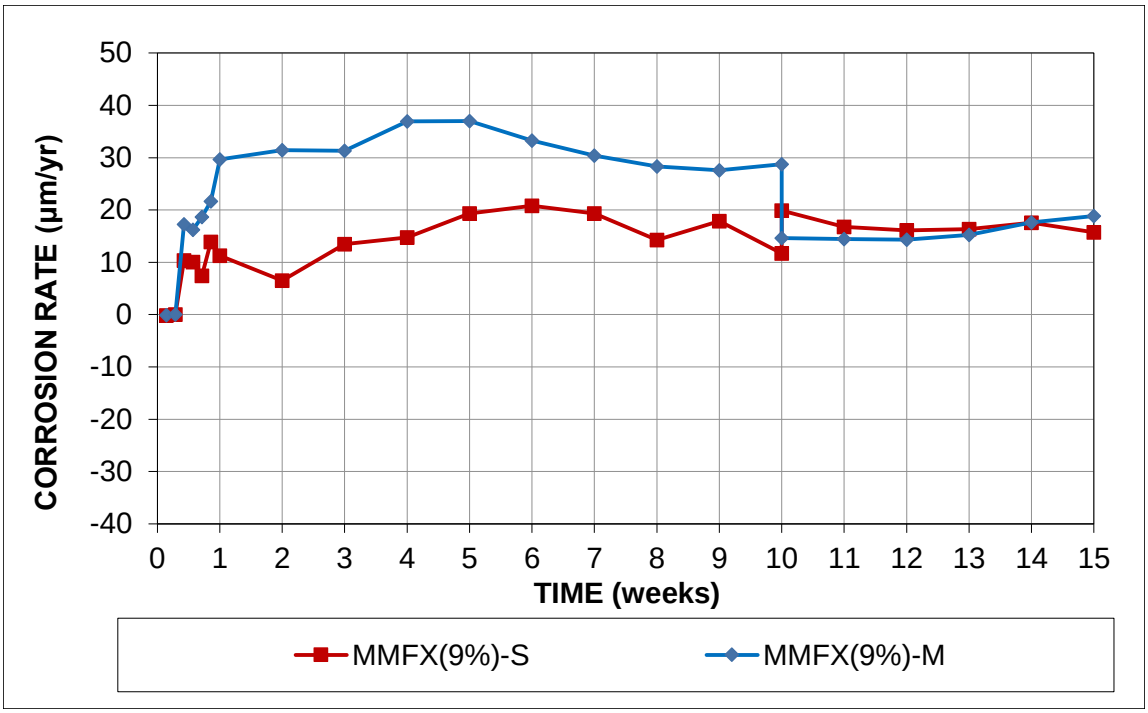

Figure 3.15: Rapid macrocell test. Average corrosion rates (µm/yr) of MMFX (9%) bar in standard (S) and modified (M) pore solutions

Figure 3.16 shows the average anode potentials, taken with respect to a saturated calomel electrode (SCE), for the MMFX bar specimens tested in standard and modified pore solutions. The anode and cathode potentials for individual specimens are shown in Appendix A. During the 15 weeks of testing, the specimens tested in the modified pore solution exhibit a more negative anode potential than the specimens tested in the standard pore solution. The average anode potentials for the specimens tested in the modified pore solution ranges between –0.476 V and –0.511 V, whereas the average anode potentials for the specimens tested in the standard pore solution ranges between –0.433 V and –0.497 V during the period of the test.

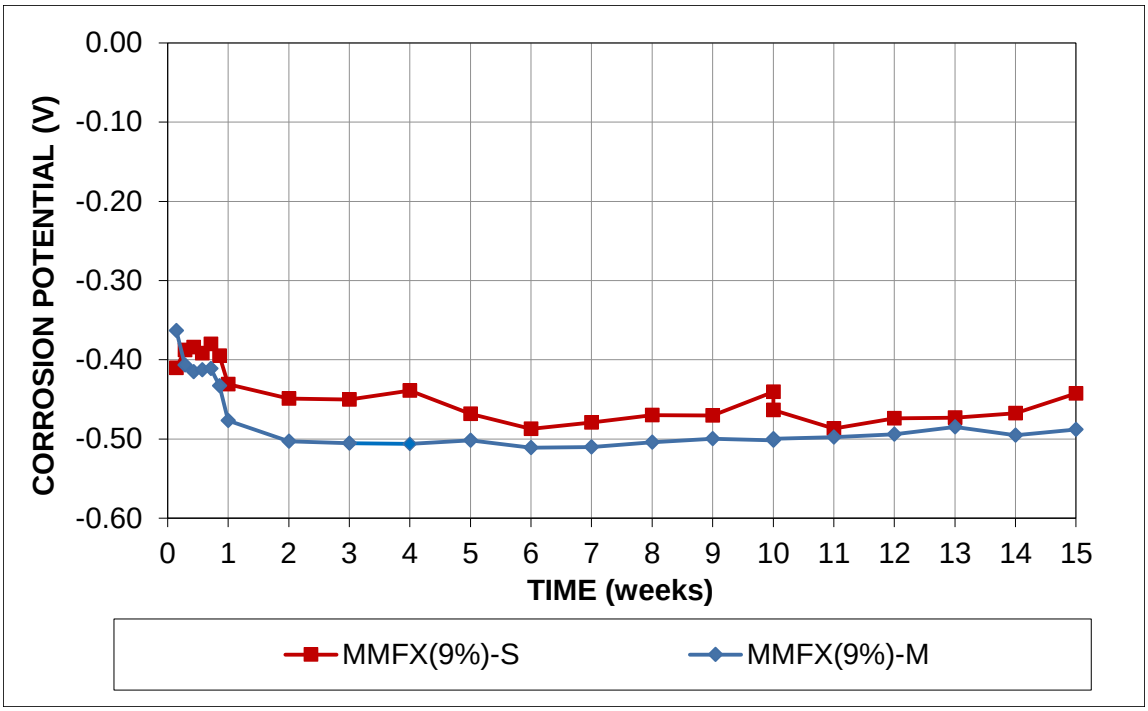

Figure 3.16: Rapid macrocell test. Average corrosion anode potentials (SCE) of MMFX (9%) bar in standard (S) and modified (M) pore solutions

The average corrosion rates obtained from LPR test results for the MMFX bar specimens are shown in Figure 3.17. During the 15 weeks of testing, the specimens tested in the modified pore solution generally exhibit higher corrosion rates than the specimens tested in the standard pore solution. At the end of test (week 15), the specimens tested in the modified pore solution exhibit a peak corrosion rate of 55.26 µm/yr, whereas the peak corrosion rate exhibited by the specimens tested in the standard pore solution is 30.43 µm/yr. The difference in LPR corrosion rates is statistically significant (p = 0.004).

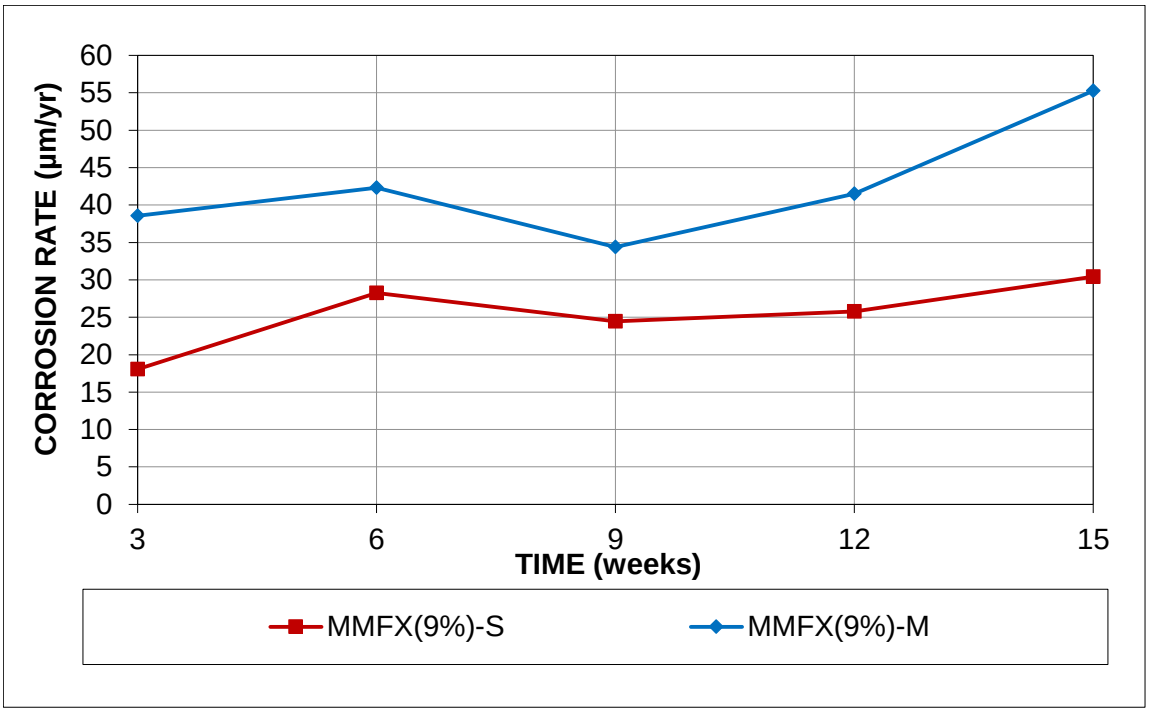

Figure 3.17: Rapid macrocell test. Average corrosion rates (µm/yr) of MMFX (9%) bar in standard (S) and modified (M) pore solutions from LPR test results

Figure 3.18 shows the average corrosion losses based on average corrosion rates obtained from LPR test results for the MMFX bar specimens. The specimens tested in the modified pore solution exhibit corrosion losses 1.6 times greater than that of specimens tested in the standard pore solution. The average corrosion loss of the specimens tested in the modified pore solution after 15 weeks is 12.23 µm, whereas the specimens tested in the standard pore solution exhibit lower average corrosion loss (7.33 µm). The difference in corrosion loss between specimens tested in standard and modified pore solutions is statistically significant ($p = 3.84\times10^{-5}$).

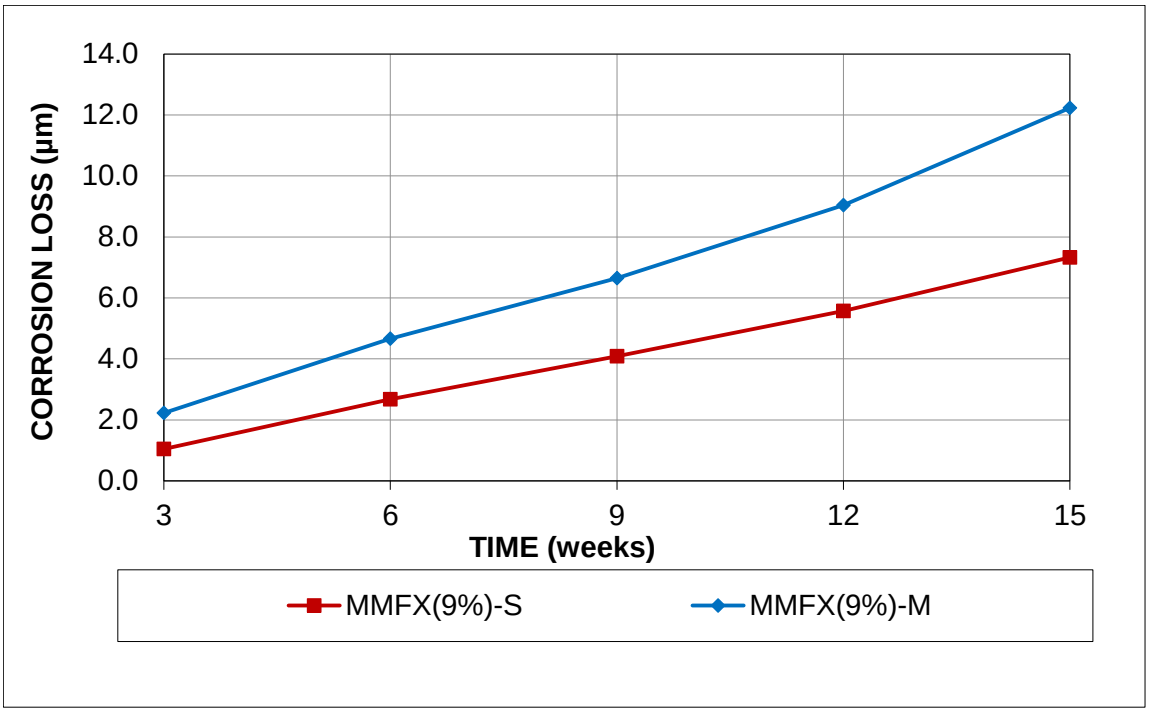

Figure 3.18: Rapid macrocell test. Average corrosion losses (µm) of MMFX (9%) bar in standard (S) and modified (M) pore solutions based on average corrosion rates obtained from LPR test results

For MMFX(9%) reinforcement, corrosion products were observed, as shown in Figures 3.19 (a) and 3.20 (a), on all anode bars for specimens tested in standard and modified pore solutions, predominantly at and above the surface level of the solution. Representative cathode bars for specimens tested in standard and modified pore solution are shown in Figures 3.19 (b) and 3.20 (b) respectively. No cathode bars showed signs of corrosion.

(a)

(b)

Figure 3.19: Rapid macrocell test, anode bar (a) and cathode bars (b) of specimen MMFX(9%)-5 in standard pore solution (S) after 15 weeks

(a)

(b)

Figure 3.20: Rapid macrocell test, anode bar (a) and cathode bars (b) of specimen MMFX(9%)-1 in modified pore solution (S) after 15 weeks

3.2.4 Galvanized Reinforcing Bar

The average corrosion rates for galvanized reinforcing bar specimens tested in standard and modified pore solutions are shown in Figure 3.21. Corrosion rates for individual specimens are shown in Appendix A. During the first week of testing, the specimens tested in the modified pore solution exhibit significantly greater corrosion rates than specimens tested in the standard pore solution. An increase in corrosion rates was observed for the specimens tested in the standard pore solution in weeks 2, 6, 7 and 11. The corrosion rates observed for the specimens tested in both solutions from weeks 8 to 10 and weeks 13 to 15 are comparable. The specimens tested in the standard pore solution exhibit a peak corrosion rate of 184.3 µm/yr at week 6, whereas the peak corrosion rate exhibited by the specimens tested in the modified pore solution is 165.7 µm/yr at week 1.

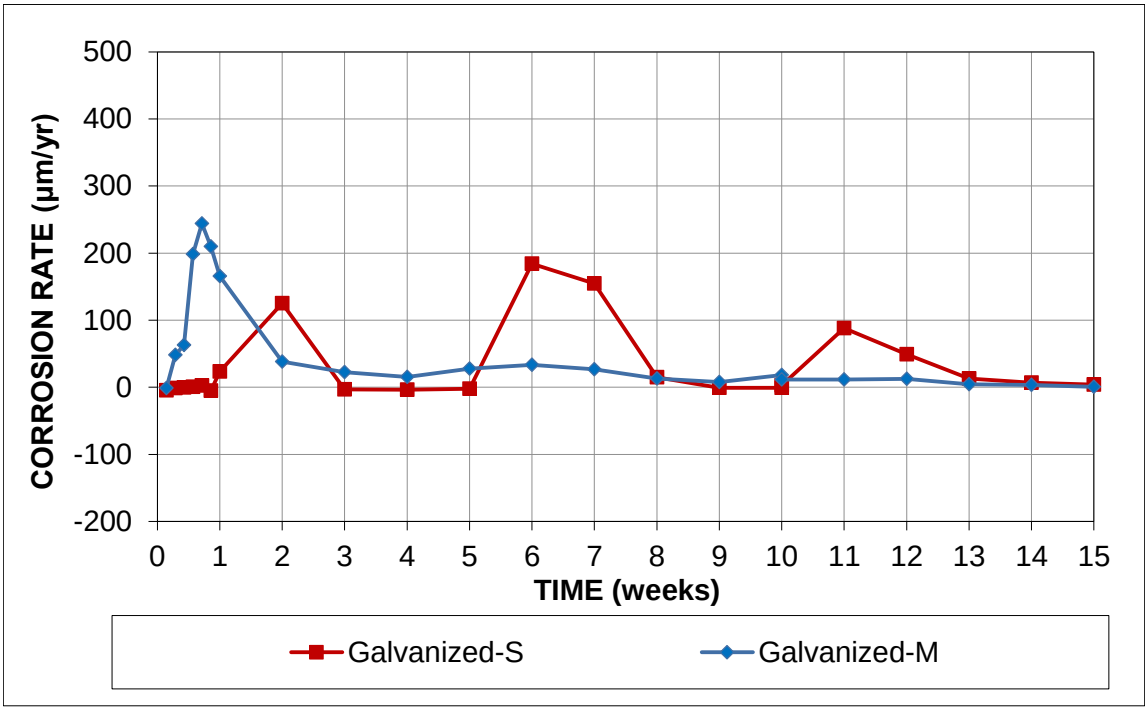

Figure 3.21: Rapid macrocell test. Average corrosion rates (µm/yr) of galvanized bar in standard (S) and modified (M) pore solutions

Figure 3.22 shows the average anode potentials, taken with respect to a saturated calomel electrode (SCE), for galvanized reinforcing bar specimens tested in standard and modified pore solutions. The anode and cathode potentials for individual specimens are shown in Appendix A. During the first 2 weeks of testing, the corrosion potentials of the specimens tested in standard pore solution are relatively close to the corrosion potentials of the specimens tested in the modified pore solution. Otherwise, the specimens tested in the modified pore solution generally show a more negative anode potential than the specimens tested in the standard pore solution during the period of the test. The average anode potentials for the specimens tested in the modified pore solutions ranges from –1.194 V and –0.419 V, whereas the average anode potentials for the specimens tested in the standard pore solution ranges between –1.396 V and –0.234 V after the first week of testing. A drop in potential for specimens tested in both standard and modified pore solutions was observed at weeks 6 and 11, one week after changing the pore solutions. This is most likely due to the increase in pH level of the pore solutions, which occurs after the solutions are changed.

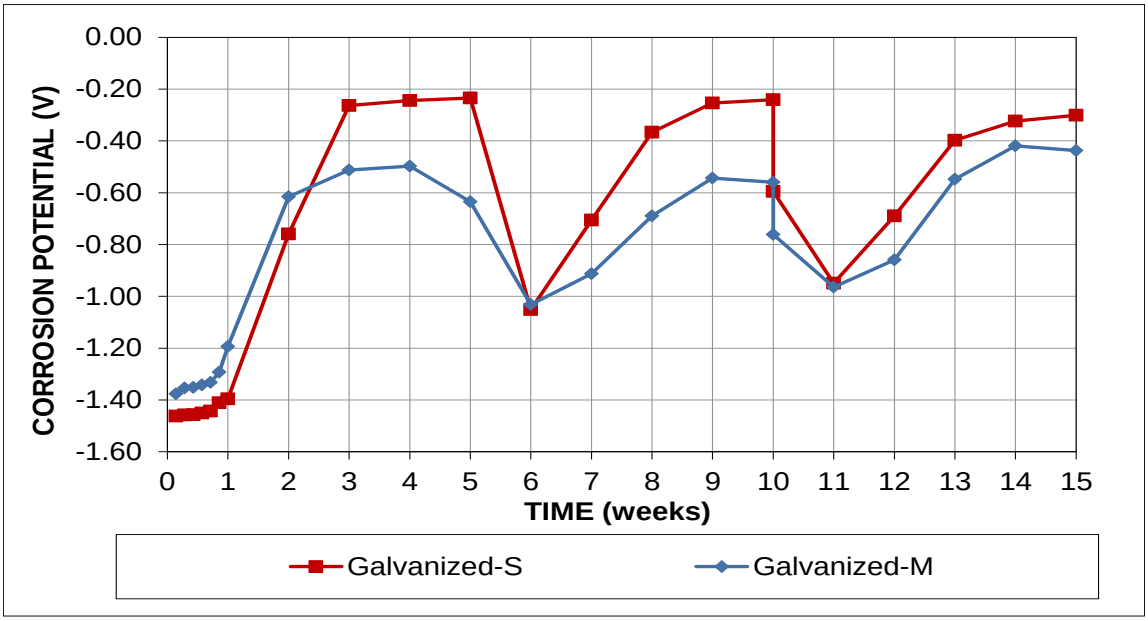

Figure 3.22: Rapid macrocell test. Average corrosion anode potentials (SCE) of galvanized bar in standard (S) and modified (M) pore solutions

The average corrosion rates obtained from LPR test results for the galvanized bar specimens are shown in Figure 3.23. Between weeks 3 and 6, the specimens tested in the standard pore solution exhibit significantly higher corrosion rates than the specimens tested in the modified pore solution. A significant decrease in corrosion rates was observed for all specimens tested in the standard and modified pore solutions between weeks 6 and 9 and weeks 12 and 15. The specimens tested in the modified pore solution exhibit a higher corrosion rate than that of the specimens tested in the standard pore solution between weeks 9 and 12. The specimens tested in the modified pore solution exhibit a peak corrosion rate of 1029 µm/yr at week 6, whereas the peak corrosion rate exhibited by the specimens tested in the standard pore solution is 261.9 µm/yr at week 12. The difference in LPR corrosion rate between specimens tested in standard and modified pore solutions is statistically significant (p = 0.014).

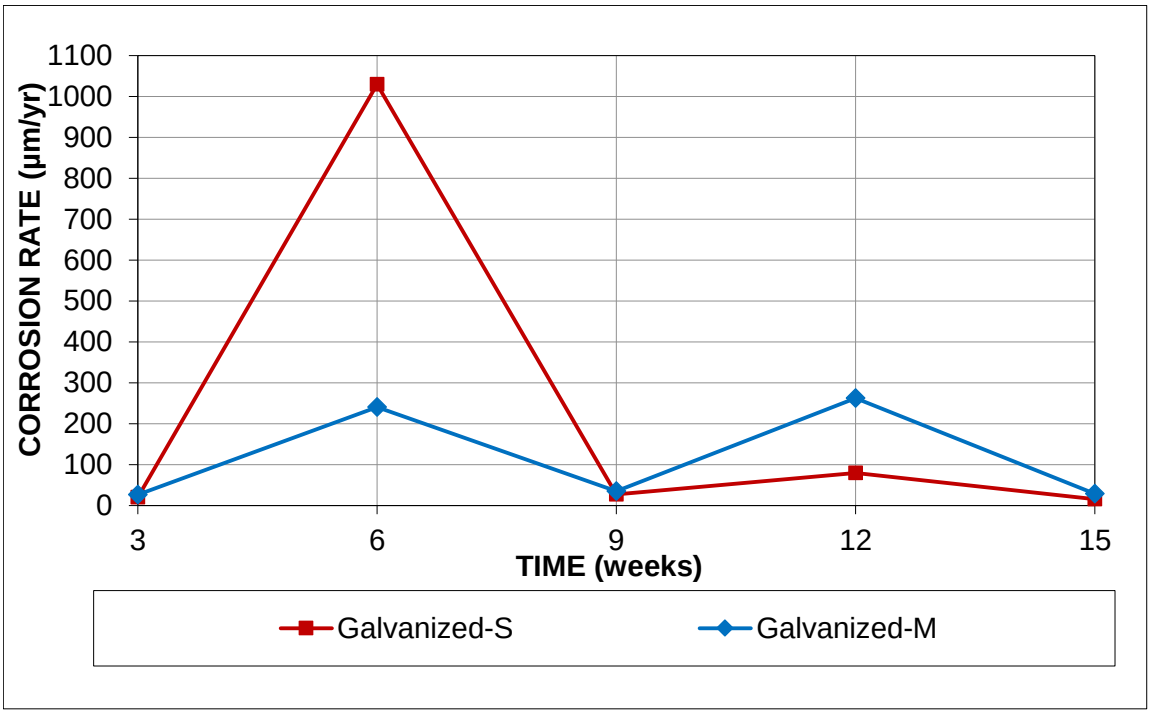

Figure 3.23: Rapid macrocell test. Average corrosion rates (µm/yr) of galvanized bar in standard (S) and modified (M) pore solutions from LPR test results

Figure 3.24 shows the average corrosion losses based on average corrosion rates obtained from LPR test results for the galvanized bar specimens. The specimens tested in the standard pore solution exhibit greater corrosion losses than specimens tested in the modified pore solution. After 15 weeks of testing, corrosion loss of the specimens tested in the modified pore solution is 34.16 µm, approximately half of the corrosion loss of the specimens tested in the standard pore solution, 67.62 µm. The difference in corrosion loss between specimens tested in standard and modified pore solutions is statistically significant (p =0.003).

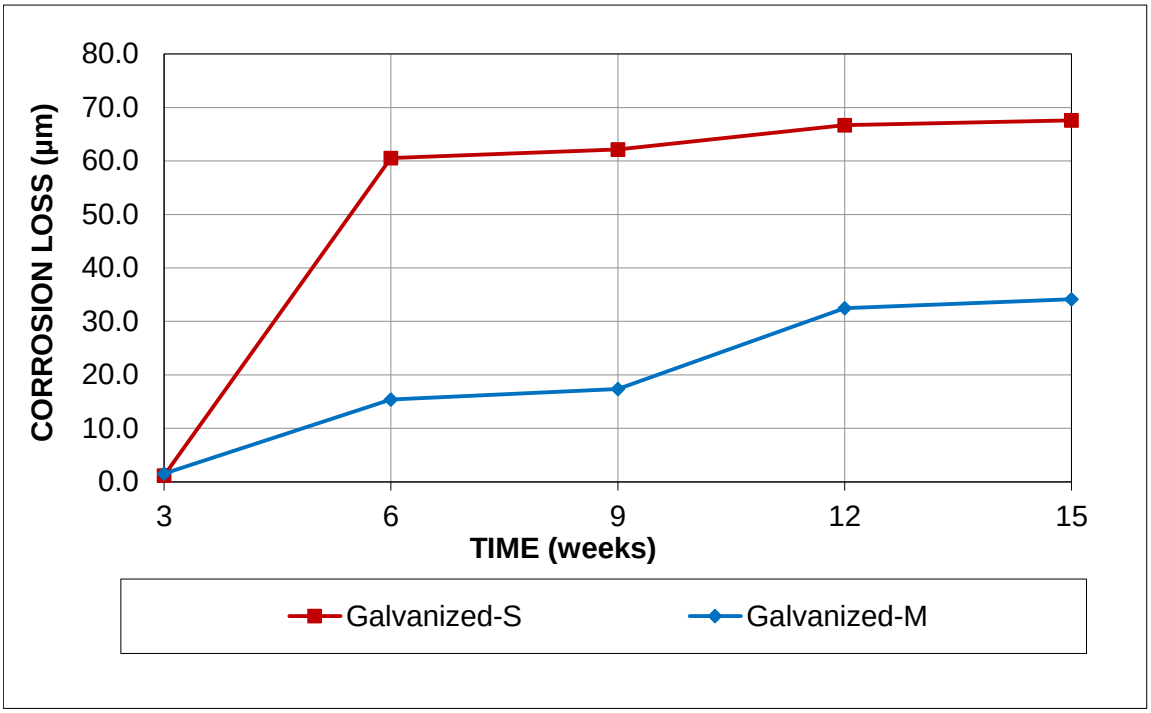

Figure 3.24: Rapid macrocell test. Average corrosion losses (µm) of galvanized bar in standard (S) and modified (M) pore solutions

Fore galvanized reinforcement tested in standard and modified pore solutions, shown in Figure 3.25 (a) and 3.26 (a), the zinc layer was consumed at different sites on the anode bar surface, corrosion products from the underlying steel, were also observed at the surface level of the solution. No corrosion under the cap was observed. Representative cathode bars for specimens

tested in standard and modified pore solution are shown in Figures 3.25 (b) and 3.26 (b) respectively.

(a)

(b)

Figure 3.25: Rapid macrocell test, anode bar (a) and cathode bars (b) of specimen galvanized-5 in standard pore solution (S) after 15 weeks

(a)

(b)

Figure 3.26: Rapid macrocell test, anode bar (a) and cathode bars (b) of specimen galvanized-4 in modified pore solution (M) after 15 weeks

3.2.5 Dual-coated reinforcing bars

The average corrosion rates based on total area for the dual-coated reinforcing bar specimens tested in standard and modified pore solutions are shown in Figure 3.27. Corrosion rates for individual specimens are shown in Appendix A. The specimens tested in the modified pore solution generally show greater corrosion rates than specimens tested in the standard pore solution during the period of the test. The specimens tested in the modified and standard pore solution exhibited a peak corrosion rate of 3.03 µm/yr at week 11 and 2.90 µm/yr at week 15 respectively.

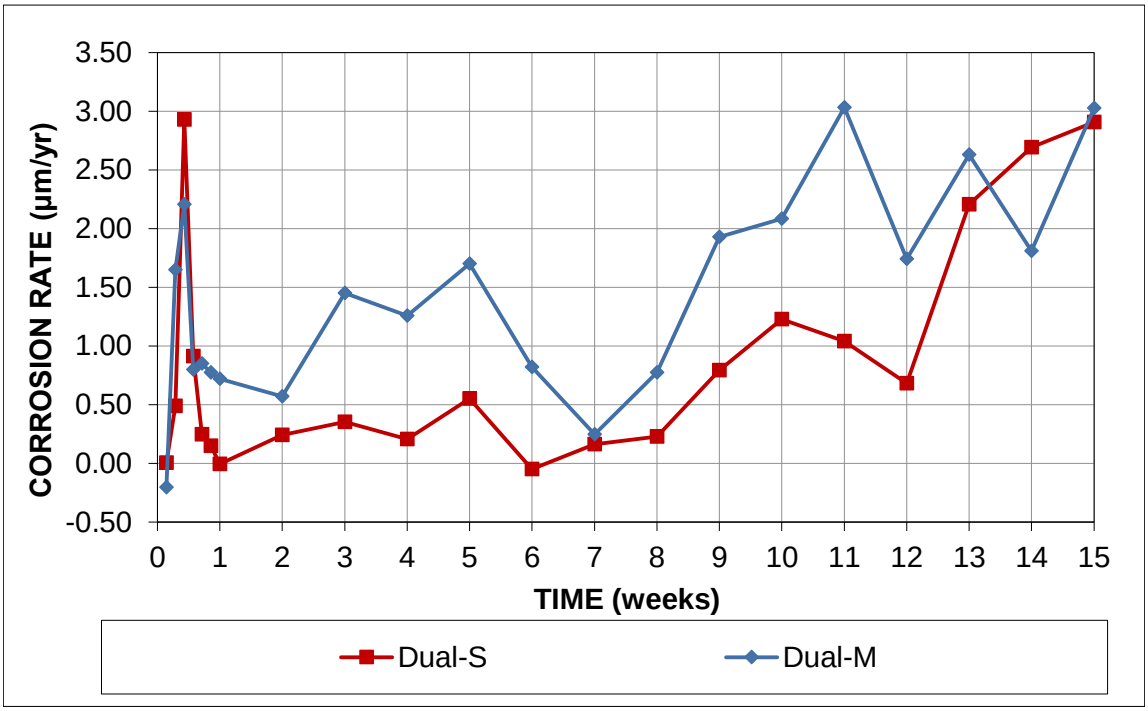

Figure 3.27: Rapid macrocell test. Average corrosion rates (µm/yr) of dual-coated bar in standard (S) and modified (M) pore solutions based on total area

Figure 3.28 shows the average anode potentials, taken with respect to a saturated calomel electrode (SCE), for the dual-coated reinforcing bar specimens. The anode and cathode potentials for individual specimens are shown in Appendix A. During the 15 weeks of testing, the specimens tested in the modified pore solution approximately exhibit a more negative anode potential than

the specimens tested in the standard pore solution. The average anode potentials for the specimens tested in the modified pore solution ranges between –0.543 V and –0.812 V, whereas the average anode potentials for the specimens tested in the standard pore solution ranges between –0.387 V and –0.761 V during the period of the test.

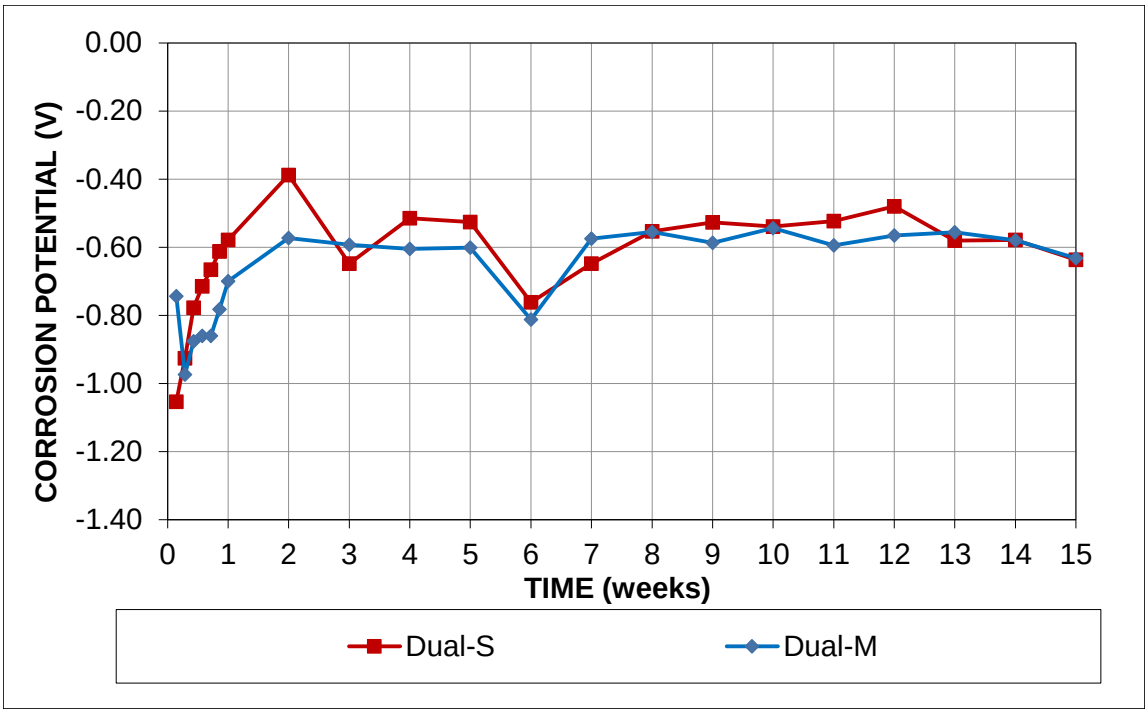

Figure 3.28: Rapid macrocell test. Average corrosion anode potentials (SCE) of dual-coated bar in standard (S) and modified (M) pore solutions based on total area

The average corrosion rates obtained from LPR test results for the dual-coated reinforcing bar specimens are shown in Figure 3.29. The specimens tested in the modified pore solution exhibit greater corrosion rates than the specimens tested in the standard pore solution during the period of the test. At the end of test (week 15), the specimens tested in the modified pore solution exhibit a peak corrosion rate of 6.47 µm/yr, whereas the peak corrosion rate exhibited by the specimens tested in the standard pore solution is 2.47 µm/yr. The difference in LPR corrosion rate between specimens tested in standard and modified pore solutions is statistically significant (p = 0.037).

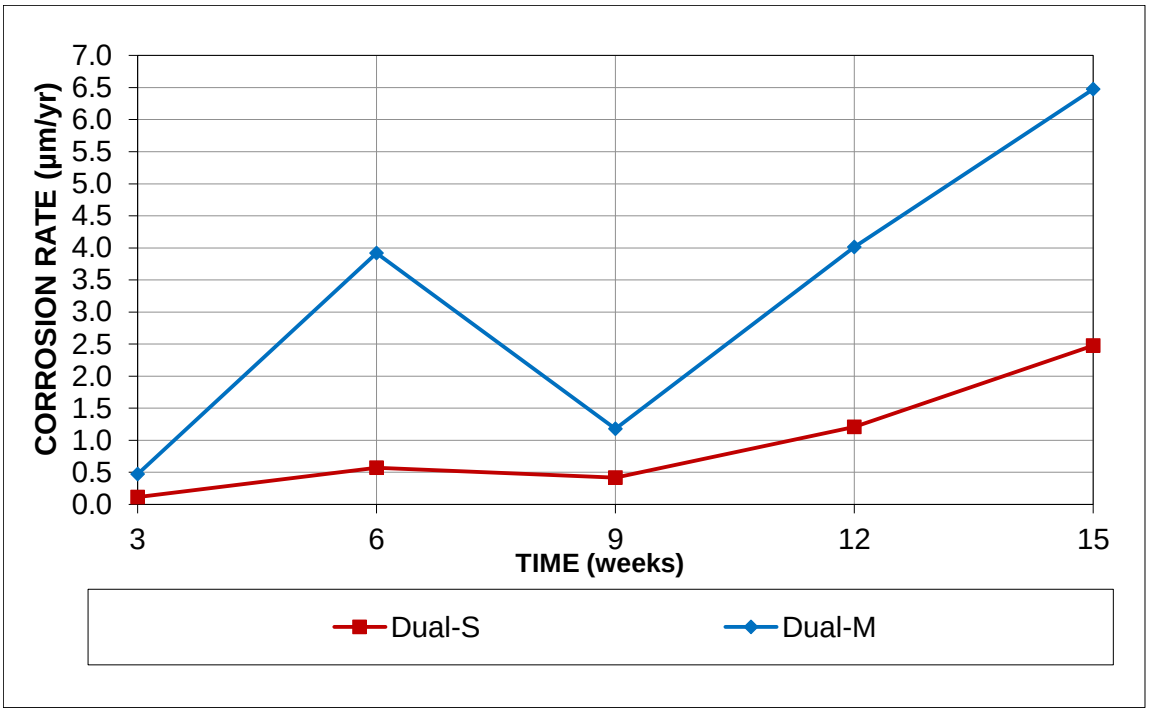

Figure 3.29: Rapid macrocell test. Average corrosion rates (µm/yr) of dual-coated bar in standard (S) and modified (M) pore solutions from LPR test results based on total area

Figure 3.30 shows the average corrosion losses based on average corrosion rates obtained from LPR test results for the dual-coated reinforcing bar specimens. The specimens tested in the modified pore solution exhibit greater corrosion losses than specimens tested in the standard pore solution. After 15 weeks of testing, corrosion loss of the specimens tested in the modified pore solution is 0.93 µm, more than twice the corrosion loss of the specimens tested in the standard pore solution, 0.28 µm. The difference in corrosion losses is statistically significant (p = 0.002).

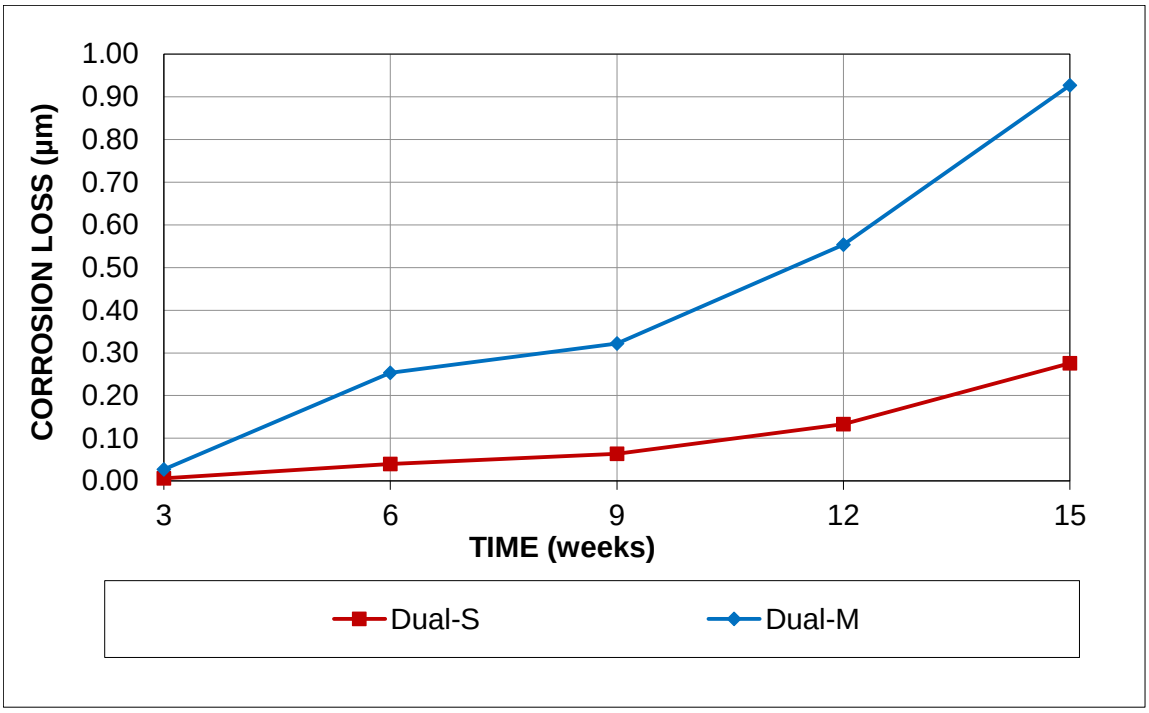

Figure 3.30: Rapid macrocell test. Average corrosion losses (µm) of dual-coated bar in standard (S) and modified (M) pore solutions based on total area

For the dual-coated reinforcement, dark orange iron corrosion products, as shown in Figures 3.31 (a) and 3.32 (a), were visible at the intentionally damaged sites for the anode bars tested in standard and modified pore solutions. No corrosion under the cap was observed for all bars, as shown in Figure 3.33. Representative cathode bars for specimens tested in standard and modified pore solution are shown in Figures 3.31 (b) and 3.32 (b) respectively.

For each anode bar, a disbondment test is performed at all four intentional damaged areas of the epoxy layer of the dual-coated reinforcement specimens. A ring of darkened metal around the damage sites was observed where disbondment occurred, indicating the zinc in this region has been consumed, surrounded by a larger area of light gray corrosion products, most likely from corroding zinc, as shown in Figures 3.34 and 3.35, for specimens tested in standard and modified pore solutions, respectivly. The disbonded area of anode bars of dual-coated reinforcement tested in standard and modified pore solutions versus their total corrosion loss obtained from LPR test

results (week 15) are tabulated in Table 3.1. The average corrosion loss (0.28 µm) and disbanded area (0.06 in^2 (41.40 mm^2)) of specimens tested in standard pore solution were approximately 30% and 55% of those obtained from specimens tested in modified pore solution (0.93 µm as average corrosion loss and 0.11 in^2 (70.43 mm^2) as average disbonded area).

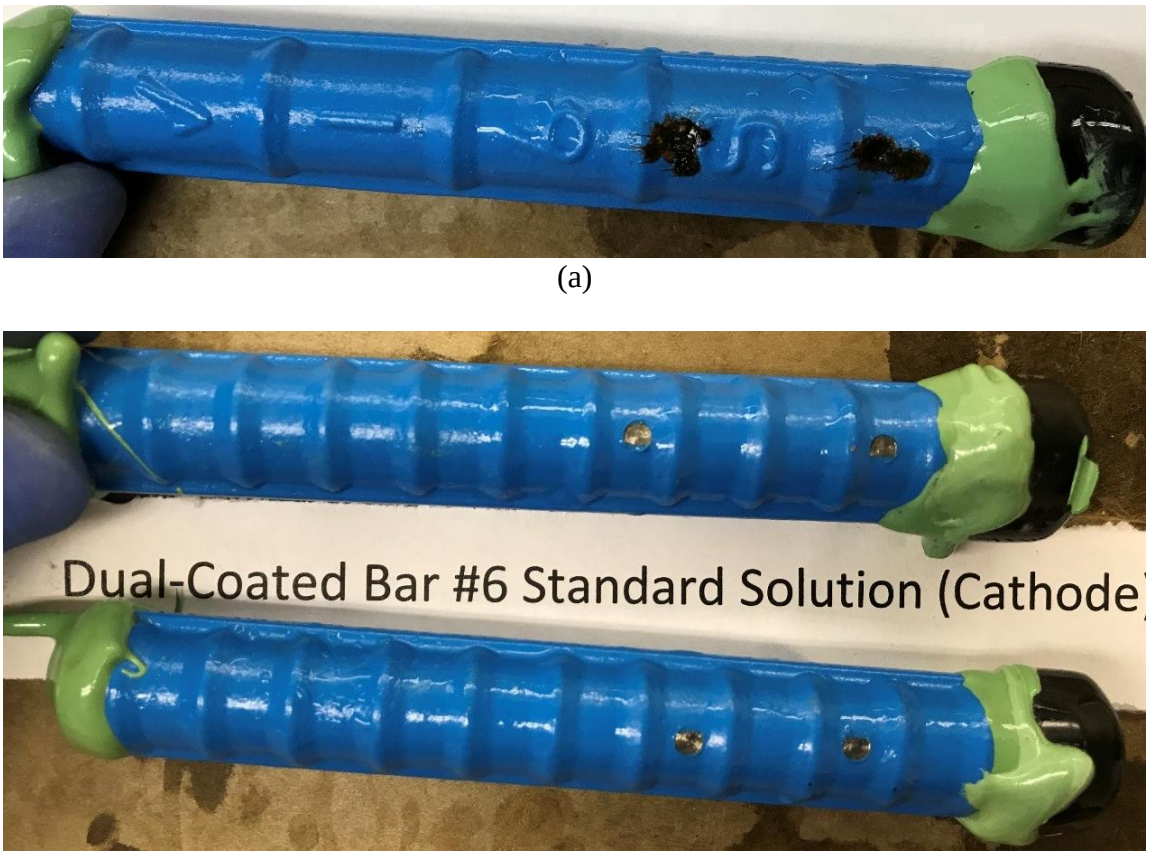

(a)

(b)

Figure 3.31: Rapid macrocell test, anode bar (a) and cathode bars (b) of specimen dual-coated-6 in standard pore solution (S) after 15 weeks

(a)

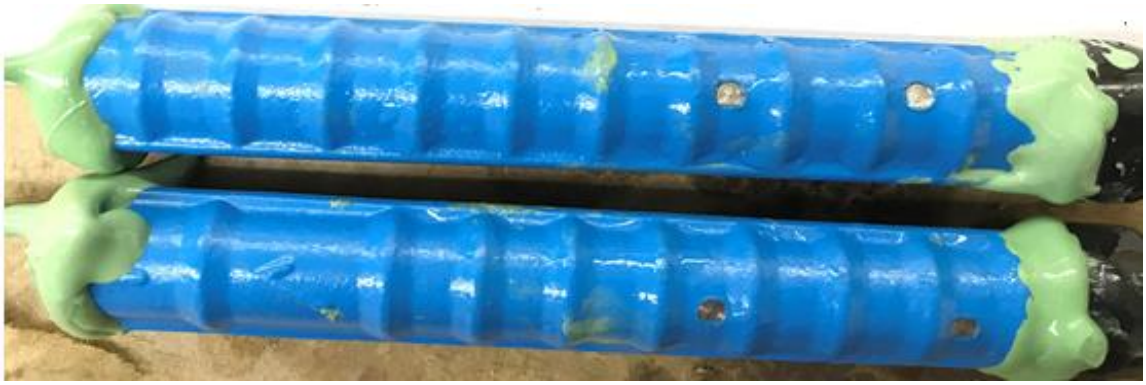

(b)

Figure 3.32: Rapid macrocell test, anode bar (a) and cathode bars (b) of specimen dual-coated-3 in modified solution (M) after 15 weeks

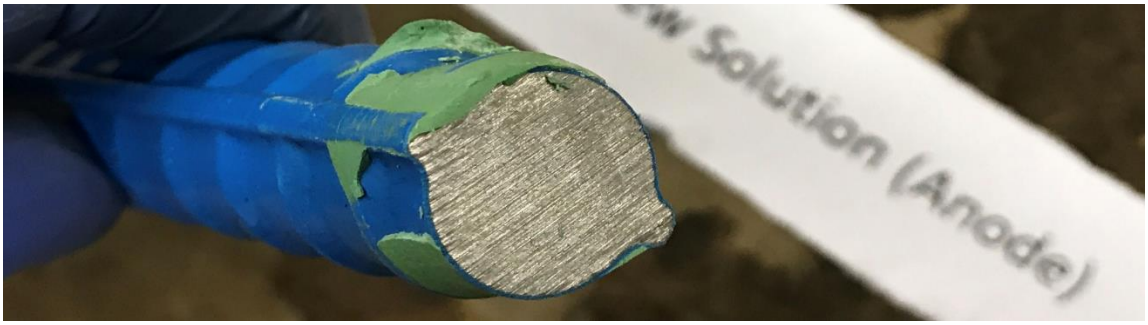

Figure 3.33: Rapid macrocell test, anode bar of specimen dual-coated-2 (no corrosion under the cap) in modified pore solution (M) after 15 weeks

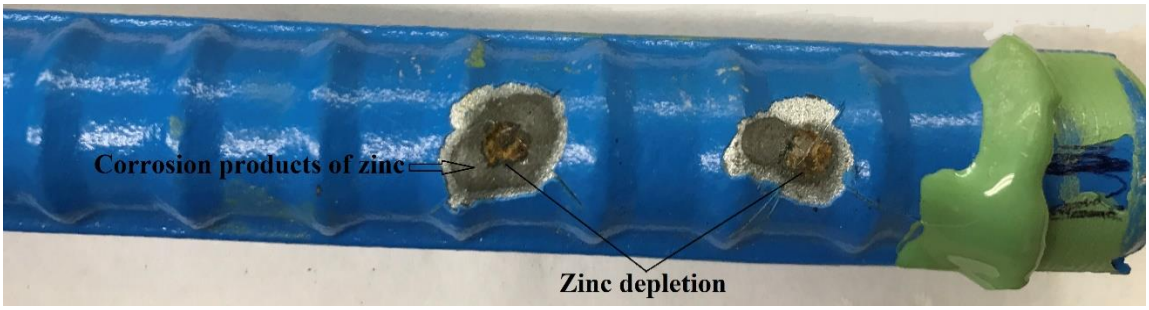

Figure 3.34: Rapid macrocell test, anod bar of specimen dual-coated-5 in standard pore solution (S) after 15 weeks, after disbondment test

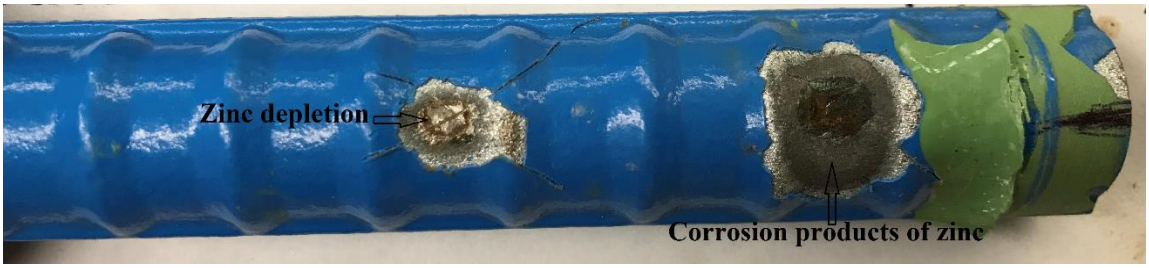

Figure 3.35: Rapid macrocell test, anod bar of specimen dual-coated-3 in modified pore solution (M) after 15 weeks, after disbondment test

Table 3.1: Disbonded area and total corrosion loss at week 15 for the dual-coated reinforcement in rapid macrocell test, standard (S) and modified (M) pore solutions

Specimen	Total Corrosion Loss (µm) Standard Solution (S)	Total Corrosion Loss (µm) Modified Solution (M)	Average Disboned Area (in2) Standard Solution (S)	Average Disboned Area (in2) Modified Solution (M)
1	0.08	1.29	0.02	0.12
2	0.15	0.53	0.05	0.11
3	0.14	1.39	0.05	0.14
4	0.27	0.99	0.06	0.08
5	0.49	0.63	0.11	0.11
6	0.53	0.74	0.11	0.11
Average	0.28	0.93	0.06	0.11

3.3 DISCUSSION

This section summarizes the test results covered in this chapter, including discussion, comparison, and analysis of various corrosion protection systems, taking the influence of pH level of the pore solutions on the corrosion performance of reinforcement into account as a criterion for comparing each type of reinforcing bar tested in standard and modified pore solutions (with pH values of 13.9 and 13.5 respectively), simulating the condition found in concrete environments, using the rapid macrocell tests.

Table3.2 shows the corrosion losses for each type of reinforcing bar tested in standard and modified pore solutions.

Table 3.2: Average of Corrosion Loss (µm) and Student's T-Test Results (*p* Values) for Corrosion Losses at Week 15 for Rapid Macrocell Specimens Based on LPR Test Results, Standard (S) and Modified (M) Pore Solutions

System	Average of Total Corrosion Loss (µm) Standard Solution (S)	Average of Total Corrosion Loss (µm) Modified Solution (M)	Student T-test (*p*)
2304	0.040	0.070	0.229
304 Clad	0.039	0.035	0.776
MMFX(9%)	7.33	12.23	3.83E-05
Galvanized	67.62	34.16	0.014
Dual	0.28	0.93	0.002

A reduction in the pH value of the concrete (or of the test solution) typically reduces the corrosion resistance of reinforcing bars (Verbeck 1975). The results from the analysis of corrosion losses from the rapid macrocell tests (Table 3.2) show statistically significant differences between the specimens tested in both standard and modified pore solutions for MMFX(9%) bar, galvanized bar, and dual-coated bar. The 2304 duplex stainless steel and 304 stainless steel clad bars, however, show no statistically significant differences between the specimens tested in both standard and modified pore solutions (as shown in Table 3.2); this is likely due to the low corrosion losses on stainless steel bars. Based on these results, the pH of the concrete (or of the testing pore solution) has a significant influence on the corrosion resistance of the reinforcement. For steel reinforcement, the simulated pore solution with pH 13.9 (standard pore solution) generally provided more protection against corrosion compared to the simulated pore solution with pH 13.5 (modified pore solution). Test specimens of the galvanized bar tested in standard pore solution,

however, exhibit corrosion losses about twice that observed in the specimens tested in modified pore solution. This is because the protective layer of calcium hydroxyzincate is more stable in lower pH (Maslehuddin et al. 1994; Yeomans 2004). However, in environments with higher pH, calcium hydroxyzincate forms large isolated crystals that cannot protect the underlying steel from corrosion (Andrade & Macias 1988).

CHAPTER 4: SUMMARY AND CONCLUSIONS

4.1 SUMMARY

The effect of the pH of concrete pore solution on the corrosion performance of reinforcing bars is evaluated. The corrosion protection systems (reinforcement) tested in this study include:

- Type 2304 duplex stainless steel reinforcing bar;
- Type 304 stainless steel-clad carbon reinforcing bar;
- MMFX reinforcing bar containing 9% chromium (ASTM A1035 Type CS);
- Galvanized reinforcing bar;
- Dual-coated reinforcing bars (epoxy-coated reinforcement with a 2-mil (0.05-mm) thick zinc coating underneath the epoxy coating)

The corrosion performance of all systems is evaluated using the rapid macrocell test outlined in Annex A2 of ASTM A955. Two different simulated concrete pore solutions (standard and modified) are used during the test to evaluate the effect of the pH of concrete pore solution on the corrosion performance of reinforcement. The standard and modified pore solutions have pH values of 13.9 and 13.5, respectively. A disbondment test is performed to evaluate the integrity of the epoxy of the dual-coated reinforcement. The results of the rapid macrocell tests for both standard and modified pore solutions are used to evaluate the influence of the pH of the pore solution on the corrosion behavior of each type of reinforcing bar.

4.2 CONCLUSIONS

The following conclusions are based on the results and analysis presented in this study:

1. The pH of the pore solution (or of the concrete) has a major influence on the corrosion resistance of reinforcing bars, and it plays a major role in determining the initiation of corrosion.
2. Corrosion resistance of MMFX(9%) and dual-coated reinforcement increases as the pH of the pore solution of concrete increases.
3. Corrosion resistance of galvanized reinforcement decreases as pH increases, likely due to the formation of large isolated hydroxyzincate crystals.
4. Stainless steel reinforcement generally exhibits similar corrosion resistance in the standard and modified pore solutions.

REFERENCES

Ahmad, S. (2003). "Reinforcement Corrosion in Concrete Structures, its Monitoring and Service Life Prediction—a Review," *Cement and Concrete Composites,* Vol. 25, No. 4, pp. 459-471.

Ai, Z., Jiang, J., Sun, W., Song, D., Ma, H., Zhang, J., & Wang, D. (2016). "Passive Behaviour of Alloy Corrosion-Resistant Steel Cr10Mo1 in Simulating Concrete Pore Solutions with Different pH," *Applied Surface Science,* Vol. 389, pp. 1126-1136.

Alvarez, S., Bautista, A., & Velasco, F. (2011). "Corrosion Behaviour of Corrugated Lean Duplex Stainless Steels in Simulated Concrete Pore Solutions," *Corrosion Science,* Vol. 53, No. 5, pp. 1748-1755.

Andrade, M., & Macias, A. (1988). "Galvanized Reinforcements in Concrete," *Surface Coatings—2,* pp. 137-182.

ASTM A775/A775M-16. (2016). "Standard Specification for Deformed and Plain Stainless-Steel Reinforcing Bars for Concrete Reinforcement," *ASTM International,* West Conshohocken, PA. 11 pp.

ASTM A934/934M-07. (2007). "Standard Specification for Epoxy-Coated Prefabricated Steel Reinforcing Bars," *ASTM International,* West Conshohocken, PA. 17 pp.

ASTM A955/A955M-14. (2014). "Standard Specification for Deformed and Plain Stainless-Steel Reinforcing Bars for Concrete Reinforcement," *ASTM International,* West Conshohocken, PA. 13 pp.

ASTM D3963/D3963M-15. (2015). "Standard Specification for Fabrication and Jobsite Handling of Epoxy-Coated Steel," *ASTM International,* West Conshohocken, PA. 3 pp.

Balma, J., Darwin, D., Browning, J. P., and Locke, C. E. (2005) "Evaluation of Corrosion Protection Systems and Corrosion Testing Methods for Reinforcing Steel in Concrete," *SM Report* No. 76, University of Kansas Center for Research, Inc., Lawrence, Kansas, 517 pp.

Berkeley, K., & Pathmanaban, S. (1990). "Cathodic Protection of Reinforcement Steel in Concrete," London: *Butterworths & Co. Ltd*. 158 pp.

Broomfield, J. P. (1997). "Corrosion of Steel in Concrete: Understanding, Investigation and Repair," London *E&FN Spon.* 240 pp.

Byfors, K. (1987). "Influence of Silica Fume and Flyash on Chloride Diffusion and pH Values in Cement Paste," *Cement and Concrete research,* Vol. 17, No.1, pp. 115-130.

Chen, L., Tan, H., Wang, Z., Li, J., & Jiang, Y. (2012). "Influence of Cooling Rate on Microstructure Evolution and Pitting Corrosion Resistance in the Simulated Heat-Affected Zone of 2304 Duplex Stainless Steels. *Corrosion Science,* Vol. 58, pp. 168-174.

Clear, K. C. (1995). "Performance of Epoxy-Coated Reinforcing Steel in Highway Bridges," *Transportation Research Board,* Vol. 370, 153 pp.

Clear, K. C., & Virmani, Y. P. (1983). “Corrosion of Non-Specification Epoxy-Coated Rebars in Salty Concrete,” *Public Roads,* Transportaion Research Board, National Research Council, Vol. 47 No. 1, pp. 1-10.

Clemeña, G. G. (2004). “Resistance of a Stainless Steel-Clad reinforcing Bar to chloride-Induced Corrosion in Concrete,” *Virginia Transportation Research Council Charlottesville* VA 22903, Principal Research Scientist (Ret.).

Clemena, G. G., & Virmani, Y. P. (2002). “Testing of Selected Metallic Reinforcing Bars for Extending the Service Life of Future Concrete Bridges: Testing in Outdoor Concrete Blocks,” *Federal Highay Administration,* VTRC 03-R6, 24 pp.

Clemeña, G. G., Kukreja, D. N., & Napier, C. S. (2003). “Trial Use of a Stainless Steel-Clad Steel Bar in a New Concrete Bridge Deck in Virginia,” *Federal Highay Administration,* VTRC 04-R5, 26 pp.

Clifton, J. R., Beeghly, H. F., & Mathey, R. G. (1975). “Protecting Reinforcing Bars from Corrosion with Epoxy Coatings,” *Special Publication,* Vol. 49, pp. 115-132.

Cross, W. M., Duke, E. F., Kellar, J. J., Han, K. N., & Johnston, D. (2001). “Stainless Steel Clad Rebar in Bridge Decks,” *SD* 200-04-F, South Dakota School of Mines and Technology.

Darwin, D., Browning, J , O’Reilly, M, & Lihua Xing, a. J. J. (2009). "Critical Chloride Corrosion Threshold of Galvanized Reinforcing Bars," *ACI Materials Journal,*Vol. 106, No. 2, pp. 176-183.

Darwin, D., Browning, J., Locke, C. E., Jr., & Nguyen, T. V. (2007). “Multiple Corrosion Protection Systems for Reinforced Concrete Bridge Components,” Publication No. FHWA-HRT-07-043, Federal Highway Administration, *SM Report* No. 84, University of Kansas Center for Research, Inc., Lawrence, Kansas, 92 pp.

Darwin, D., Browning, J., Nguyen, T.V., and Locke, C.E., Jr. (2002). "Mechanical and Corrosion Properties of a High-Strength, High Chromium Reinforcing Steel for Concrete," *SM Report* No. 66, University of Kansas Center for Research, Inc., Lawrence, Kansas, 142 pp.; also South Dakota Department of Transportation Report, SD2001-05-F.

Darwin, D., Browning, J., O'Reilly, M., Locke, C.E., and Virmani, Y. P. (2011) "Multiple Corrosion Protection Systems for Reinforced Concrete Bridge Components," Publication No. FHWA-HRT-11-060, Federal Highway Administration, *SM Report* No. 101, University of Kansas Center for Research, Inc., Lawrence, Kansas, 255 pp.

Darwin, D., Locke Jr, C. E., Balma, J., & Kahrs, J. T. (1999). “Evaluation of Stainless Steel Clad Reinforcing Bars,” *SL Report* No. 99-3, The University of Kansas Center for Research, Inc., Lawrence, Kansas, 43 pp.

Diab, A. M., Elyamany, H. E., & Elmoty, A. E. M. A. (2011). “Effect of Mix Proportions, Seawater Curing Medium and Applied Voltages on Corrosion Resistance of Concrete Incorporating Mineral Admixtures,” *Alexandria Engineering Journal,* Vol. 50, No. 1, pp. 65-78.

Diamond, S. (1981). “Effects of Two Danish Flyashes on Alkali Contents of Pore Solutions of Cement-Flyash Pastes,” *Cement and Concrete research,* Vol. 11, No. 3, pp. 383-394.

Diamond, S. (1983). “Effects of Microsilica (Silica Fume) on Pore-Solution Chemistry of Cement Pastes,” *Journal of the American Ceramic Society,* Vol. 66, No. 5, pp C-82-C84.

Draper, J., Darwin, D., Browning, J. P., Locke, C. E. (2009), "Evaluation of Multiple Corrosion Protection Systems for Reinforced Concrete Bridge Decks," *SM Report 96,* University of Kansas Center for Research, Inc., Lawrence, Kansas, 429 pp.

Duarte, R., Castela, A., Neves, R., Freire, L., & Montemor, M. (2014). “Corrosion Behavior of Stainless Steel Rebars Embedded in Concrete: An Electrochemical Impedance Spectroscopy Study,” *Electrochimica Acta,* Vol. 124, pp. 218-224.

Erdoğdu, Ş., Bremner, T., & Kondratova, I. (2001). “Accelerated Testing of Plain and Epoxy-Coated Reinforcement in Simulated Seawater and Chloride Solutions,” *Cement and Concrete research,* Vol. 31, No. 6, pp. 861-867.

Fanous, F., & Wu, H. (2005). “Performance of coated reinforcing bars in cracked bridge decks,” *Journal of Bridge Engineering,* Vol. 10, No. 3, pp. 255-261.

Farshadfar, O. (2017). “Performance Evaluation of Corrosion Protection Systems for Reinforced Concrete,” *University of Kansas,* 345 pp.

FHWA. (2016). "Deficient Bridges by State and Highway Systems," https://www.fhwa.dot.gov/bridge/nbi/no10/defbr16.cfm. Accessed 12/30/2016.

Figueira, R. B., Silva, C. J., & Pereira, E. V. (2015). “Hybrid Sol–Gel Coatings for Corrosion Protection of Hot-Dip Galvanized Steel in Alkaline Medium,” *Surface and Coatings Technology,* Vol. 265, pp. 191-204.

Flint, G., & Cox, R. (1988). “The Resistance of Stainless Steel Partly Embedded in Concrete to Corrosion by Seawater,” *Magazine of concrete research,* Vol. 40, No. 142, pp. 13-27.

Freire, L., Carmezim, M., Ferreira, M. a., & Montemor, M. (2010). “The Passive Behaviour of AISI 316 in Alkaline Media and the Effect of pH: A Combined Electrochemical and Analytical Study,” *Electrochimica Acta,* Vol. 55, No. 21, pp. 6174-6181.

Gong, L., Darwin, D., Browning, J. P., & Carl E. Locke, J. (2003). "Evaluation of Mechanical and Corrosion Properties of MMFX Reinforcing Steel for Concrete," *Kansas Department of Transportation, Report FHWA-KS-02-8,* 114 pp.

Gong, L., Darwin, D., Browning, J. P., & Locke, C. E. (2002). “Evaluation of Mechanical and Corrosion Properties of MMFX Reinforcing Steel for Concrete,” *Kansas Department of Transportation, Report FHWA-KS-02-8,* 114 pp.

Gong, L., Darwin, D., Browning, J., & Locke Jr, C. E. (2006). “Evaluation of Multiple Corrosion Protection Systems and Stainless Steel Clad Reinforcement for Reinforced Concrete,” *SM Report* No. 82, The University of Kansas Center for Research, Inc., Lawrence, Kansas, 540 pp.

Grubb, J. A., Limaye, H. S., & Kakade, A. M. (2007). “Testing pH of concrete,” *Concrete International,* Vol. 29, No. 04, pp. 78-83.

Haran, B. S., Popov, B. N., Petrou, M. F., & White, R. E. (2000). "Studies on Galvanized Carbon Steel in $Ca(OH)_2$ Solutions," *Materials Journal,* Vol. 97, No. 4, pp. 425-431.

Hartt, W. H., & Nam, J. (2008). "Effect of Cement Alkalinity on Chloride Threshold and Time-to-Corrosion of Reinforcing Steel in Concrete," *Corrosion,* Vol. 64, No. 8, pp. 671-680.

Hartt, W. H., Powers, R. G., Leroux, V., & Lysogorski, D. (2004). "A Critical Literature Review of High-Performance Corrosion Reinforcements in Concrete Bridge Applications," *Federal Highay Administration,* FHWA-RD-04-093, 54 pp.

Hartt, W., Kim, K., Jingak, N., & Li, L. (2003). "Effect of Cement Alkalinity Upon Time-to-Corrosion of Reinforcing Steel in Concrete Undergoing Chloride Exposure," *Corrosion 2003,* NACE International.

Hausmann, D. (1967). "Steel Corrosion in Concrete," *Materials protection,* Vol. 6, No. 11, pp. 19-22.

Head, M., Ashby-Bey, E., Edmonds, K., Efe, S., Grose, S., & Mason, I. (2015). "Stainless Steel Prestressing Strands and Bars for Use in Prestressed Concrete Girders and Slabs," *MSU-* 2013-02, Morgan State University Clarence M. Mitchell, Jr., School of Engineering Department of Civil Engineering, 121 pp.

Hime, W., & Machin, M. (1993). "Performance Variances of Galvanized Steel in Mortar and Concrete," *Corrosion,* Vol. 49, No. 10, pp. 858-860.

Ji, J. (2005). "Corrosion Resistance of Microcomposite and Duplex Stainless Steels for Reinforced Concrete Bridge Decks," *SM Report* 76, University of Kansas Center for Research, Lawrence, Kansas, 517 pp.

Ji, J., Darwin, D., and Browning, J. P. (2005). "Corrosion Resistance of Duplex Stainless Steels and MMFX Microcomposite Steel for Reinforced Concrete Bridge Decks," *SM Report* 80, University of Kansas Center for Research, Inc., Lawrence, Kansas, 507 pp.

Jones, D. A. (1996). "Principles and Prevention of Corrosion," New York: *Macmillan Publising Co.* 500 pp.

Kahl, S. (2007). "Corrosion Resistant Alloy Steel (MMFX) Reinforcing Bar in Bridge Decks," *Michigan Department of Transportation Construction and Technology Division* No. R-1499, 31 pp.

Kahrs, J. T., Darwin, D., & Locke, C. E. (2001). "Evaluation of Corrosion Resistance of Type 304 Stainless Steel Clad Reinforcing Bars," *SM Report* No. 65, The University of Kansas Center for Research, Inc., Lawrence, Kansas, 76 pp.

Kepler, J. L., Darwin, D., & Locke Jr, C. E. (2000). "Evaluation of Corrosion Protection Methods for Reinforced Concrete Highway Structures," *SM Report* No. 58, University of Kansas Center for Research, Inc, Lawrence, Kansas, 231 pp.

King, D., Fict, H., Dip, M., & Chartered, M. C. I. M. (2012). "The Effect of Silica Fume on the Properties of Concrete as Defined in Concrete Society Report 74, Cementitious Materials," Singapore: *37th Conference on our world in concrete and structures,* pp. 29-31.

Koch, G. H., Brongers, M. P., Thompson, N. G., Virmani, Y. P., & Payer, J. H. (2002). "Corrosion Cost and Preventive Strategies in the United States," *Federal Highay Administration,* FHWA-RD-01-156, 784 pp.

Lafikes, J., Storm, S., Darwin, D., Browning, J., & O'Reilly, M. (2011). "Stainless Steel Reinforcement as a Replacement for Epoxy Coated Steel in Bridge Decks," *SL Report* 11-4, University of Kansas Center for Research, Lawrence, Kansas, 152 pp.

Lambert, P., Page, C., & Vassie, P. (1991). "Investigations of Reinforcement Corrosion. 2. Electrochemical Monitoring of Steel in Chloride-Contaminated Concrete," *Materials and Structures,*Vol. 24, No. 5, pp. 351-358.

Li, L., Sagüés, A. A., & Poor, N. (1999). "In Situ Leaching Investigation of pH and Nitrite Concentration in Concrete Pore Solution," *Cement and Concrete research,* Vol. 29, No. 3, pp. 315-321.

Liu, J., Qiu, Q., Chen, X., Xing, F., Han, N., He, Y., & Ma, Y. (2017). "Understanding the Interacted Mechanism Between Carbonation and Chloride Aerosol Attack in Ordinary Portland Cement Concrete," *Cement and Concrete research,* Vol. 95, pp. 217-225.

Mammoliti, L., Brown, L., Hansson, C., & Hope, B. (1996). "The Influence of Surface Finish of Reinforcing Steel and pH of the Test Solution on the Chloride Threshold Concentration for Corrosion Initiation in Synthetic Pore Solutions," *Cement and Concrete research,* Vol. 26, No. 4, pp. 545-550.

Manning, D. G. (1996). "Corrosion Performance of Epoxy-Coated Reinforcing Steel: North American Experience," *Construction and Building Materials,*Vol. 10, No. 5, pp. 349-365.

Maslehuddin, M., Al-Amoudi, O., & Al-Mana, A. (1994). "Concrete Durability in a Very Aggressive Environment," *Special Publication,* Vol. 144, pp. 191-212.

McDonald, D. B., Pfeifer, D. W., & Sherman, M. R. (1998). "Corrosion Evaluation of Epoxy-Coated, Metallic-Clad and Solid Metallic Reinforcing Bars in Concrete," *Federal Highay Administration*, No. FHWA-RD-98-153, 140 pp.

McDonald, D. B., Sherman, M. R., Pfeifer, D. W., & Virmani, Y. P. (1995). "Stainless Steel Reinforcing as Corrosion Protection," *Concrete International,* Vol. 17, No. 5, pp. 65-70.

Muralidharan, S., Parande, A., Saraswathy, V., Kumar, K., & Palaniswamy, N. (2008). "Effect of Silica Fume on the Corrosion Performance of Reinforcements in Concrete," *Zastita materijala,* Vol. 4, No.49, pp. 3-9.

O'Reilly, M., Darwin, D., Browning, J.P., and Locke, Jr., C. E. (2011), "Evaluation of Multiple Corrosion Protection Systems for Reinforced Concrete Bridge Decks," *SM Report 100,* University of Kansas Center for Research, Inc., Lawrence, Kansas, 535 pp.

Ortolan, V., Mancio, M., & Tutikian, B. (2016). "Evaluation of the Influence of the pH of Concrete Pore Solution on the Corrosion Resistance of Steel Reinforcement," *Journal of Building Pathology and Rehabilitation,* Vol. 1, No. 1, 10 pp.

Page, C., & Vennesland, Ø. (1983). "Pore Solution Composition and Chloride Binding Capacity of Silica-Fume Cement Pastes," *Matériaux et Construction,* Vol. 16, No. 1, pp. 19-25.

Phares, B. M., Fanous, F. S., Wipf, T. J., Lee, Y.-S., & Jolley, M. J. (2006). "Evaluation of Corrosion Resistance of Different Steel Reinforcement Types," *Center for Transportation Research and Education* No. 02-103, 79 pp.

Ranjith, A., Rao, K. B., & Manjunath, K. (2016). "Evaluating the Effect of Corrosion on Service Life Prediction of RC Structures–A Parametric Study," *International Journal of Sustainable Built Environment,* Vol. 5, No. 2, pp. 587-603.

Rasheeduzzafar, Dakhil, F. H., Bader, M. A., & Khan, M. M. (1992). "Performance of Corrosion-Resisting Steels in Chloride-Bearing Concrete," *Materials Journal,* Vol. 89, No. 5, pp. 439-448.

Roventi, G., Bellezze, T., Giuliani, G., & Conti, C. (2014). "Corrosion resistance of galvanized steel reinforcements in carbonated concrete: effect of wet–dry cycles in tap water and in chloride solution on the passivating layer," *Cement and Concrete research,* Vol. 65, pp. 76-84.

Sagüés, A., Powers, R., & Kessler, R. (1994). "Corrosion Processes and Field Performance of Epoxy-Coated Reinforcing Steel in Marine Substructures," *NACE International, Houston, TX (United States)* No. CONF-940222.

Samples, L. M. (1998). "Durability of Concrete Bridge Decks with Emphasis on Epoxy-Coated Bars," (Ph.D), *Purdue University*. 271 pp.

Saraswathy, V., & Song, H. W. (2005). "Performance of Galvanized and Stainless Steel Rebars in Concrete Under Macrocell Corrosion Conditions," *Materials and Corrosion,* Vol. 56, No. 10, pp. 685-691.

Šiler, P., Kolářová, I., Sehnal, T., Másilko, J., & Opravil, T. (2016). "The Determination of the Influence of pH Value of Curing Conditions on Portland Cement Hydration," *Procedia Engineering,* Vol. 151, pp. 10-17.

Smith, J. L., & Virmani, Y. P. (1996). "Performance of Epoxy-Coated Rebars in Bridge Decks," *Public Roads,* Vol. 60, No. 2. pp. 6-12.

Smith, L., Kessler, R., & Powers, R. G. (1993). "Corrosion of Epoxy-Coated Rebar in a Marine Environment," *Transportation Research Circular,* No. 403, pp. 36-45.

Smith, R. J., Pfeifer, D. W., Landgre, R. J., Buttke, B., & McDonald, D. B. (1992). "Laboratory and Field Corrosion Test Methods for Highway Metals Exposed to Inhibited Rock Salt," *Transportaion Research Record,* No. 1347, pp. 66-68.

Srensen, B., Jensen, P., & Maahn, E. (1990). "The Corrosion Properties of Stainless Steel Reinforcement," *Corrosion of Reinforcement in Concrete*, pp. 601-610.

Tan, H., Wang, Z., Jiang, Y., Yang, Y., Deng, B., Song, H., & Li, J. (2012). Influence of Welding Thermal Cycles on Microstructure and Pitting Corrosion Resistance of 2304 Duplex Stainless Steels. *Corrosion Science,* Vol. 55, pp. 368-377.

Thomas, M. (1996). "Chloride Thresholds in Marine Concrete," *Cement and Concrete Research,*Vol. 26, No. 4, pp. 513-519.

Treadaway, K., & Davies, H. (1989). "Performance of Fusion-Bonded Epoxy-Coated Steel Reinforcement," *Structural Engineer,*Vol. 67, No. 6, pp. 99-108.

Treadaway, K., Cox, R., & Brown, B. (1989). “Durability of Corrosion Resisting Steel in Concrete,” *Proceedings of the Institution of Civil Engineers,* Vol. 86, No. 2, pp. 305-331.

Vassie, P. (1996). “A Discussion of Methods for Preventing Reinforcement Corrosion in Bridges,” London: *Corrosion of Reinforcement in Conceret Constructure,* Special Publication No. 183, pp. 654-661.

Verbeck, G. (1975). "Mechanisms of Corrosion of Steel in Concrete," *American Concrete Institute, Farmington Hills, MI*, 17 pp.

Weyers, R. E., Pyc, W., & Sprinkel, M. M. (1998). "Estimating the Service Life of Epoxy-Coated Reinforcing Steel," *ACI Materials Journal,*Vol. 95, No. 5, pp. 546-557.

Yeomans, S. (2004). “Galvanized Steel Reinforcement in Concrete,” *Elsevier*, 293 pp.

Zhang, F., Pan, J., & Lin, C. (2009). “Localized Corrosion Behaviour of Reinforcement Steel in Simulated Concrete Pore Solution,” *Corrosion Science,* Vol. 51, No. 9, pp. 2130-2138.

Zoob, A., Le Claire, P., & Pfeifer, D. (1985). “Corrosion Protection Tests on Reinforced Concrete With Solid Stainless Steel Reinforcing Bars for Joslyn Stainless Steels,” *Wiss, Janney, Elstner Associates,* Inc., Report.

APPENDIX A

MACROCELL RATE AND CORROSION POTENTIAL OF ANODE AND CATHODE OF INDIVIDUAL SPPECIMENS TESTED IN STANDARD (S) AND MODIFIED (M) PORE SOLUTIONS

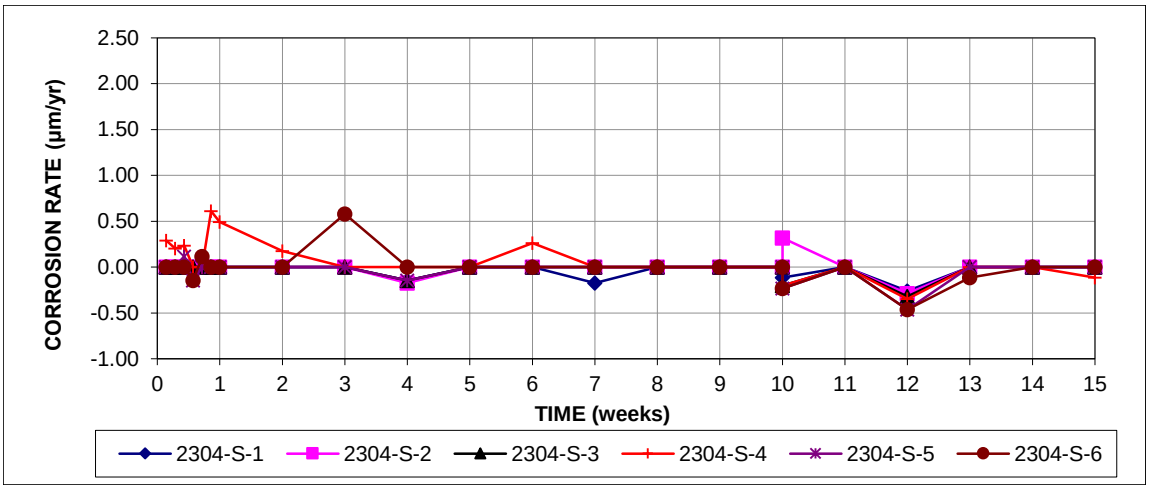

(a)

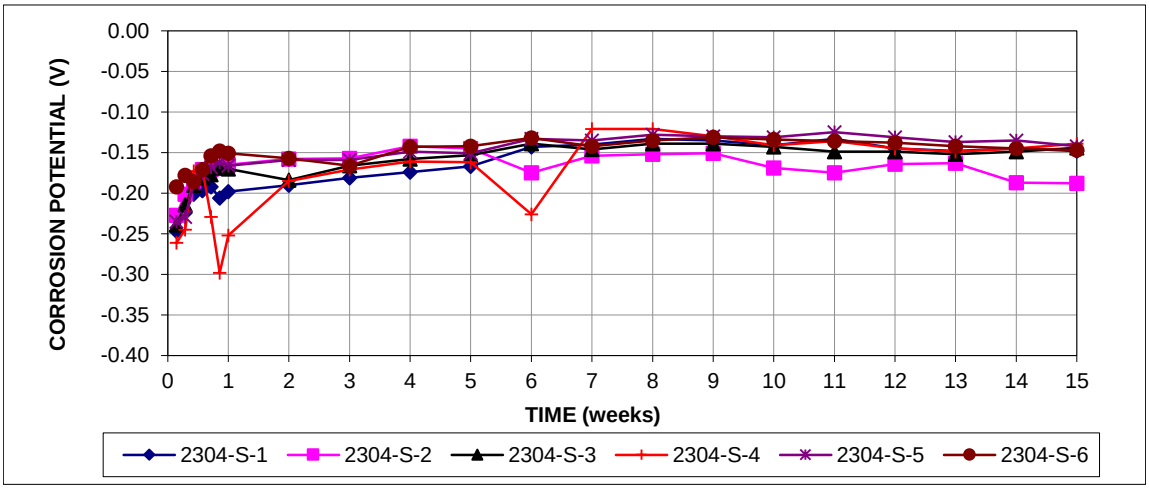

(b)

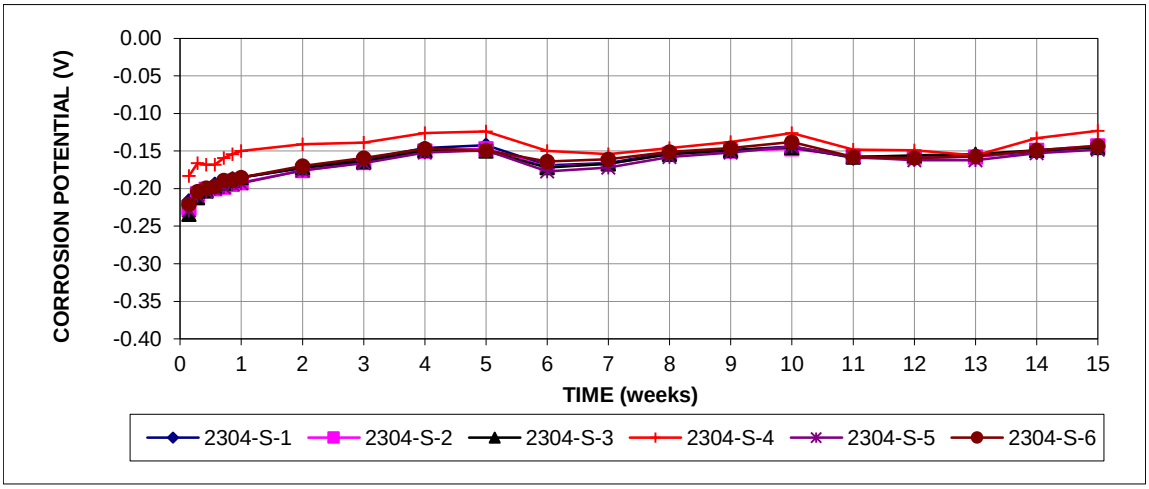

(c)

Figure A.1: Rapid macrocell test, corrosion rates (a), anode potentials (b) and cathode potentials (c) of 2304 bars in standard (S) pore solution.

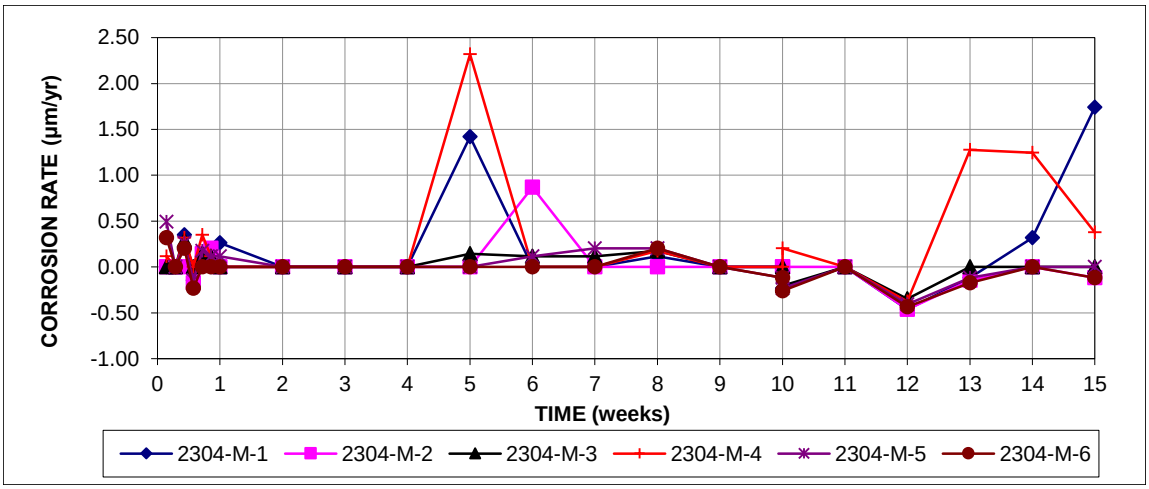

(a)

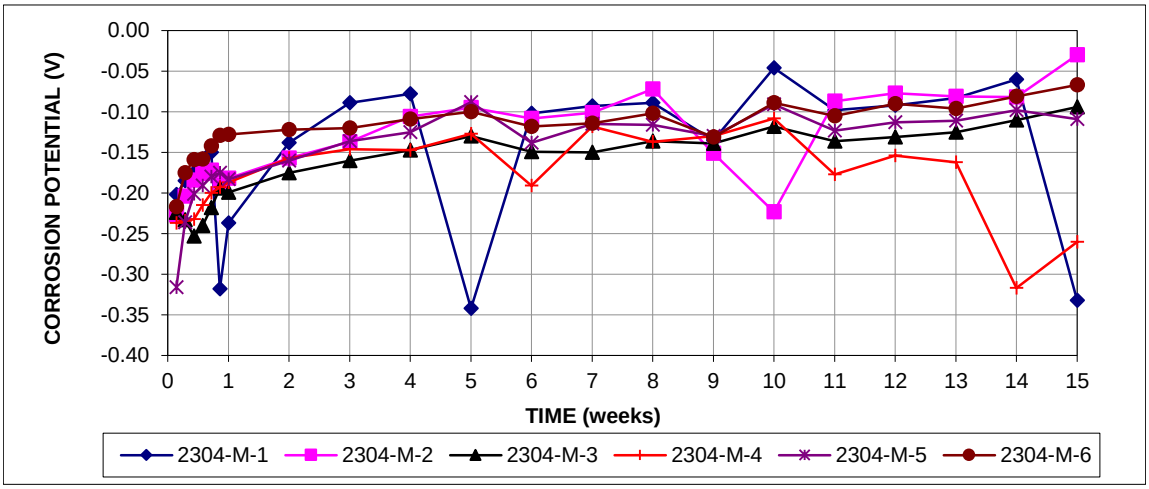

(b)

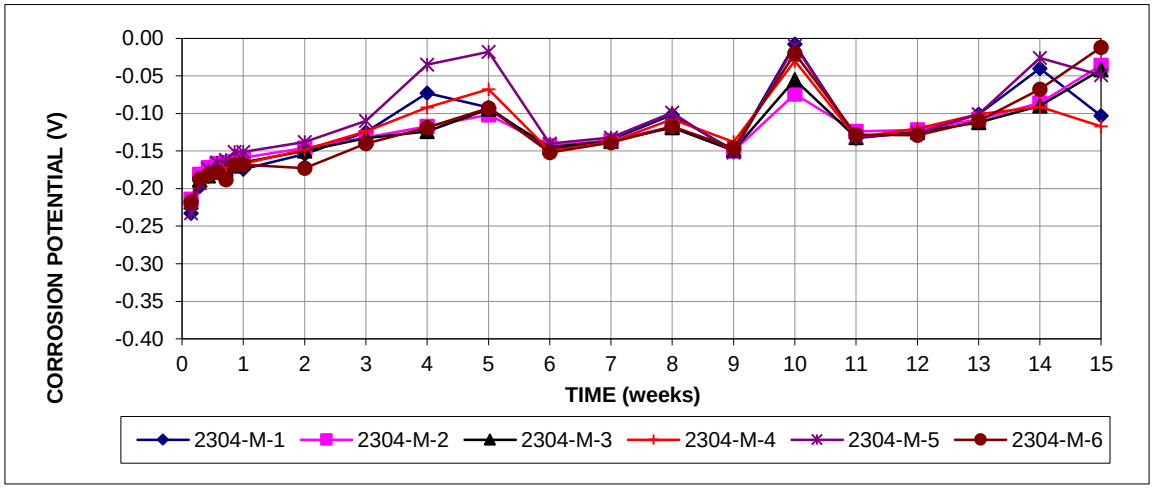

(c)

Figure A.2: Rapid macrocell test, corrosion rates (a), anode potentials (b) and cathode potentials (c) of 2304 bars in modified (M) pore solution.

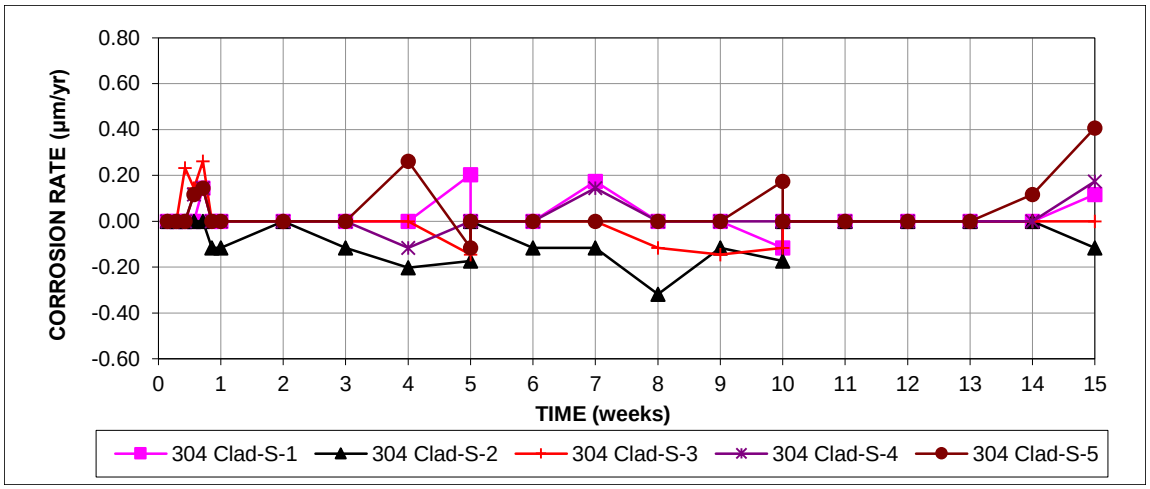

(a)

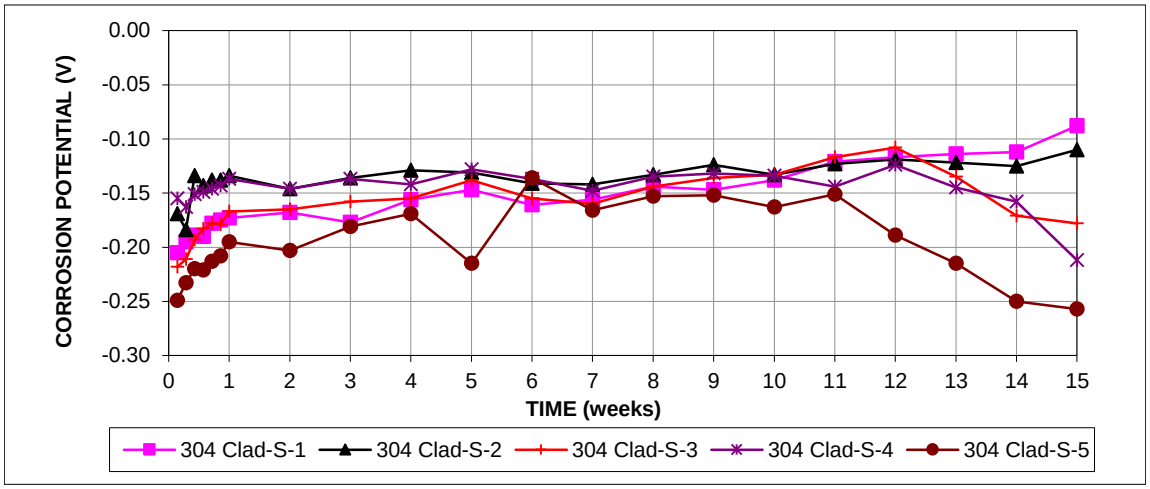

(b)

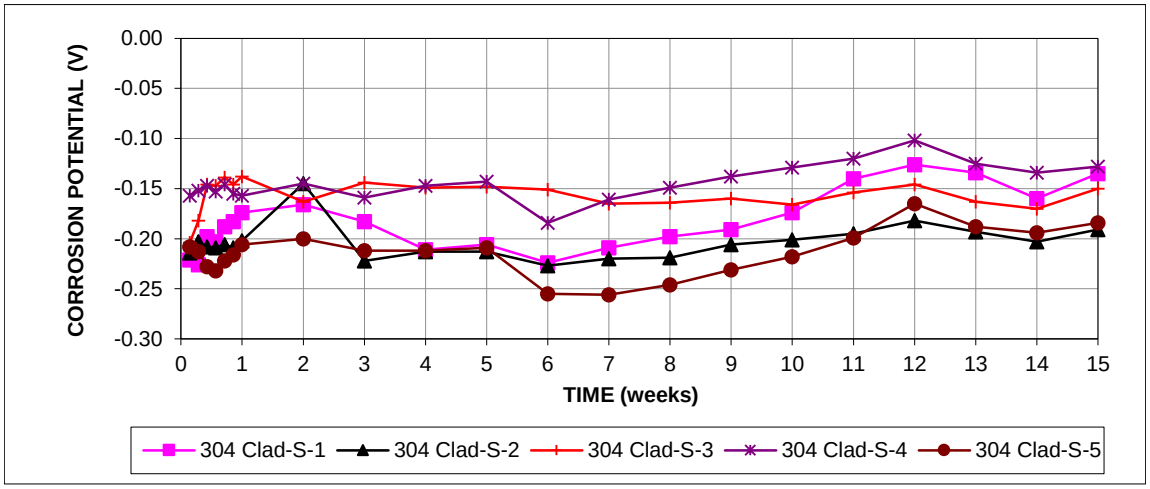

(c)

Figure A.3: Rapid macrocell test, corrosion rates (a), anode potentials (b) and cathode potentials (c) of 304 clad bars in standard (S) pore solution.

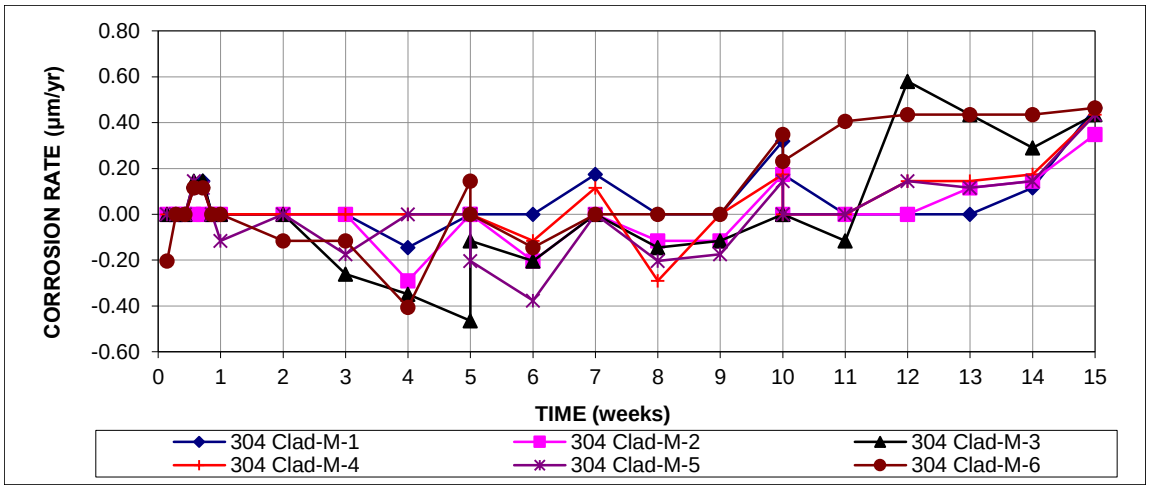

(a)

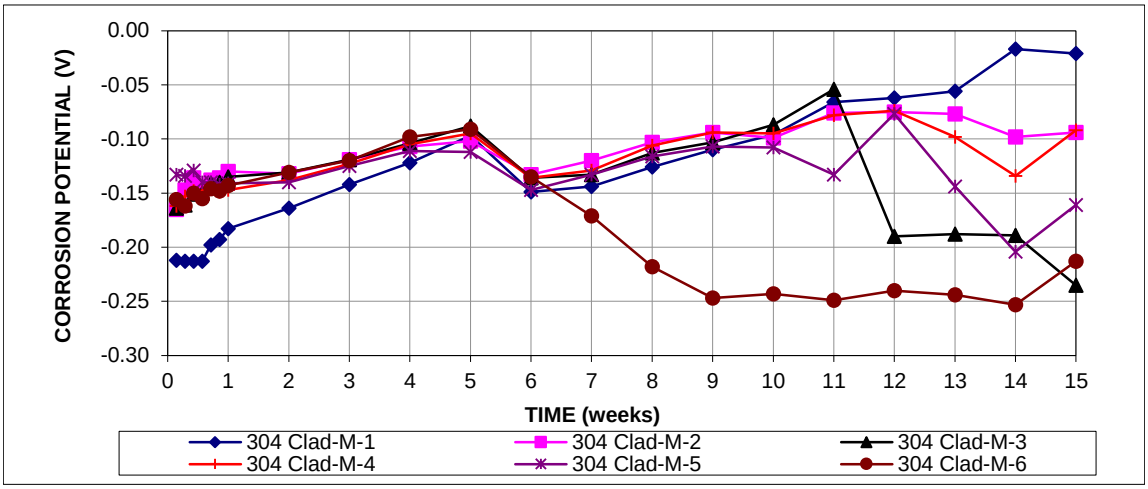

(b)

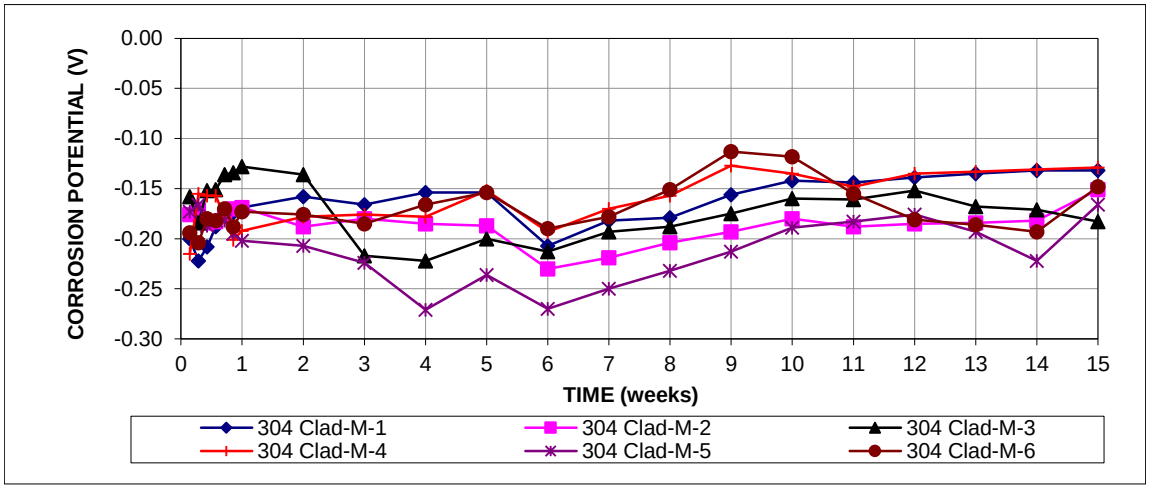

(c)

Figure A.4: Rapid macrocell test, corrosion rates (a), anode potentials (b) and cathode potentials (c) of 304 clad bars in modified (M) pore solution.

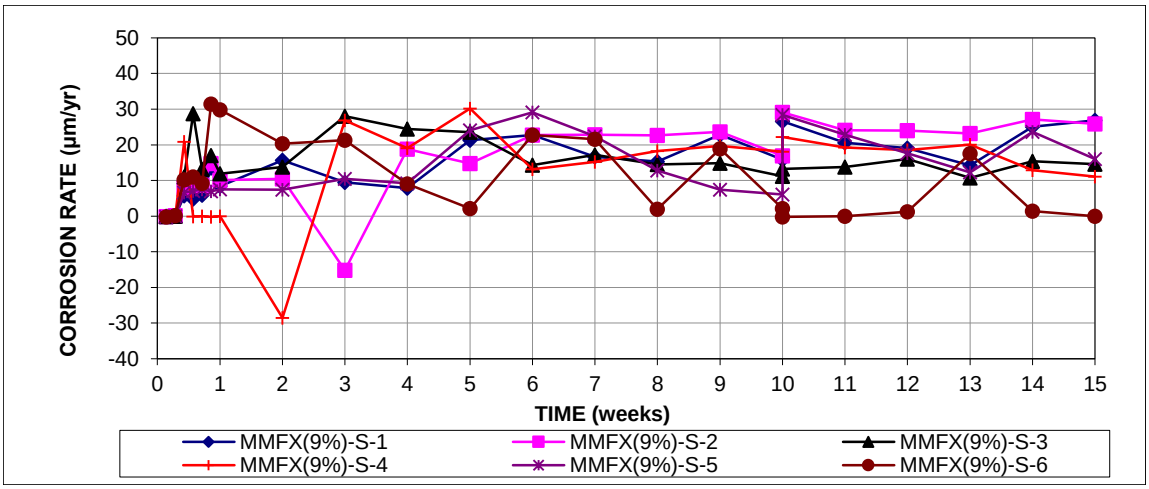

(a)

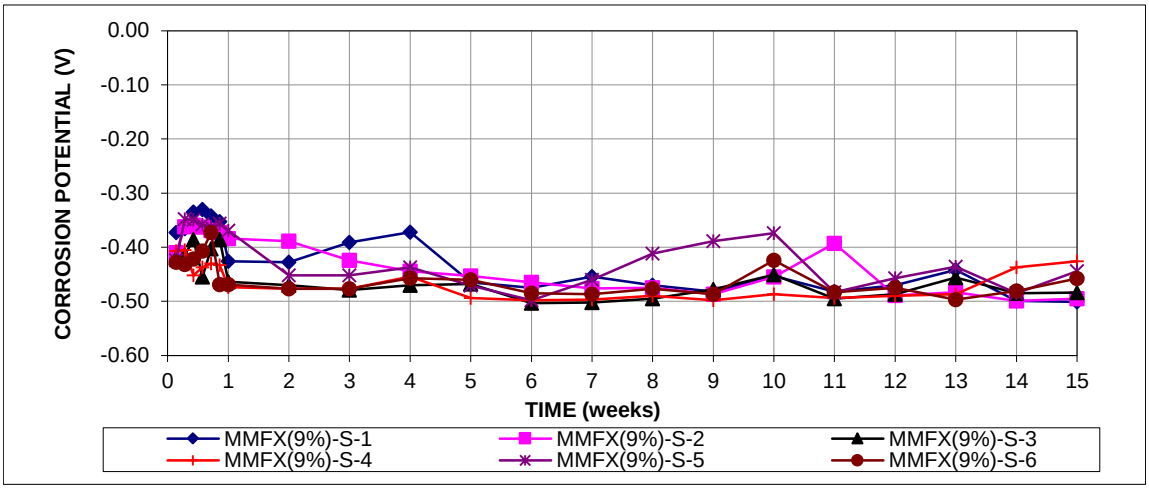

(b)

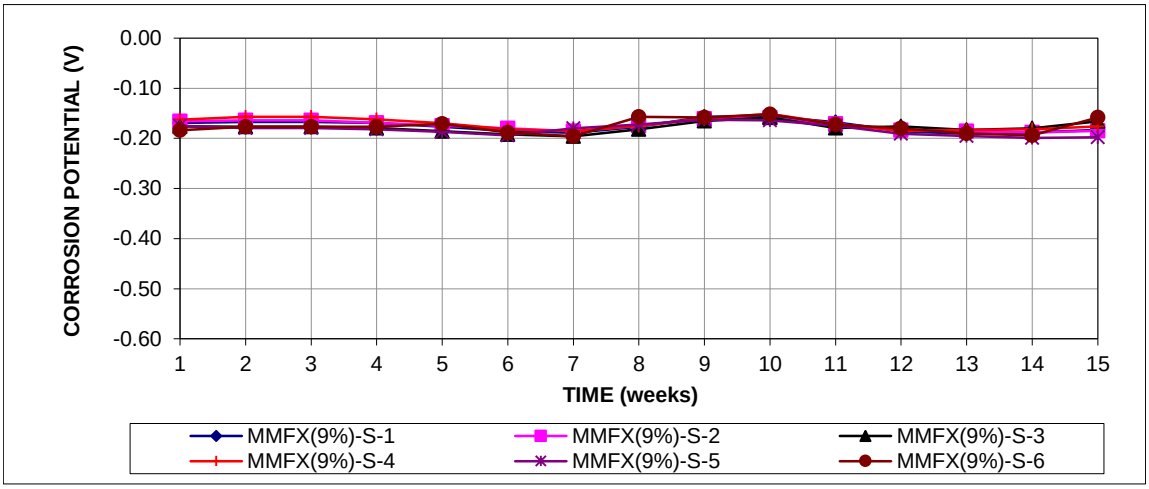

(c)

Figure A.5: Rapid macrocell test, corrosion rates (a), anode potentials (b) and cathode potentials (c) of MMFX(9%) bars in standard (S) pore solution.

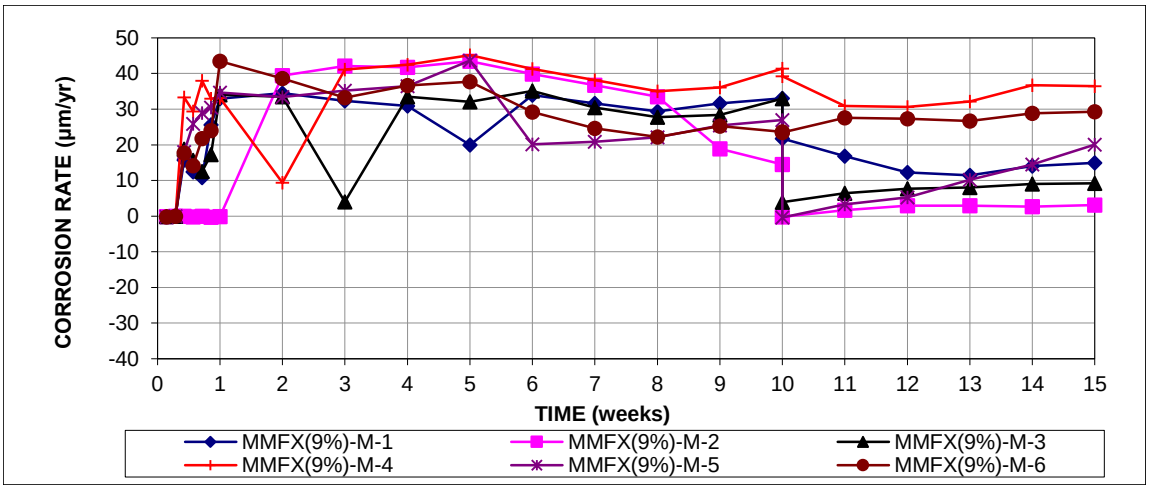

(a)

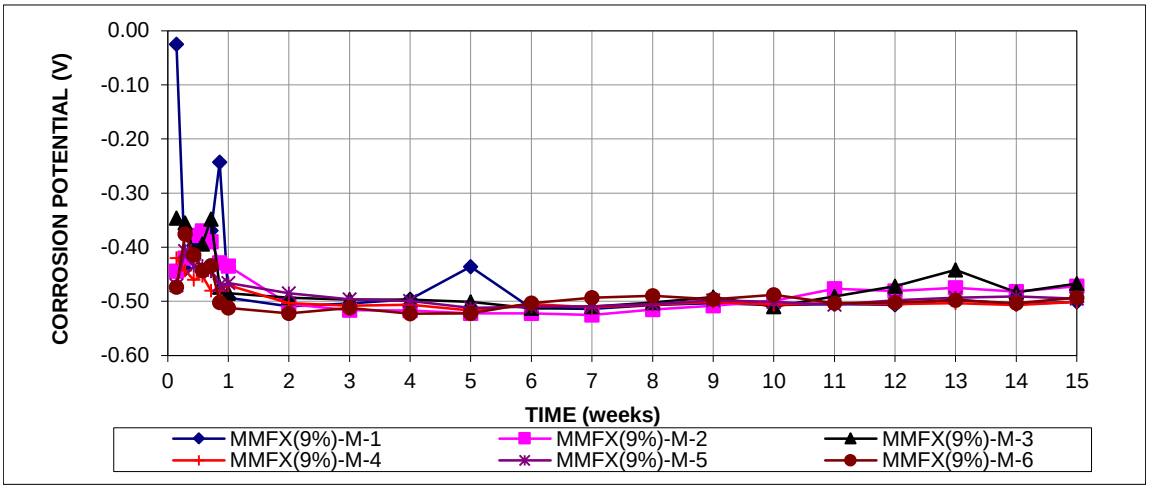

(b)

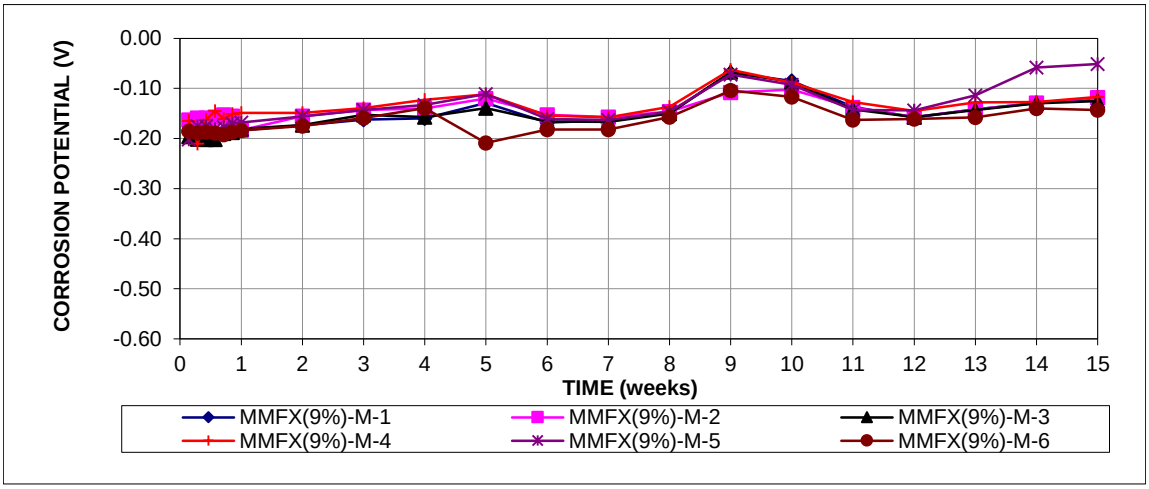

(c)

Figure A.6: Rapid macrocell test, corrosion rates (a), anode potentials (b) and cathode potentials (c) of MMFX(9%) bars in modified (M) pore solution

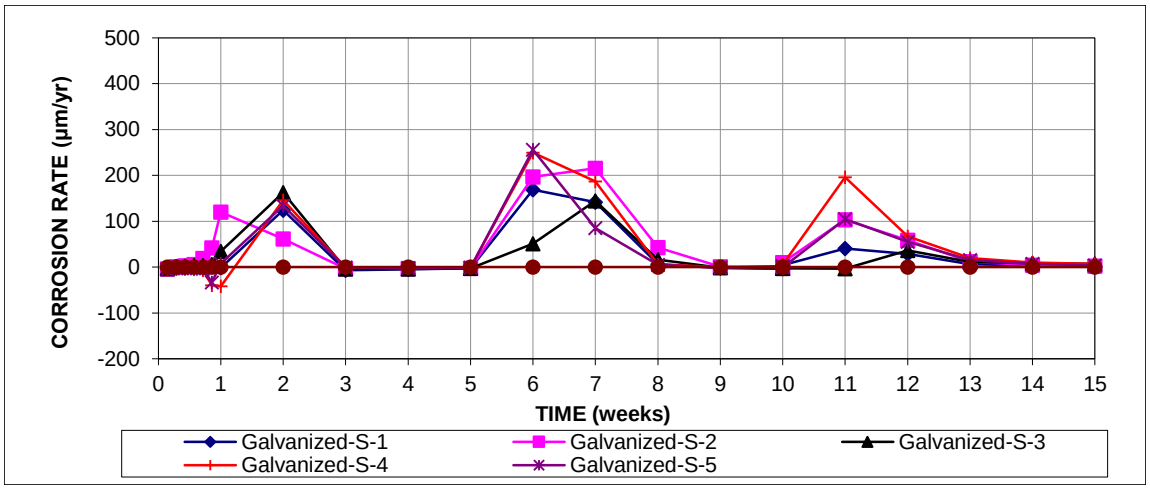

(a)

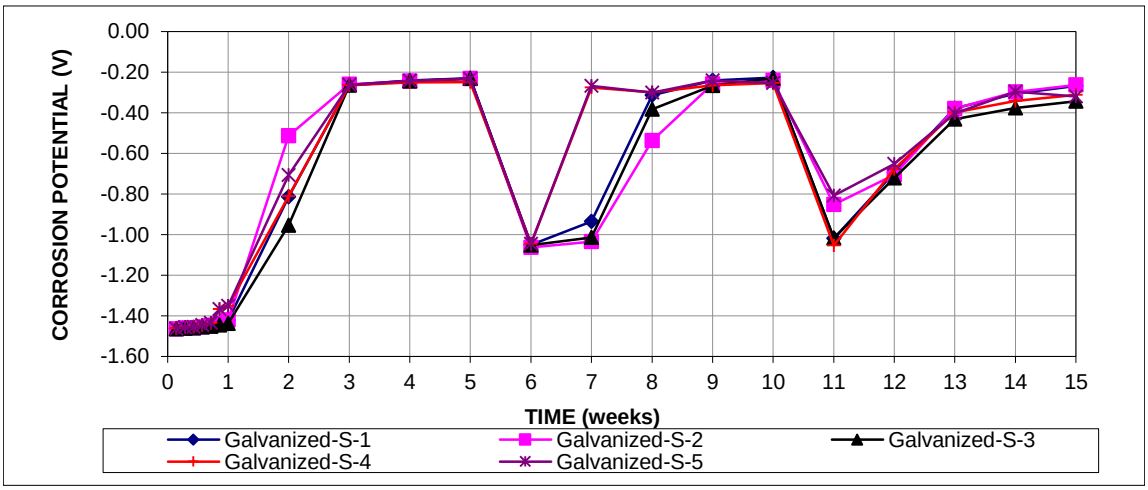

(b)

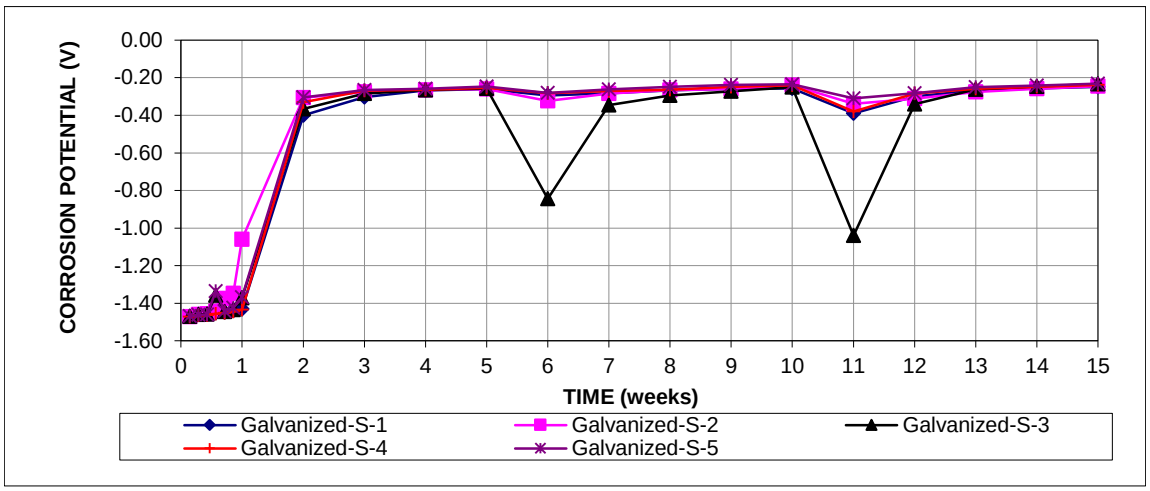

(c)

Figure A.7: Rapid macrocell test, corrosion rates (a), anode potentials (b) and cathode potentials (c) of galvanized bars in standard (S) pore solution.

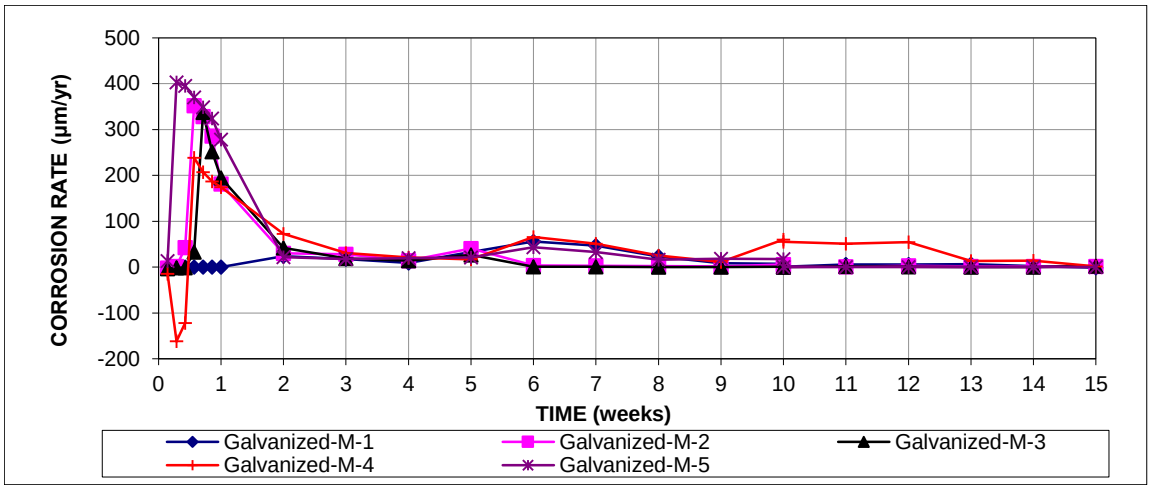

(a)

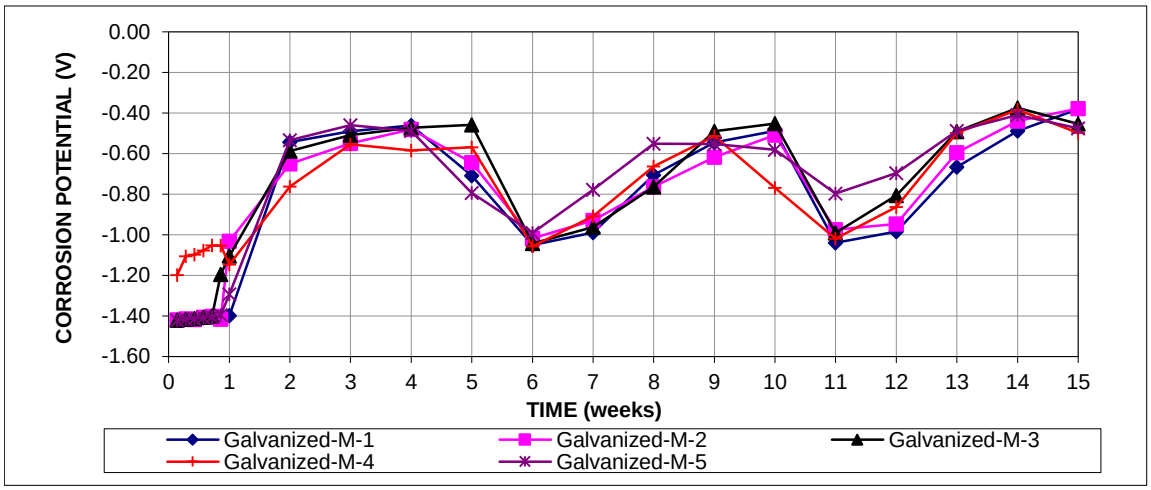

(b)

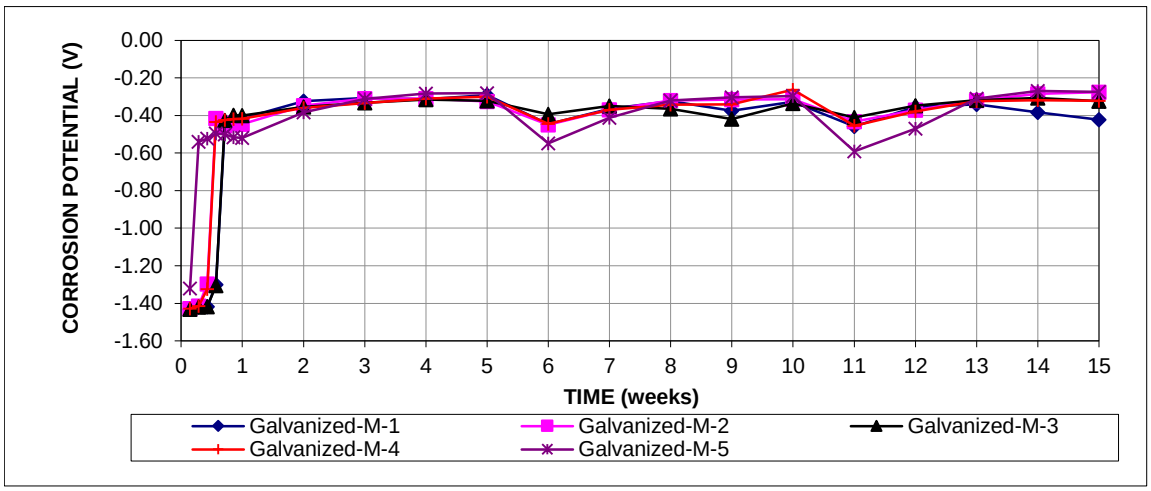

(c)

Figure A.8: Rapid macrocell test, corrosion rates (a), anode potentials (b) and cathode potentials (c) of galvanized bars in modified (M) pore solution

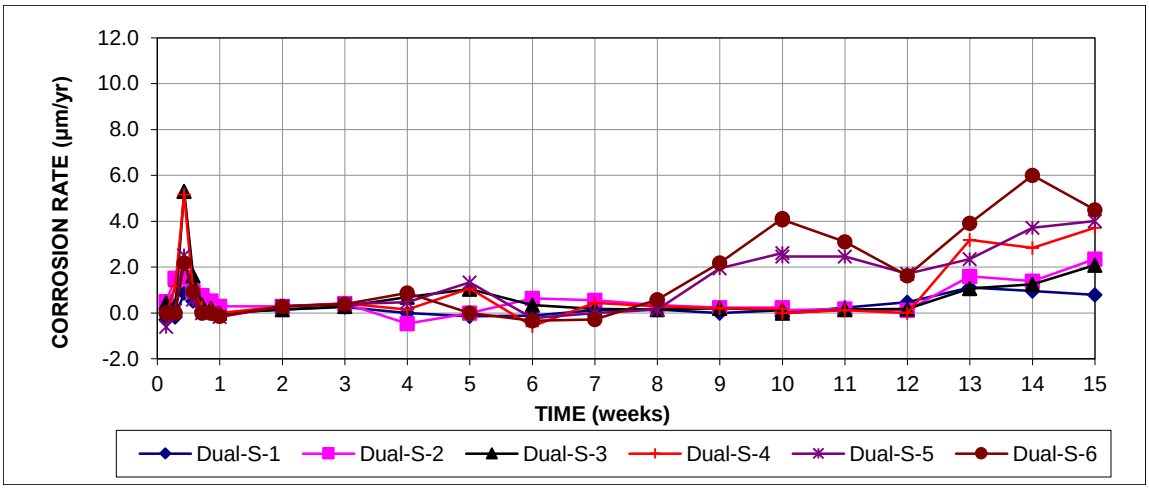

(a)

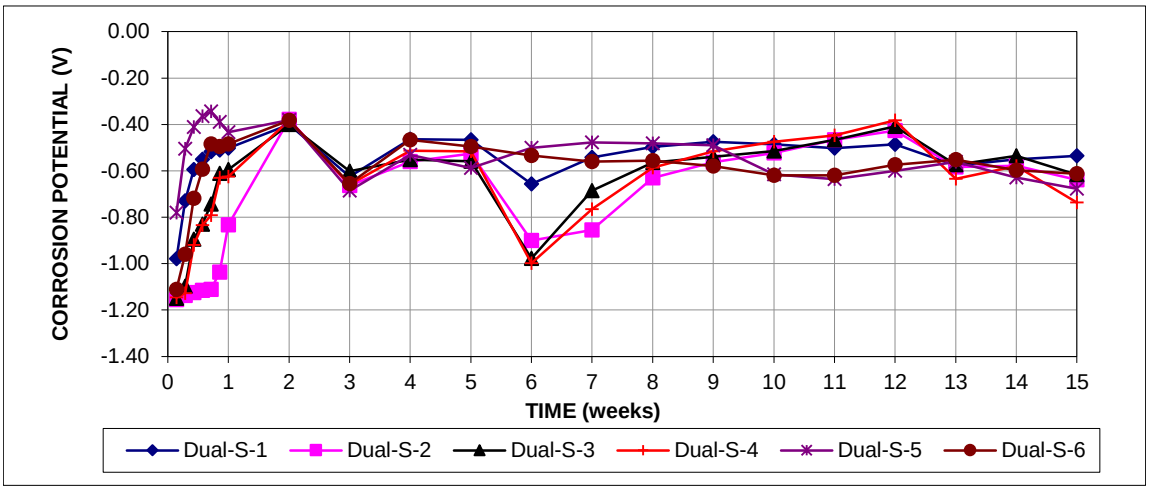

(b)

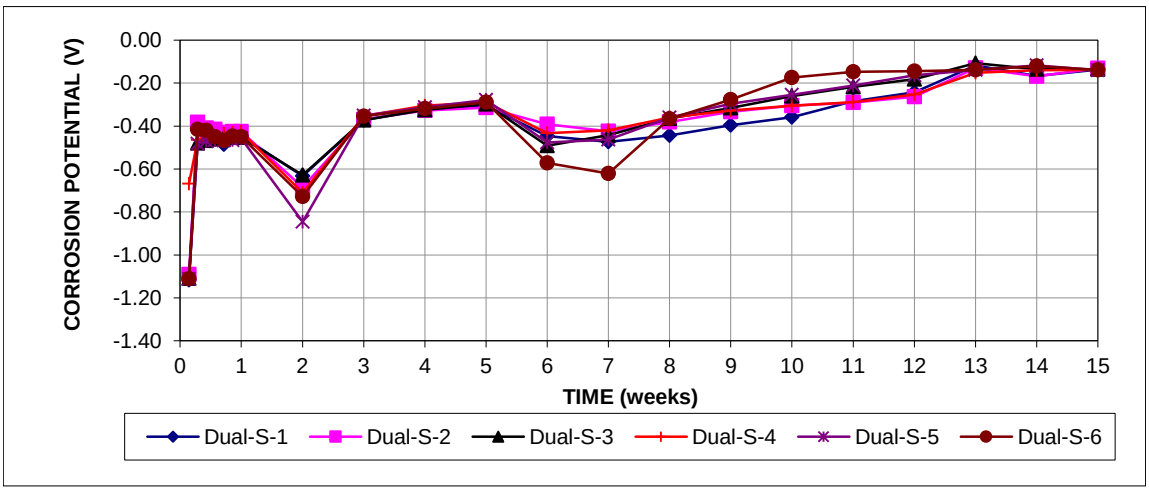

(c)

Figure A.9: Rapid macrocell test, corrosion rates (a), anode potentials (b) and cathode potentials (c) of dual-coated bars in standard (S) pore solution.

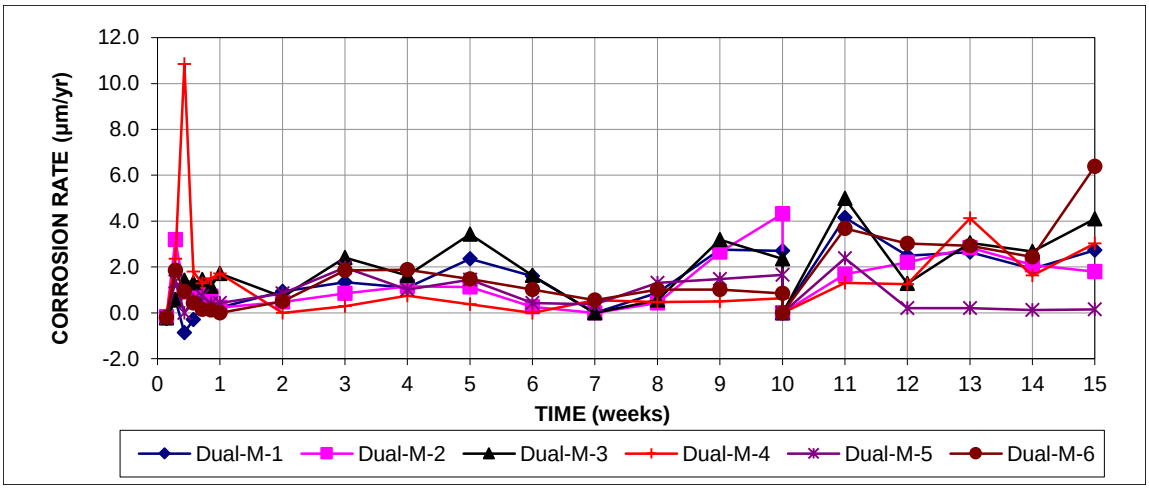

(a)

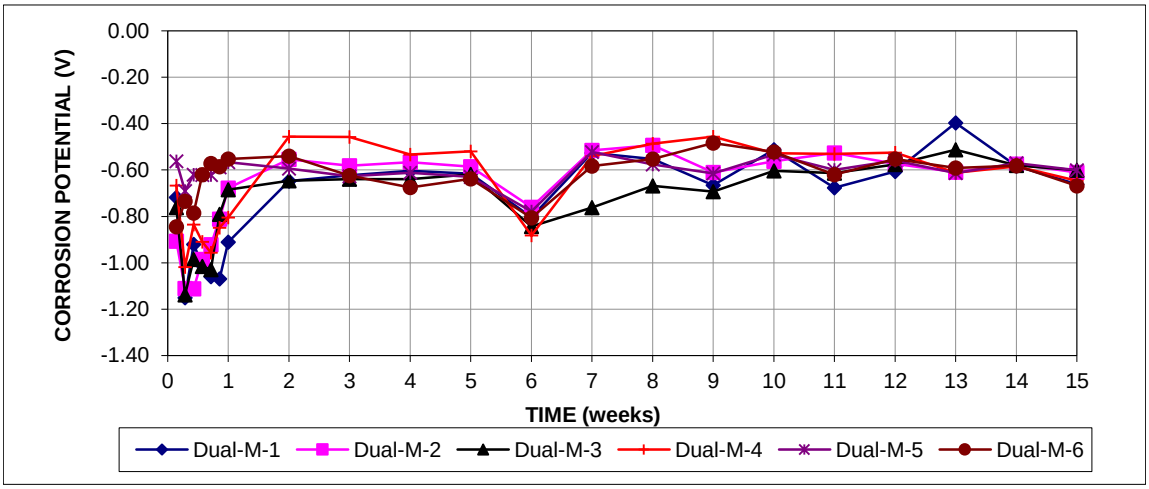

(b)

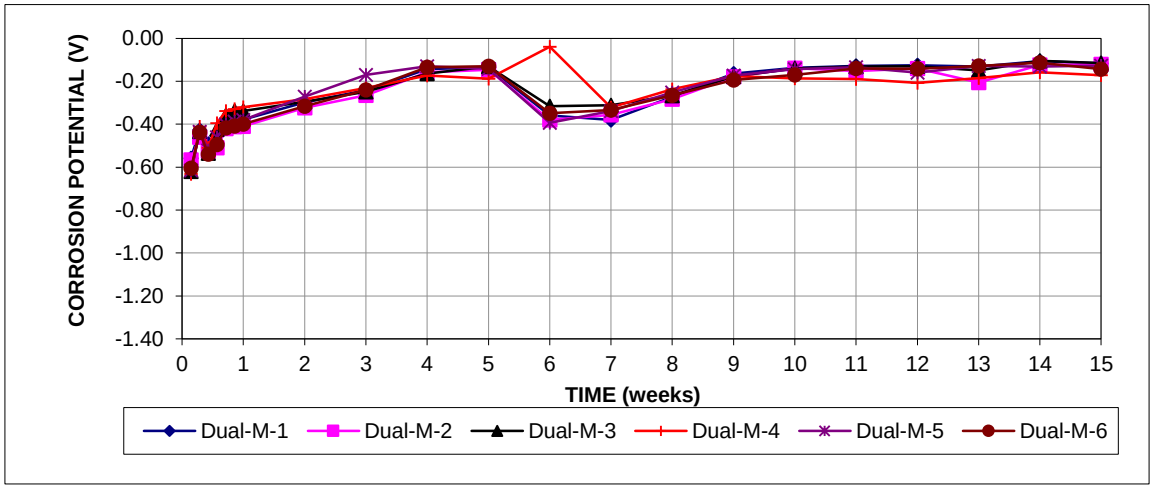

(c)

Figure A.10: Rapid macrocell test, corrosion rates (a), anode potentials (b) and cathode potentials (c) of dual-coated bars in modified (M) pore solution